



Ph.D. Thesis

Mikael Palner

**Development & Evaluation of
Monoaminergic Agonist PET Tracers**

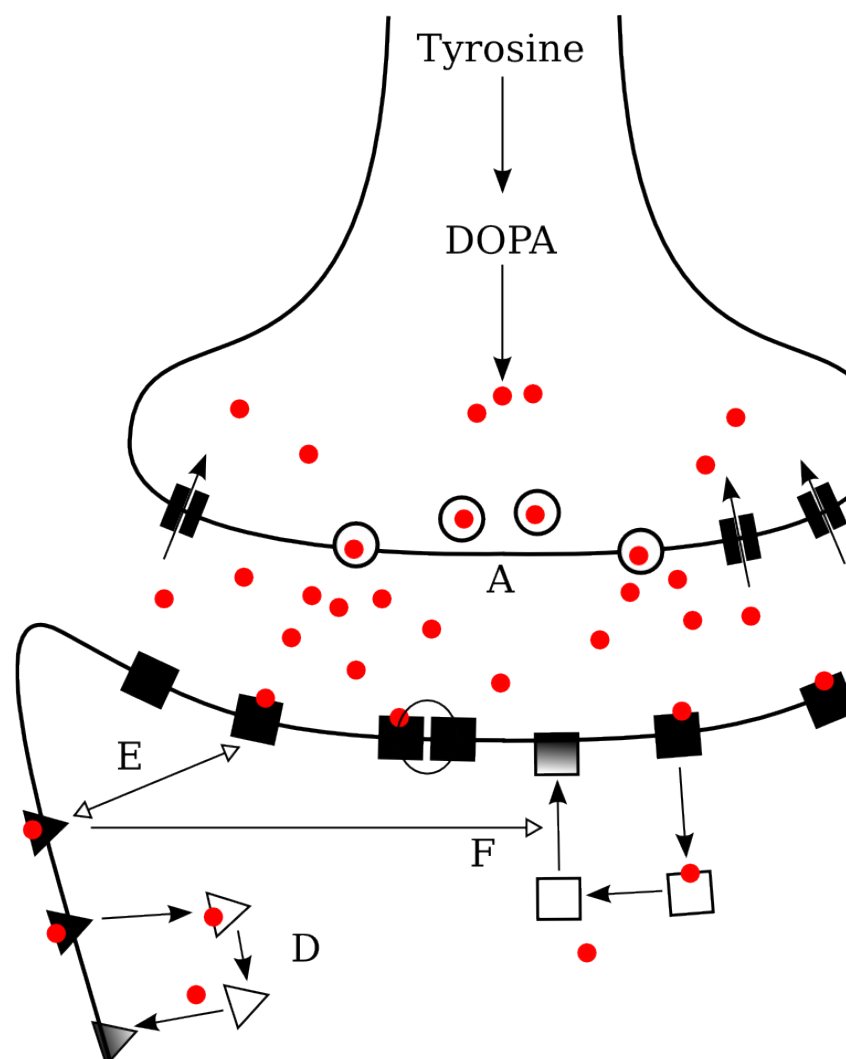


Table of Contents

Project Details.....	3
Summary.....	4
Dansk Resumé.....	5
Papers Included in This Ph.D Thesis.....	6
Abbreviations.....	8
Introduction.....	10
The Dopaminergic & Serotonergic Transmitter Systems.....	11
Dopamine and Serotonin GPCR affinity states.....	14
The Ternary Model of GPCRs.....	15
PET and Radioligands.....	17
The Competition Model.....	18
Agonist Radioligand Development.....	21
Aims and Delineation of the Problem.....	23
Methodological Considerations.....	24
Properties of Agonist Radioligands.....	24
Quantitative Methods for Studying the Uptake and Distribution.....	25
Radionuclide Decay and Detection.....	25
Positron Emission Tomography.....	26
Quantifying PET Data.....	27
Ex Vivo Experiments.....	29
Ex Vivo Autoradiography.....	30
Metabolism of Radioligands.....	30
Binding Competition.....	31
Direct Competition.....	31
Endogenous Competition - Release.....	31
Endogenous Competition - Depletion	32
Results & Discussion.....	34
Chemical Properties of Agonist Radioligands.....	34

Studying the Uptake and Distribution of Radioligands.....	34
Metabolism of Radioligands.....	36
Binding Competition.....	38
Endogenous Competition - Release.....	38
Endogenous Competition - Depletion	40
The in vivo Competition Model Expanded.....	41
Conclusion.....	45
Acknowledgments.....	46
References.....	47
Appendices.....	58
Radiosynthesis and <i>ex vivo</i> evaluation of (R)-(-)-2-chloro-N-[1- ¹¹ C-propyl]n-propylnorapomorphine.....	59
Systemic catechol-O-methyl transferase inhibition enables the D1 agonist radiotracer R-[¹¹ C]SKF 82957.....	65
Effects of unilateral 6-OHDA lesion on [³ H]NPA binding in striatum <i>ex vivo</i> , and vulnerability to amphetamine-evoked dopamine release in rat.....	72
<i>Ex vivo</i> binding and pharmacological challenges of the serotonin 1A receptor agonist [³ H]CUMI-101 in awake rats.....	77
Radiosynthesis and evaluation of [¹¹ C]Cimbi-5 as a 5-HT _{2A} receptor agonist radioligand for positron emission tomography.....	86

Project Details

Title: Development & Evaluation of Monoaminergic Agonist PET Tracers

Title in Danish: Udvikling & Evaluering af Monoaminerge Agonist PET Sporstoffer

Author: Mikael Palner

Main Academic Advisor:

Gitte M. Knudsen, Professor, Center for Integrated Molecular Brain Imaging, Department of Neurology, Copenhagen University Hospital, Copenhagen, Denmark.

Secondary Academic Advisors:

Alan A. Wilson, Associate Professor, Department of Psychiatry, University of Toronto, Toronto, Ontario, Canada.

Ramin V. Parsey, Associate Professor in Psychiatry, Columbia University, New York, New York, USA.

Paul Cumming, PD Dr., Department of Nuclear Medicine, Ludwig-Maximilian's University, Munich, Germany.

Submitted: 1st of March 2010

With Corrections: 23rd of September 2010

Defense: 11th of March 2011

Review Committee:

Albert Gjedde, Professor in Neurobiology and Pharmacology, University of Copenhagen, Copenhagen, Denmark.

Christer Halldin, Professor in Medical Radiochemistry, Karolinska Institute, Stockholm, Sweden.

Tine B. Stensbøl, Divisional Director, Discovery Pharmacology Research, H. Lundbeck A/S, Valby, Denmark.

Summary

Positron emission tomography (PET) is a non-invasive *in vivo* biomedical imaging technique, which trace radioactive isotopes. Radioactive labeled receptor ligands can be used to image G-protein coupled receptors in the living brain. Ligands for GPCRs fall into two categories; antagonists, which block receptor activation, bind to the whole population of receptors irrespective of their coupling to second messenger signaling, and agonists, which activate the receptor, bind only to those receptors which are coupled to intracellular G-proteins. All neurotransmitters are considered natural agonists for their receptors. There are numerous well-characterized antagonist PET tracers, whereas the development and validation of agonist tracers is in its infancy.

The major aim of this thesis was to evaluate a series of novel radiolabeled agonists as possible PET radioligands for G-protein coupled receptors, and to evaluate the agonist binding under pharmacologically-altered competition from endogenous neurotransmitter.

Several novel radiolabeled agonists were evaluated as possible PET radioligands. The dopamine D_{2/3} receptor agonist [¹¹C]-2Cl-NPA, the dopamine D₁ receptor agonist [¹¹C]SKF 82957, the serotonin 5-HT_{2A} receptor agonist [¹¹C]Cimbi-5 and the serotonin 5-HT_{1A} receptor agonist [³H]CUMI-101. Pharmacological challenges and neurochemical lesions altering the interstitial levels of DA and 5-HT were used to test the vulnerabilities of the agonist radioligands to competition from the endogenous agonists. The binding of the D_{2/3} agonist [¹¹C]NPA (and [³H]NPA) in rat striatum was challenged with amphetamine-induced dopamine release and neurotoxic lesioning. The D₁ agonist [¹¹C]SKF 82957 was challenged by amphetamine induced dopamine release and alpha-methyle tyrosine inhibition of dopamine synthesis, leading to substantial depletion. And finally, the cerebral binding of the 5-HT_{1A} agonist [³H]CUMI-101 was challenged by blocking the serotonin reuptake with citalopram, inducing serotonin release with fenfluramine and inhibiting serotonin synthesis with *para*-chloro-*D,L*-phenylalanine. Most of the tracers, except for the classic example with [³H]NPA, did not respond to these treatments.

Dansk Resumé

Positron emission tomography (PET) er en ikke-invasiv billeddannelsesteknik, der kan spore radiomærkede stoffer. Ved at radiomærke en receptor ligand kan man måle mængden af G-protein-koblede receptorer i den levende menneskehjerne. Der findes to typer af ligander til denne receptorgruppe: antagonist, der blokerer for receptoraktivering og binder til hele populationen af receptorer uanset deres kobling til G-proteiner, og agonister, der aktiverer receptoren og binder den del af receptorpopulationen, der er koblet til G-proteiner. Alle naturligt forekommende neurotransmittere er agonister. Der er mange veldokumenterede antagonist PET sporstoffer, mens udviklingen af agonister stadig er i opstartsfasen.

Målet med projektet var, at evaluere en række nyudviklede agonister som mulige PET sporstoffer for G-protein-koblede receptorer, og derudover måle ændringen i binding efter farmakologisk induceret konkurrence mellem neurotransmitter og de receptorbundne sporstoffer.

Flere nye agonister er blevet evalueret som mulige PET sporstoffer: Dopamin D₂ receptor agonisten, [¹¹C]-2Cl-NPA, dopamin D₁ receptor agonisten, [¹¹C]SKF 82957, serotonin 5-HT_{1A} receptor agonisten, [³H]CUMI-101, og serotonin 5-HT_{2A} receptor agonisten, [¹¹C]Cimbi-5. Farmakologisk og læsions-inducerede ændringer af dopamin og serotonin neurotransmitter-niveauer blev brugt til at teste følsomheden af de forskellige agonist radioligander til konkurrence fra endogene agonister. De fleste af de testede sporstoffer, på nær det klassiske eksempel med [³H]-NPA, var ufølsomme overfor konkurrence fra de endogene agonister.

Papers Included in This Ph.D Thesis

- I. **Mikael Palner**, Patrick McCormick, Nic Gillings, Mikael Begtrup, Alan A. Wilson, Gitte M. Knudsen (2010) Radiosynthesis and *ex vivo* evaluation of (*R*)-(-)-2-chloro-*N*-[1-¹¹C-propyl]*n*-propylnorapomorphine. *Nucl Med Biol* 37(1):35-40
- II. **Mikael Palner**, Patrick McCormick, Jun Parkes, Gitte M Knudsen, Alan A. Wilson (2010) Systemic catechol-O-methyl transferase inhibition enables the D₁ agonist radiotracer *R*-[¹¹C]SKF 82957. *Nucl Med Biol* 37(7):837-43
- III. **Mikael Palner**, Celia Kjaerby, Gitte M Knudsen, Paul Cumming (2011) Effects of unilateral 6-OHDA lesion on [³H]NPA binding in striatum *ex vivo*, and vulnerability to amphetamine-evoked dopamine release in rat. *Neurochemistry International* 58: 243-247
- IV. **Mikael Palner**, Mark Underwood, Dileep Kumar, Victoria Arango, Gitte M Knudsen, J. John Mann, Ramin V. Parsey (2010) *Ex vivo* binding and pharmacological challenges of the serotonin 1A receptor agonist [³H]CUMI-101 in awake rats. In Press, *Synapse*
- V. Anders Ettrup, **Mikael Palner**, Nic Gillings, Martin A. Santini, Martin Hansen, Birgitte R. Kornum, Lars K. Rasmussen, Kjell Någren, Jacob Madsen, Mikael Begtrup, Gitte M Knudsen (2010) Radiosynthesis and evaluation of [¹¹C]Cimbi-5 as a 5-HT_{2A} receptor agonist radioligand for positron emission tomography. *Journal of Nuclear Medicine* 51:1-8

Other papers not included in this thesis but where the author has contributed during the Ph.D. period.

- I. Kramer V, Herth MM, Santini MA, **Palner M**, Knudsen GM, Rösch F (2010) Structural Combination of Established 5-HT Receptor Ligands: New Aspects of the Binding Mode. *Chem Biol Drug Des*, In Press
- II. Prabhakaran J, Majo VJ, Milak MS, Kassir SA, **Palner M**, Savenkova L, Mali P, Arango V, Mann JJ, Parsey RV, Kumar JS (2010) Synthesis, *in vitro* and *in vivo* evaluation of [¹¹C]MMTP: a potential PET ligand for mGluR1 receptors. *Bioorg Med Chem Lett* 15;20(12):3499-501.
- III. Herth MM, Kramer V, Piel M, **Palner M**, Riss PJ, Knudsen GM, Rösch F (2009) Synthesis and *in vitro* affinities of various MDL 100907 derivatives as potential ¹⁸F-radioligands for the 5-HT_{2A} receptor imaging with PET, *Bioorg Med Chem* 17(8): 2989-3002
- IV. Syvänen S, Lindhe O, **Palner M**, Kornum BR, Rahman O, Långström B, Knudsen GM, Hammerlund-Udenaes M, (2009) Species difference in blood-brain barrier transport of three positron emission tomography radioligands with emphasis on P-glycoprotein transport, *Drug Metab Dispos* 37(3):635-643
- V. Herth MM, Debus F, Piel M, **Palner M**, Knudsen GM, Lüddens H, Rösch F, (2008) Total synthesis and evaluation of [¹⁸F]MHMZ, *Bioorg Med Chem* 18(4):1515-1519

Abbreviations

A	An unspecified agonist
α -MT	Alpha-methyl- <i>para</i> -tyrosine, dopamine synthesis inhibitor
B	An unspecified agonist, different from A
BBB	Blood brain barrier
B/F	Bound over free radioligand
B_{max}	The maximum binding to a receptor population
BP	The binding potential
BP _{ND}	The non-displaceable binding potential
cAMP	Cyclic adenosine monophosphate
C _{FT}	The free concentration in tissue
C _{ND}	The non-displaceable compartment
C _P	The plasma (input) compartment
C _S	The specific binding compartment
C _T	The total accumulation compartment
COMT	Catechol- <i>O</i> -methyltransferase
DA	Dopamine
DAT	Dopamine reuptake transporter
D _x	Dopamine receptor type X
D _x ^{Low}	The low affinity state of the dopamine receptor type X
D _x ^{High}	The high affinity state of the dopamine receptor type X
G-protein	A guanine nucleotide-binding protein
GPCR	G-protein coupled receptor
5-HIAA	5-hydroxy indole acetic acid
5-HT	Serotonin (5-Hydroxy-tryptamine)
5-HT _x	Serotonin receptor type X
5-HT _x ^{Low}	The low affinity state of the serotonin receptor type X
5-HT _x ^{High}	The high affinity state of the serotonin receptor type X
5-HTP	5-hydroxytryptophan
HPLC	High performance liquid chromatography
HVA	Homovanillic acid
IC ₅₀	The concentration of a compound evoking 50% inhibition of some process
k _A	Dissociation equilibrium constant between A and R ^{Low}

k_A^*	Dissociation equilibrium constant between A and R ^{High}
F	The concentration of free radioligand
K_D	Dissociation equilibrium concentration
K_i	Inhibition equilibrium concentration
K_1	The unidirectional blood-brain clearance of a substance
k_2	The fractional rate constant for washout from brain
k_3	The <i>in vivo</i> dissociation constant
k_4	The <i>in vivo</i> association constant
L	Tissue dependent constant for the ratio between R ^{Low} and R ^{high}
L-DOPA	Levodopa
MAO	Monoamine oxidase
6-OHDA	6-hydroxydopamine, a toxin for catecholamine neurons
pCPA	<i>para</i> -chloro- <i>D,L</i> -phenylalanine, serotonin synthesis inhibitor
PET	Positron emission tomography
R	An unspecified G-protein coupled receptor
R ^{Low}	An unspecified G-protein coupled receptor in the low affinity state
R ^{High}	An unspecified G-protein coupled receptor in the high affinity state
ROI	Region of interest
RTI-32	A tropane-based selective dopamine reuptake inhibitor
SERT	Serotonin reuptake transporter
SPECT	single photon emission computed tomography
SUV	Standardized uptake value
SBR	Specific binding ratio
SSRI	Selective serotonin reuptake inhibitors
$t_{1/2}$	Half-life for radioactive decay
TAC	Time activity curve
VMAT	Vesicular monoamine transporter
V_{FT}	The volume of distribution of free concentration in tissue
V_{ND}	The volume of distribution of the non-displaceable compartment
V_P	The volume of distribution of the plasma (input) compartment
V_S	The volume of distribution of the specific binding compartment
V_T	The volume of distribution of the total accumulation compartment

Introduction

One can consider the human brain and its relationship to mind from many perspectives. In a modern form of Cartesian dualism, it can be seen as the seat of consciousness (and perhaps the soul) or merely a complicated machine, an input-output device composed of neurons, the particular nature of which is an expression of genes encoded in our DNA. Whatever preferred perspective, it remains a valid endeavor to understand the mechanisms by which the brain actually sends and receives signals, how thoughts are turned into action, and how neuropharmacological and neurobiological functions are involved in normal behavior. It is a natural extension of this mechanistic perspective to seek causes for neurological diseases such as Parkinson's disease, and psychiatric illnesses such as schizophrenia and depression. This is proving to be a tremendous task.

The brain consists of numerous connecting neurons. There is 21 billion (21×10^9) nerve cells in the cerebral cortex alone (Pakkenberg et al. 1997). Typical neurons consists of a cell body, the soma, which has an extended arborization of dendrites and a long extension known as an axon, which transmits a wave of depolarization away from its origin in the soma, at the axon hillock. The axon terminates in specialized structures, the axon terminal, which are in close apposition to the membrane of another neuron, the synapse. In fact, it has been estimate that we have an amazing 0.15 quadrillion (0.15×10^{15}) synapses in the cerebral cortex, i.e. some 10.000 per neuron (Pakkenberg et al. 2003), which implies a structure of astronomical complexity.

Different classes of neurons express one or more neurotransmitter substances, either small molecules such as the biogenic amines and certain amino acids or polypeptides, which are stored at high concentrations in synaptic vesicles. The arrival of a depolarizing signal at the axon terminal evokes an exocytotic process, by which synaptic vesicles fuse with the plasma membrane, releasing its contents into the synaptic cleft between the axon terminal and recipient neuron. Neurotransmitters then diffuse to the other side of the synaptic cleft, where they can bind to receptor proteins, which generally have a large specificity for a particular neurotransmitter. Receptors fall into two broad classes; ligand gated ion channels, which upon activation open a membrane spanning ion channel, and metabotropic receptors, which are linked to intracellular messenger pathways.

Individual synapses can be resolved by light microscopy, and in some detail through electron microscopy. However, autoradiographic procedures allow for indirect visualization of synapses. Here a radiolabeled compound is selected on the basis of its high affinity and selectivity for a receptor. We are then able to quantify the amount of radioactive compound, and thereby the amount of receptors. This method was first developed for *in vitro* determination of the abundance of binding sites in frozen brain sections. It was subsequently employed for detection of receptors in living human brain, either by positron emission tomography (PET) or single photon emission computed tomography (SPECT). The radiolabeled receptor ligands used in these techniques are called radioligands. Whereas the great majority of radioligands are antagonists, there has in recent years arisen a particular interest in developing agonist radioligands, which share the natural neurotransmitters ability to activate the signal of a receptor. This thesis deals with the evaluation of receptor agonist ligands, with application of *in vitro* principles for agonist radioligand development, and finally the testing and evaluation of novel agonist radioligands *ex vivo*.

The Dopaminergic & Serotonergic Transmitter Systems

There are three major dopaminergic brain pathways 1) The nigrostriatal pathway, which originates in the substantia nigra and projects into the striatum. 2) The mesocortical and mesolimbic pathway, which originates in the ventral tegmental area and projects to the frontal cortex, the cingulate gyrus and the striatum. 3) The tuberoinfundibular pathway, which descends from the arcuate nucleus to the pituitary. Serotonergic neurons mainly descend from the raphe nucleus and project throughout the brain, mainly to the cerebral cortex and hippocampus (Dahlström & Fuxe 1964, Fuxe et al. 1996).

Dopamine (DA) and serotonin (5-HT) are two types of neurotransmitters belonging to the class of biogenic amines. They are formed in specific neurons from their respective aromatic amino precursors. Dopamine originates from the amino acid tyrosine, which in the dopaminergic neurons is converted into L-DOPA (levodopa) by the enzyme tyrosine hydroxylase. L-DOPA is subsequently converted so rapidly to DA by aromatic amino acid decarboxylase that L-DOPA levels in the brain are negligible under normal conditions. Serotonin on the other hand originates from tryptophan which is slowly hydroxylated by tryptophan hydroxylase into 5-hydroxytryptophan (5-HTP). 5-HTP is then, in a manner similar to DA, converted into 5-HT by aromatic amino acid decarboxylase. After

synthesis, both DA or 5-HT are transported into synaptic vesicles, by the vesicular monoamine transporter (VMAT) and released into the synapse by calcium dependent exocytose (Langley and Grant, 1997, Olivier et al. 2000).

After release, DA and 5-HT are removed from the synapse by reuptake into the presynaptic terminal by the monoamine transporter's (DAT and SERT) and thereby reincorporated into vesicles by VMAT or metabolized by internal monoamine oxidase (MAO) (Olivier et al. 2000). Free synaptic DA is converted through sequential actions of catechol-O-methyltransferase (COMT) and external MAO, into 3-methoxytyramine and homovanillic acid (HVA) (Trouvin et al. 1986, Sjostrom et al. 1975). Free synaptic 5-HT is converted either by MAO into 5-hydroxy indole acetic acid (5-HIAA) or by sequential actions of 5-HT N-acetylase and 5-hydroxy indole O-methyl transferase into melatonin.

DA targets at least five known receptors, categorized into D₁-like (D₁ and D₅) and D₂-like (D₂, D₃ and D₄) receptors (Stoof and Keabian, 1984, Sunahara et al. 1990, Van Tol et al. 1991, Sokoloff et al. 1990). Serotonin targets an even more diverse range of receptors, at least 14 different. Each of these receptors has a different distribution in the brain, and is responsible for their own distinct intracellular response to DA and 5-HT binding, which mediate specific neurobiological functions. During the development of new agonist tracers, we have been focusing on four receptor subtypes, namely the D₁ and D₂ receptors, and the 5-HT_{1A} and 5-HT_{2A} receptors.

All four receptors share some biological features and can be considered as typical representatives of the superfamily of metabotropic receptors, also commonly called G-protein coupled receptors (GPCR), which are of universal importance for all biological signaling, not just in the nervous system. The metabotropic receptors are the largest group of cell surface proteins involved in signal transduction and represent a total of 1% of the human genome code. All members contain seven-transmembrane domains, build by seven α -helices crossing the cell membrane, each connected by cytoplasmic and extracellular loops (Hermans, 2003). They have an extracellular binding site for their respective neurotransmitter and ligands, and an intracellular coupling to a guanine nucleotide-binding protein (G-protein), which initiates further signaling.

The D₁ receptor is involved in different types of memory function (Williams et al. 1995; Arnsten et al. 1994; Seamans et al. 1998) and reduced expression has been implicated in the cognitive deficits of schizophrenic patients (Goldman-Rakic et al. 2004; Hirvonen et

al. 2006). D₁ receptors are mainly located postsynaptically in the regions of striatum, nucleus accumbens, olfactory tubercle, and substantia nigra, and are also expressed in the cerebral cortex. Agonism of D₁ receptors stimulates intracellular adenylate cyclase, mainly leading to elevated formation of cyclic adenosine monophosphate (cAMP). However, D₁ has also been found to stimulate phosphoinositol hydrolysis (Jaber et al. 1996).

D₂ receptors are the main site of action of DA antagonists used to alleviate certain symptoms of schizophrenia (Seeman et al. 2006) whereas DA agonism (either direct or indirect through L-DOPA therapy) is beneficial for the alleviation of motor symptoms of Parkinson's disease (Dentresangle et al. 1999). D₂ receptors are located in general in the same brain regions as D₁ receptors, but serve an additional autoreceptor function when expressed on presynaptic elements of DA neurons (Missale et al. 1998, Vallone et al. 2000). A variety of different signal have been described for the D₂-like receptors (Missale et al. 1998, Jaber et al. 1996). The most abundant is the inhibition of adenylate cyclase (De Camilli et al. 1979), but they also mediate changes in intracellular calcium and potassium levels (Lledo et al. 1990a, 1990b) and release arachidonic acid (Piomelli et al. 1991).

The 5-HT_{1A} receptors have been implicated in the pathophysiologies of mood (De Boer et al. 2005), sleep (Wilson et al. 2005), eating (Ebenezer et al. 2007a), schizophrenia (Goldman-Rakic et al. 2004), anxiety (Brunelli et al. 2009), and cognition (Borg 2008). At present, 5-HT_{1A} agonists are being evaluated as novel antipsychotic drugs with fewer side effects than the current market drugs, which can evoke extrapyramidal side effects due to substantial blockade of D₂ receptors (Kleven et al. 2005). 5-HT_{1A} receptors are mainly located in regions of cortex and hippocampus, and in the raphe nuclei where they serve an autoreceptor function controlling the activity of the serotonin neurons. Agonist stimulation of 5-HT_{1A} receptors can lead to diverse intracellular responses, depending on where they are located and the particular G-protein to which they are coupled. The known intracellular responses include inhibition of adenylate cyclase, opening of potassium channels and closing of calcium channels (Clawges et al. 1997, Lanfumey et al. 2004)

The 5-HT_{2A} receptors are implicated in pathophysiology of depression (Frøkjær et al. 2008, Abbas et al. 2008), Alzheimer's disease (Marner et al. 2010), obsessive compulsive

disorder (Adams 2005, Kim et al. 2009), and schizophrenia (Rasmussen 2010) and are thought to mediate the hallucinogenic effects of LSD (González-Maeso et al. 2007). The 5-HT_{2A} receptors are homogeneously distributed throughout the neocortex and to a lesser amount in the hippocampus. Agonist stimulation of 5-HT_{2A} receptors lead to intracellular signaling by several different pathways, again according to the particular G-protein to which they are coupled; phospholipase A2 (Kurrasch-Orbaugh et al. 2003a) and phospholipase C (Kurrasch-Orbaugh et al. 2003b) activation are two of the best described responses.

Dopamine and Serotonin GPCR affinity states

Monod and Changeux was the first to present a model for the interactions between ligands and enzyme binding sites (Monod et al. 1965). Since then, extensive *in vitro* research has been made on the existence of distinct affinity states of GPCRs with respect to their endogenous neurotransmitters and exogenous agonist ligands. Zahniser and Molinoff were the first to demonstrate the coupling of DA receptors with G-proteins (Zahniser et al. 1978). Subsequently, Sibley and Creese showed that DA D₂ receptors in membrane preparations exist in two binding states towards agonists; a high affinity state coupled to a G-protein, called D₂^{High}, and a low affinity state decoupled from a G-protein, called D₂^{Low} (Sibley et al. 1979, 1982). They found that competition between an antagonist and an antagonist radioligand was monophasic, consistent with a single binding site, and that competition between an agonist and an antagonist radioligand was biphasic, suggesting the existence of two affinity states for agonists. Similar results were later found for antagonist ligands of the D₁ receptor (Leff et al. 1985). The addition of guanine nucleotides to the incubation medium, which cause dissociation of the receptor-G-protein complex, induces complete conversion of D₂^{High} into D₂^{Low} (Richfield et al. 1986, 1989; Grigoriadis et al. 1985; Skinbjerg et al. 2009) and likewise conversion of D₁^{High} into D₁^{Low} (Farrell et al. 1994; Richfield et al. 1989; Sidhu et al. 1992).

Similar evidence of multiple agonist affinity states has been seen for 5-HT_{1A} and 5-HT_{2A} receptors. In particular, the 5-HT_{1A} agonists have a higher binding to 5-HT_{1A} receptors in membrane preparations in the absence of guanine nucleotides (Gozlan et al. 1995; Clawges et al. 1997). The saturation binding of the 5-HT_{1A} agonist [³H]8-OH-DPAT in brain homogenates is biphasic, supporting the existence of two binding sites. Conversion of 5-HT_{1A}^{High} sites to 5-HT_{1A}^{Low} by addition of guanine nucleotide to the incubation medium lowers the binding maximum (B_{max}) of [³H]8-OH-DPAT for the 5-HT_{1A}^{High} binding

component which concomitantly increases the B_{max} for the 5-HT_{1A}^{Low} component (Mongeau et al. 1992). The 5-HT_{2A} receptor also exists in two different affinity states towards agonists (Shi et al. 2007; Song et al. 2005), but new research extends the model with two affinity states to a more complicated ternary model, possibly applicable for other GPCR as well (Egan et al. 2000; Roth et al. 1997).

The Ternary Model of GPCRs

The two affinity states *in vitro* can be described in a model, which relies on the principles of allosterism first proposed by Monod for enzymes, and later extended to the case of acetylcholine GPCRs (Monod et al. 1965; Karlin 1967). The ternary model, as shown in figure 1, was proposed by De Lean as an explanation of the agonist-specific binding to β -adrenergic GPCRs (De Lean et al. 1980; Kenakin 2004; Leff 1995). The ternary model is simplified and does not describe the entire process of agonism at GPCRs. For example, it neglects the mechanistic complexities associated with the interaction between receptor and G-protein (Egan et al. 2000; Roth et al. 1997). This is potentially an issue in the case of the 5-HT_{2A} receptor, with which several G-proteins can interact, activating different second messenger systems (Kurrasch-Orbaugh et al. 2003a). The model also neglects quaternary structures such as dimerization of receptors (Brea et al. 2009) and the agonist induced internalization of receptors (Roth et al. 1998), which is well documented for the 5-HT and DA receptors. Nevertheless, the ternary model is useful, due to its simplicity, for making predictions of agonist (**A**) and receptor (**R**) binding, and the effects of environment (**L**).

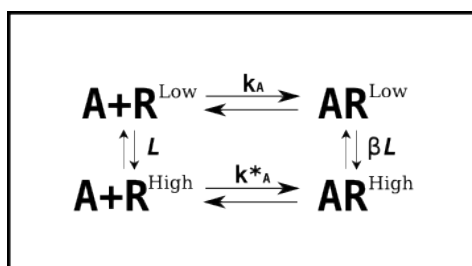


Figure 1: The ternary model for receptor-ligand, **A** and **R**, interactions. The dissociation equilibrium constants k and k^* describe the affinities of the ligand to the receptor in high R^{High} and low R^{Low} affinity states towards agonists, while the environment constant L describe the environmental effect on the ratio of R^{High} to R^{Low} .

The parameters in the ternary model can be described as follows (Leff 1995).

$$L = [R^{Low}]/[R^{High}] \quad (1)$$

$$k_A = [R^{Low}][A]/[AR^{Low}] \quad (2)$$

$$k^*_A = [R^{High}][A]/[AR^{High}] \quad (3)$$

The total amount of receptors ($\mathbf{R}_{\text{total}}$) in the four different states is given by

$$[\mathbf{R}_{\text{total}}] = [\mathbf{R}^{\text{Low}}] + [\mathbf{AR}^{\text{Low}}] + [\mathbf{R}^{\text{High}}] + [\mathbf{AR}^{\text{High}}] \quad (4)$$

A ligand binding in an antagonistic matter will have equal affinity towards \mathbf{R}^{High} and \mathbf{R}^{Low} ($\mathbf{k}_A = \mathbf{k}^*_A$), and an agonist will have higher affinity towards \mathbf{R}^{High} ($\mathbf{k}_A > \mathbf{k}^*_A$). On the other hand, inverse agonists, which oppose the constitutive activity of a receptor, will have higher affinity towards \mathbf{R}^{Low} ($\mathbf{k}_A < \mathbf{k}^*_A$). The affinity of full agonists will therefore be approximately equal to \mathbf{k}^*_A , whereas the affinity of a partial agonist will depend on both \mathbf{k}_A and \mathbf{k}^*_A .

In this model \mathbf{L} is the environment constant, describing changes in the environment leading to altered agonist affinities (**1**). For example, addition of guanine nucleotides evokes a higher concentration of \mathbf{R}^{Low} by changing the environment, thereby changing \mathbf{L} . An agonist in one tissue environment can consequently act as an antagonist in another tissue environment. Assessment of agonist properties in the right physiological environment is therefore very important.

On the basis of this model, several distinct paradigms can be proposed that must be true if the model has any relevance *in vivo*.

1. Saturation binding experiments with a full agonist radioligand should be best fitted with a two binding site model, whereas saturation binding experiments with an antagonist should be best fitted with a one binding site model.
2. Competition between a full agonist and an antagonist radioligand should be best fitted with a two binding site competition model.
3. Competition between a full agonist and an agonist radioligand should be best fitted with a one binding site competition model.
4. Competition between a full agonist and an agonist radioligand should be higher than between an agonist and an antagonist radioligand.

PET and Radioligands

PET is a non-invasive *in vivo* biomedical imaging technique used to monitor the distribution of radioligands in the living human or animal. Ligands of biological interest are labeled with short-lived positron emitting radionuclides, such as ^{11}C , ^{13}N , ^{15}O , ^{18}F or ^{68}Ga , enabling PET recordings to follow their uptake and distribution in the brain or other target organs. The methodology of PET will be described in the method section.

PET has found a number of uses in pharmacokinetic studies. Dynamic PET recordings can; 1) follow the administration, distribution and elimination of a radiolabeled drug, 2) monitor the distribution and quantify the amount of radioligand binding in a target organ, and 3) measure the effect of a pharmacological or cognitive stimulus on cellular or body physiology, as revealed by changes in radioligand kinetics (Hartvig et al. 2001; Syvänen 2008). Most importantly, PET can reveal pathophysiological changes. Among many possible examples of uses of PET, the cerebral uptake and distribution of [^{11}C]verapamil has been found to correlate with local activity of the efflux transporter P-glycoprotein residing in the blood-brain barrier (BBB) (Syvänen et al. 2009). The distribution of the novel 5-HT₄ receptor radioligand [^{11}C]SB207145 has been evaluated in pigs (Kornum et al. 2009) and humans (Marner et al. 2009). Also, radiolabeled water, [^{15}O]H₂O, has been used in numerous studies to map local brain activation under different cognitive and motor challenges (Bie-Olsen et al. 2009).

PET have emerged as an important tool for investigating the physiological basis of neuropsychiatric disorders such as mood disorders, Schizophrenia, Alzheimer's and Parkinson's diseases (Frøkjær et al. 2008; Guo et al. 2003; Dentresangle et al. 1999; Rabinovici et al. 2007), for pre-clinical neuropharmacological experiments, and for cutting costs in new drug development, where the occupancy of drugs at their receptor targets can be determined with fewer subjects, or indeed on an individual basis (Lee et al. 2006).

The brain receptor systems most widely investigated by PET include the D₁, D₂, 5-HT_{1A} and 5-HT_{2A} receptors. These four receptors have in the past 25 years been intensively investigated under neuropharmacological challenges, and in a wide variety of neuropsychiatric conditions, as well as in relation to normal function. The most widely used PET radioligands for human D₁ receptor brain imaging are [^{11}C]SCH 23390 (Farde et al. 1987; Halldin et al. 1998) and [^{11}C]NNC 112 (Halldin et al. 1998). Other, but less

widely used radioligands are [^{11}C]NNC 756 (Halldin et al. 1993; Laihinen et al. 1994), [^{11}C]A-69024 (Kassiou et al. 1995; Besret et al. 2008) and the ^{18}F -labeled compound (3-[^{18}F]-fluoropropyl)-SCH 38548 (Yang et al. 1996). All the above radioligands are antagonists and consequently should, in relation to the ternary receptor model, be expected to label both states of the D_1 receptors. A number of these radioligands suffer from incomplete selectivity to D_1 receptors, having also a $5\text{-HT}_{2\text{A}}$ binding component. Recently, a D_1 agonist has been developed, and methods developed for its analysis, for eventual applications in human PET studies (DaSilva et al. 1999; Paper II).

There are several well-characterized antagonist radioligands for imaging the human $\text{D}_{2/3}$ receptor; including the most used antagonist radioligand [^{11}C]raclopride, and also high affinity antagonists such as [^{18}F]fallypride, and [^{11}C]epidepride (Langer et al. 1999; Mukherjee et al. 2002; Farde et al. 1987). Recently, several suitable dopamine $\text{D}_{2/3}$ agonist radioligands have been developed; including the apomorphines [^{11}C]NPA (Hwang et al. 2000) and [^{11}C]MNPA (Finnema et al. 2005), and the naphthoxazine [^{11}C]PHNO (Wilson et al. 2005). Another agonist is the fluorinated tetralin analogue [^{18}F]5-OH-FPPAT (Shi et al. 2004).

Two antagonist radioligands have frequently been used to measure the $5\text{-HT}_{1\text{A}}$ receptor in human brain; [^{18}F]MPPF (Sanabria-Bohórquez et al. 2002) and [^{11}C]WAY 100635 (Oikonen et al. 2000; Gunn et al. 1998). Recently, a novel agonist [^{11}C]CUMI-101 has been developed and evaluated in baboon and rat (Kumar et al. 2007; Paper IV).

The $5\text{-HT}_{2\text{A}}$ antagonist PET ligands [^{18}F]altanserin (Sadzot et al. 1995) and [^{11}C]MDL100907 (Ito et al. 1998) have been characterized and found wide used in humans PET studies. A novel agonist PET radioligand [^{11}C]Cimbi-5 has recently been developed and characterized in rats and pigs (Paper V).

The Competition Model

The D_2 receptor has been the target of the preponderance of molecular imaging studies considering *in vivo* receptor affinity states. In the context of a competition model (Laruelle 2000), the magnitude of \mathbf{R}^{High} *in vivo* is calculated when the endogenous neurotransmitter DA competes with radioligands for binding to the D_2 receptor in living brain (figure 2).

Classical Occupancy Model

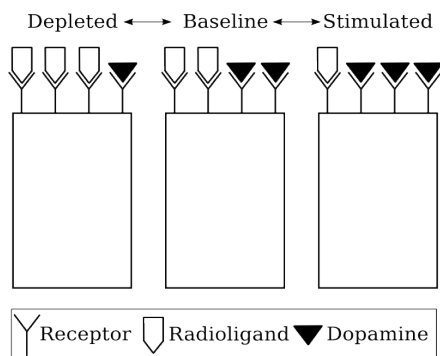


Figure 2: The classical *in vivo* occupancy model show the binding of a radioligand in competition with endogenous neurotransmitter. Depletion of dopamine will increase radioligand binding, while release of dopamine will decrease radioligand binding.

Many competition experiments have been carried out before and under condition of amphetamine-evoked DA release (Kahlig et al. 2005). For example, reduced binding of D_2 antagonist radioligands following a amphetamine challenge has been reported in rats (Pedersen et al. 2007), pigs (Lind et al. 2005), non-human primates (Mukherjee et al. 2005; Narendran et al. 2005) and humans (Laruelle et al. 1995, 1997; Breier et al. 1997). DA is the endogenous agonist for these receptors; and in accordance with the ternary model, DA is expected to have a higher affinity for D_2^{High} , and exert little competition against the proportion of radiolabeled antagonist binding to the D_2^{Low} state of the D_2 receptor. In PET studies with amphetamine-evoked dopamine release cited above, no more than 38% displacement of radiolabeled antagonist has been observed *in vivo*, a phenomenon known as the ceiling effect (Laruelle 2000). This displacement is assumed to represent the fraction of receptors in high affinity state and thereby the fraction of receptors vulnerable to competition from released DA (figure 3).

Based on the assumption that agonists should compete with agonists in a manner described by a single-site binding model, it would follow that agonist radioligand would be inherently more vulnerable to competition from DA than antagonist radioligands, as mentioned in paradigm 4 above. In support of this conjecture, a dual tracer *ex vivo* study in awake mice revealed that the binding of the $D_{2/3}$ DA receptor agonist [^3H]NPA was 60% more vulnerable to amphetamine challenge than [^{11}C]raclopride (Cumming et al. 2002), a finding which was essential replicated in PET study of non-human primates using the agonists [^{11}C]MNPA (Seneca et al. 2006) or [^{11}C]NPA (Narendran et al. 2005).

Of course, some DA is present in the interstitial fluid, even without amphetamine-evoked DA release. This baseline presence of DA results in a certain tonic occupancy at D_2

binding sites. Pharmacological treatments lowering the baseline level of DA, should increase the binding of radioligands. Since DA favors the D_2^{High} sites, a proportionally larger binding increase would be expected for an agonist radioligand than for an antagonist radioligand in the condition of DA depletion. Treatment with reserpine and/or alpha-methyl-*para*-tyrosine (α -MPT) evokes a substantial loss of brain DA. This treatment preferentially increased the binding of the agonist ligand [^{11}C]NPA in an *ex vivo* mouse study (Cumming et al. 2002), and likewise evoke higher increases in PET studies with the agonists [^{11}C]NPA and [^{11}C]MNPA, as much as 50% above baseline (Ginovart et al. 2006; Seneca et al. 2006). Whereas relatively moderate increases in the binding of [^{11}C]raclopride in human striatum have been reported (Martinez et al. 2009; Paper III), in line with the proposed competition model.

However, despite it being general accepted, the competition model fails to account for several relevant phenomena. In particular, the *in vivo* displacement of the $D_{2/3}$ antagonist, [^{11}C]raclopride, from striatum in non-human primate by escalating doses of the $D_{2/3}$ agonist PD 128907 was monophasic and complete, corresponding to an one-site binding model (Kortekaas et al. 2004), rather than the biphasic displacement which might have been expected if there were separate populations of D_2^{High} and D_2^{Low} . Furthermore, in a subsequent *ex vivo* dual tracer study, the displacement of the agonist [^{11}C]PHNO and the antagonist [^3H]raclopride were both monophasic and indistinguishable in rat (McCormick et al. 2008). These findings call into question the claim that distinct \mathbf{R}^{High} and \mathbf{R}^{Low} populations of DA receptors exist *in vivo*. The consequences of this objection will be covered in more detail in the discussion section.

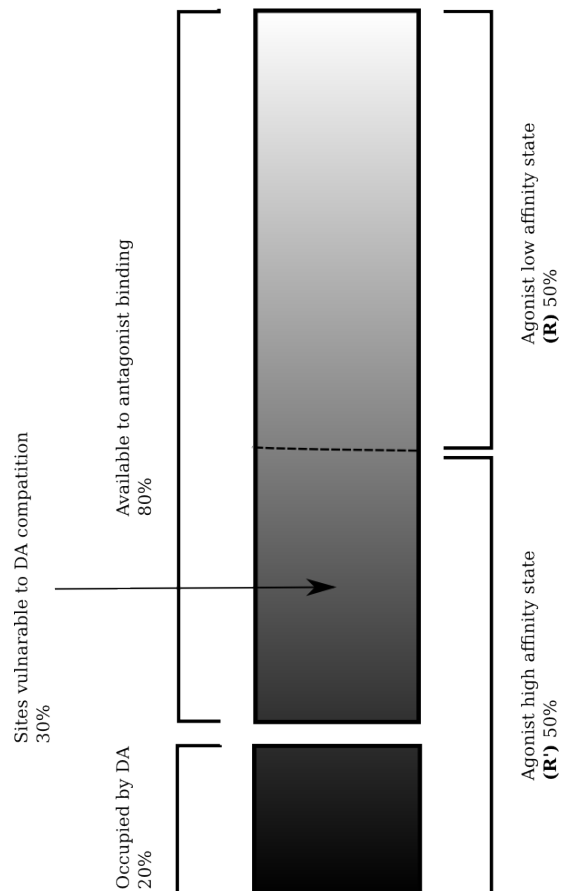


Figure 3: The receptor model based on the classical occupancy model above, as proposed by Laruelle, 2000. The binding components of the D_2 receptor are divided into high affinity state and low affinity state, the dopamine baseline occupancy is 20%, leaving only 80% for antagonist binding and 30% for agonist binding. The component of sites vulnerable to DA competition following release is estimated to 30%.

Agonist Radioligand Development

As noted above, a wide variety of antagonist radioligands for PET studies of the four receptors considered in this thesis are available already. While these radioligands are of proven utility for determining the total amount of receptors, they are not so suitable for determining changes in the environment (L) leading to changes in the fraction of R^{High} to R^{Low} receptors. The possibility of measuring specifically the R^{High} receptors would present a great contribution to the understanding of the brain. Based on measurements of the ratio between R^{High} and R^{Low} *in vitro* it has been found that the D_2^{High} fraction is increased in animal models of schizophrenia (Seeman et al. 2006; Sumiyoshi et al. 2005). The fraction of $5\text{-HT}_{2A}^{\text{High}}$ is lower in 5-HT_{2A} agonist treated animals, in spite of an increase in the total amount of receptors (Shi et al. 2008). And rats treated with cocaine show increased $5\text{-HT}_{2A}^{\text{High}}$ binding with autoradiography (Carrasco et al. 2006) and increased D_2^{High} binding in membranes (Briand et al. 2008).

Until recently, development of new PET radioligands has been focusing on antagonists, and only a handful of agonists are available for human use, mostly for the $D_{2/3}$ receptor as described above. Thus, a agonist ligand promise to selectively map receptors in their functional state, and therefore alterations in agonist binding measured *in vivo* with PET may be more relevant for assessing dysfunction in the monoaminergic receptor systems in specific patient or population groups. Furthermore, combining measurements with antagonist and agonist PET tracers would enable determination of the ratio of the R^{High} to the R^{Low} . Agonist PET tracers may also be better suited for measuring endogenous competition compared to antagonist tracers.

New agonists must meet a number of requirements (Sermons et al. 2009) in order to show usefulness for PET scanning.

- While routes to radiosynthesis of a new agonist radioligand may be theoretically possible, in practice there is a requirement for a fast and reliable procedure using only milligrams of starting material.
- The radioligand must be chemically stable and eventual radiolabeled metabolites must not interfere with the signal in the brain.

- The radioligand must be sufficiently lipophilic to pass across the blood-brain barrier, while being sufficiently hydrophilic to avoid excessive non-displaceable binding, which will lower the signal to background ration.
- In general, a good radioligand should not be a substrate for the p-glycoprotein efflux transporter and related processes.
- The pharmacological selectivity of the radioligand must be known, so that it can be certain what receptors are labeled *in vivo*.
- The affinity and kinetics of the radioligand has to suit the molecular target and the half-life of the nuclide, for example; a high affinity binding ligand with a slow dissociation from its receptor would be a poor ^{11}C radioligand, but might work with ^{18}F .

Specific traits regarding development of agonist radioligands

- The efficacy of the agonist radioligand must be tested *in vitro* and *in vivo* in order to insure agonistic properties.
- Demonstrable competition from the endogenous agonist *in vivo* would be a useful property.

Aims and Delineation of the Problem

The major aims of this thesis are:

- To evaluate a series of novel radiolabeled agonists as possible PET radioligands .
- To evaluate the susceptibility of these radioligands to changes in endogenous neurotransmitter.

This work describes evaluation of five different agonist radioligands; [¹¹C]SKF 82957 for the D₁ receptor, [¹¹C]-2Cl-NPA, [¹¹C]NPA and [³H]NPA for the D₂ receptor, [¹¹C]CUMI-101 for the 5-HT_{1A} receptor, and [¹¹C]Cimbi-5 for the 5-HT_{2A} receptor.

Methodological Considerations

As with pharmaceutical development, the project of developing a novel radioligand can begin with hundreds of possible candidates, and rarely ends in success. We started this project with a pipeline designed to eliminate unsuitable candidates before proceeding to *in vivo* PET imaging.

Properties of Agonist Radioligands

If a radioligand binds to multiple receptors in the same regions, it will be difficult to allocate the PET signal to individual receptor types. A good PET radioligand will have a nanomolar affinity to its main receptor, and in general 10-100 fold lower affinity for the next most abundant receptor that it recognizes. Some receptors are pharmacologically so similar as to make the task of obtaining a complete selective ligand almost impossible; in the case of D_{2/3} receptors, only a 10-fold selectivity for D₃ is afforded by [¹¹C]PHNO. This holds true also for 5-HT_{2A} and 5-HT_{2C} receptors, which have yet to be distinguished by selective ligands. A PET signal measured from radioligands binding to several subtypes will therefore be a combination of binding to each receptor. In the case of D_{2/3} receptors, D₂ sites are relatively more abundant in the dorsal striatum, whereas D₃ sites are mostly in nucleus accumbens. However, this anatomic segregation is incomplete, and the need for full selectivity is the rationale for paper I. In the case with 5-HT_{2A} and 5-HT_{2C} receptors, specificity is less of a problem, since 5-HT_{2A} receptors are most abundant in frontal cortex and hippocampus, where the 5-HT_{2C} receptors contribute only a tiny fraction of the PET signal in these brain areas. However, 5-HT_{2C} receptors are abundant in the choroid plexus, which may thus contaminate the PET signal in adjacent brain areas. In the case of the novel 5-HT_{1A} agonist [³H]CUMI-101, an additional binding component to the alpha₁ adrenoreceptor occurs in rat, but this is not the case in baboon brain. It is therefore essential that the binding of a new ligand be tested against batteries of cloned human receptors and not only cloned rat receptors.

An agonist is, by definition, an agent which induces a response after binding to its receptor. Therefore, a formal requirement is that a post-synaptic response can be measured not only in cell lines, but also *in vivo*.

Quantitative Methods for Studying the Uptake and Distribution

Radionuclide Decay and Detection

A radioligand contains a radioactive isotope in its chemical structure. A radioactive isotope contains a physically unstable atomic nucleus, which spontaneously decays with the release of daughter isotopes, and other particles. There are three main types of radiation arising from radioactive decay; α -radiation consists of helium nuclide, β -radiation consists of electrons (β^-) or positrons (β^+), and γ -radiation, which is electromagnetic radiation in the form of high energy photons. Nuclear decay is a stochastic process, such that it is impossible to predict when a given atom will decay, but given a large number of similar atoms the average decay rate is predictable. In the context of radioactive decay, the half-life ($t_{1/2}$) is the time which it takes for one half of the original mass to decay. The magnitude of a given isotopic half-life can be determined experimentally with considerable precision.

Henri Becquerel was the first to describe the phenomenon of radioactive decay, for which his memory is honored through the use of his name as the SI-unit for radioactivity; one Becquerel is equal to one radioactive decay per second. Another unit used by many medical doctors, especially in the English speaking world, is the Curie (Ci), equal to the decay rate of 3.7×10^{10} Bq. The radionuclide decay of Carbon-11 and the subsequent detection with PET is explained in figure 5.

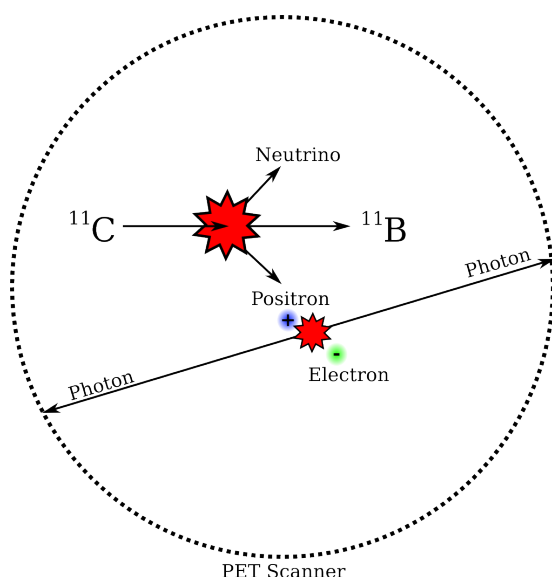


Figure 5: Decay of ^{11}C to ^{11}B is due to a conversion of a proton into a neutron, stabilizing the nucleus, and with elimination of a positron β^+ and a neutrino from the core. The positron can travel up to 5 mm through tissue before it collides with an electron. The positron-electron annihilation produces two 512 keV photons, which are emitted at an 180 degree angle; these photons travel out of the body and are detected by the PET scanner, which estimates the line of annihilation. The PET scanner will never be more precise than the average length the positron travels before annihilation.

Due to the short half-life of common positron emitters other longer-lived isotopes are some times used in the evaluation of radioligands. The two most-used isotopes in radioligand development are Iodine-125, a γ -emitter with an energy of 35.5 keV and a half-life of approximately 60 days, and Tritium, a β -emitter with an energy of 18.6 keV (of which 5.7 keV is imparted to the electron as kinetic energy), and a half-life of approximately 12 years. Both of these isotopes have a relative low energy, reducing the need for radioactive protection from external sources (although they are both toxic if ingested). However, these energies disfavor *in vivo* detection, such that they are suited for evaluation of ligands *ex vivo* and *in vitro*. The half-lives are such that the researcher need not rely on the daily production of radioligand, making the full evaluation cheaper and the experiments easier to schedule. Chemical methods exist for incorporation of both isotopes into a wide variety of organic compounds.

Positron Emission Tomography

The half-life of common PET radionuclides is relatively short: ^{15}O ($t_{1/2} = 2$ min), ^{11}C ($t_{1/2} = 20$ min), ^{18}F ($t_{1/2} = 109$ min) and ^{68}Ga ($t_{1/2} = 68$ min). This property imparts advantages and disadvantages (Antoni et al. 2008). The site of production of the radionuclides and the laboratory for synthesis of a radioligand must be in close proximity to the PET scanner, the chemical synthesis must be fast, usually within one or two half-lives, and the administration of radioligand to the subject must be performed shortly after radiosynthesis. This leaves little time for formulation and quality control of the radioligand. Therefore, it is usual for a functional PET research facility to have not only a PET scanner, but also a cyclotron, a radiochemistry laboratory and a quality control laboratory, an expense many places cannot afford. However, the short half-life is a benefit in research as it allows repeated examination of single subjects, and minimizes the dosimetry experienced by the subject.

A dynamic PET scanning gives the definitive view of the kinetics of the radioligand, with the radioactivity concentration in a given region as a function of time. Mathematical models can be applied to describe the kinetics of different ligands, from which the magnitudes of uptake and binding constants can be derived, as described in some detail below. However, a main limitation with PET is the low number of subjects who can be scanned after each production; research studies usually entail only one or two scans. Another limitation is the use of anesthesia in animal studies, this adds confounding factors related to the pharmacological effects of anesthesia.

Quantifying PET Data

Quantification of PET data relies on equations and models first derived for *in vitro* binding. The Michaelis-Menten equation can be used to quantify ligand binding (5), where the specifically bound concentration **B** is related to the free concentration of radioligand **F**, the maximal number of receptors **B_{max}**, and the equilibrium dissociation rate constant of radioligand **K_D** at equilibrium (Mintun et al. 1984).

$$\mathbf{B} = \mathbf{B}_{max} * \mathbf{F} / (\mathbf{K}_D + \mathbf{F}) \quad (5)$$

When a radioligand is administered in tracer dose (**F** << **K_D**) then **F** becomes negligible in relation to **K** and the equation can be reduced to 6.

$$\mathbf{B} = \mathbf{B}_{max} * \mathbf{F} / (\mathbf{K}_D) \quad (6)$$

The equation can be rearranged to the ratio of **B** over **F**, which is termed the binding potential **BP**.

$$\mathbf{BP} = \mathbf{B} / \mathbf{F} = \mathbf{B}_{max} / (\mathbf{K}_D) \quad (7)$$

The distribution in brain of a PET radioligand as a function of time after injection can be described by e.g. a two tissue compartmental model (figure 6). The compartments include the radioligand in the arterial plasma **C_P**, a non-displaceable binding compartment **C_{ND}** (which is composed of a non-specific bound **C_{NS}** and a free radioligand concentration in tissue water **C_{FT}**) and a specific binding compartment **C_S**. The rate constants describing the radioligand uptake and binding consist of **K₁**, the unidirectional blood-brain clearance with units of blood flow **k₂**, the fractional rate constant for washout from brain and **k₃** and **k₄**, the reversible association of the radioligand with its receptors.

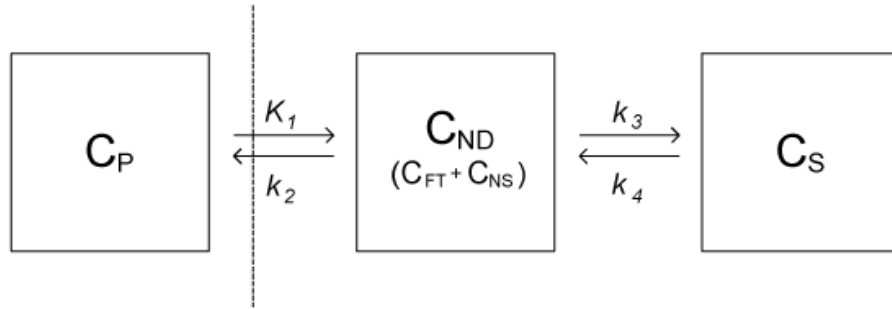


Figure 6: A two-tissue compartment model describing the distribution of radioligand in the brain at equilibrium. The compartments include the radioligand in the arterial plasma C_P , a non-displaceable binding compartment C_{ND} (which is composed of a non-specific bound C_{NS} and a free radioligand concentration in tissue water C_{FT}) and a specific binding compartment C_S . The rate constants describing the radioligand uptake and binding consist of K_1 , the unidirectional blood-brain clearance with units of blood flow k_2 , the fractional rate constant for washout from brain and k_3 and k_4 , the reversible association of the radioligand with its receptors.

PET measures a concentration of radioligand within a given volume of tissue. The volume of distribution of each compartment can be described as the ratio at equilibrium of the radioligand concentration in the compartment to that of the parent radioligand concentration in plasma, as follows in equation 8 for the non-displaceable compartment V_{ND} . V_S and V_{ND} can be determined in different ways. For example, by use of an area in the brain devoid of radioligand binding sites. This area will contain a mix of V_{FT} and V_{NS} and can thereby be used as an estimate of the V_{ND} . An area with radioligand binding can then be described as a mix of V_S and V_{ND} termed V_T (9).

$$V_{ND} = C_{ND} / C_P \quad (8)$$

$$V_T = V_S + V_{ND} \quad (9)$$

If it is assumed that V_{ND} equal the free amount of radioligand concentration in brain F , and that V_S equals the specifically bound radiotracer B , we can rearrange the equation 7 to be described by different volumes of distribution 10, this is called the non-displaceable binding potential and termed BP_{ND} .

$$BP_{ND} = B/F = V_T - V_{ND}/V_{ND} \quad (10)$$

Binding potentials of PET tracers can be expressed in other ways, but BP_{ND} has the most importance for the *ex vivo* calculations in this thesis. For a full review of PET quantification see (Innis et al. 2007)

Ex Vivo Experiments

An alternative to animal PET is *ex vivo* studies, where multiple rats are injected with a radiotracer and terminated at a certain time-point followed by quick removal of the brain for further analysis. This gives a single data point for each animal, in contrast to the dynamic time series within individuals that is afforded by PET. However, the *ex vivo* approach can reveal population-based estimates of the dynamic process, if individual animals are killed at different time points. *Ex vivo* methods have a big advantage over animal PET in that anesthesia is not required; the rat or mouse is free to move around in the interval between radioligand injection and time of decapitation. A drawback is that individual animals cannot serve as their own baseline or control, if the experiments require removal of the brain. This limitation tends to introduce variability, thus reducing the sensitivity of *ex vivo* experiments.

In the case of the D₂ agonist [¹¹C]-2Cl-NPA and the D₁ agonist [¹¹C]SKF 82957, around 30 awake rats were used for each radioligand production. This approach yielded a huge amount of data, with triplicate determination of ten treatment groups from a single radioligand production. In analogous studies with longer lived isotopes, as in the studies with [³H]CUMI-101, it was possible singlehandedly to study 12 rats in a single experiment day. In comparison, PET scanning can only provide a few scans from each production of radiotracer.

Quantification of *ex vivo* experiments is generally simpler than the full compartmental analysis of a dynamic PET scan. The radioactivity in the region of interest (ROI) at a single time point is divided by the injected radioactivity and adjusted for rat- and tissue sample weight, giving units of Standardized Uptake Value, **SUV**.

$$\mathbf{SUV = (Activity\ in\ ROI/weight\ of\ ROI)/(Activity\ injected/weight\ of\ animal)\ (11)}$$

As with PET, the occurrence of a reference brain region with negligible specific binding region is optimal for quantification of *ex vivo* experiments. In *ex vivo* experiments we measure the exact compartment concentration, and can therefore rewrite the non-displaceable binding potential equation **10** using the definition of volumes of distribution from equation **8** giving the equation **12**. The plasma concentration can be taken out of

the equation and we are left with the specific binding ratio **SBR** defined as in the equation **13**.

$$\mathbf{BP_{ND}} = (\mathbf{C_T/C_P} - \mathbf{C_{ND}/C_P})/(\mathbf{C_{ND}/C_P}) = (\mathbf{C_T} - \mathbf{C_{ND}})\mathbf{C_P}/\mathbf{C_{ND}C_P} \quad \mathbf{(12)}$$

$$\mathbf{SBR} = \mathbf{BP_{ND}} = (\mathbf{C_T} - \mathbf{C_{ND}})/\mathbf{C_{ND}} \quad \mathbf{(13)}$$

These *ex vivo* calculations are valid at equilibrium; as this is not generally the case, calculations of **SBR** in *ex vivo* studies must be interpreted with this caveat.

Ex Vivo Autoradiography

Having the option of using a longer half-life isotope, it is convenient to combine the *ex vivo* experiment with an autoradiographic experiment. After the brain has been extracted, it must be frozen quickly and then cut into thin sections, dehydrated, and then exposed to a sensitive imaging plate or X-ray film, which ultimately yields a very high resolution image of the radioligand distribution at the time of death. In principle, this procedure is also possible with [¹⁸F]-radioligands and in some cases with [¹¹C]-radioligands as described by (Bergström et al. 2003), but time is crucial. It is generally easier to conduct *in vitro* autoradiography with short-lived isotopes, but this too can be a challenge.

Metabolism of Radioligands

One major limitation with PET and *ex vivo* experiments is non-specific binding; as PET only traces the radioactivity, a false signal can arise when the radioligand is metabolized in the living organism. For example, metabolism of [¹¹C]SKF 82957 generates a lipophilic metabolite, which crosses the blood-brain barrier, ultimately making up 50-60% of the brain signal, rather than the intended parent compound (DaSilva et al. 2003, Paper II). The lipophilic metabolite is most likely the result of a methylation of one of the phenol groups by the enzyme COMT, as has been described for [¹⁸F]fluorodopa (Boyes et al. 1986) and other related catechols (Männistö et al. 1999). The examination of these radiometabolites can be carried out *ex vivo*, by injecting a high dose of radioligand, and following up with high performance liquid chromatography (HPLC) analysis of the brain and plasma extracts, as in papers I and II.

Binding Competition

The competition model and the ternary receptor model predict that agonist radioligands should be better suited to measure competition from other agonists, including the endogenous neurotransmitters. There are three main methods to test this; direct challenge, where pharmacological treatments compete directly for the receptor binding; indirect challenge, where endogenous neurotransmitter is released by a drug or stimulus; and depletion, where the endogenous neurotransmitter is removed by a drug or lesion.

Direct Competition

A typical direct challenge would be pharmacological treatment with different doses of a well-characterized agonist. For example, intravenous treatment with 8-OH-DPAT, a 5-HT_{1A} agonist, five minutes previous to the injection of [³H]CUMI-101, as reported in paper V. If the radioligand is a selective and full agonist, the treatment should evoke a competition curve as a function of dose, which should be monophasic, reflecting a single binding state.

Endogenous Competition - Release

The interstitial concentrations of DA and 5-HT in the brain can be increased by various drugs. The two biogenic amines have several similarities with respect to mechanisms of synthesis, metabolism, release, and re-uptake. Selective serotonin reuptake inhibitors (SSRIs) such as citalopram are medically used as antidepressants, by virtue of their blockade of the serotonin reuptake transporter (SERT) in the plasma membrane, which increases the amount of interstitial serotonin, as in paper IV. This same principle is behind the DA increase evoked by RTI-32 (a potent cocaine analogue), as in paper II, where RTI-32 is a selective blocker of the dopamine reuptake transporter (DAT) (Stathis et al. 1995), see figure 7. Microdialysis studies have shown increased levels of interstitial 5-HT after acute treatment with citalopram, attaining peak increases of as much as 200-400% above basal levels at 40 minutes after administration, and remaining elevated for hours thereafter (Mørk et al. 2003; Huang et al. 2006; Ceglia et al. 2004). Likewise, interstitial levels of DA have been shown to increase by up to 600% above basal levels after blockade of DAT by cocaine or its analogues, peaking almost

immediately, and remaining elevated for up to 1.5 hours (Church et al. 1987; Hurd et al. 1989).

DA and 5-HT can also be released by reversing the uptake transporter and enhancing exocytosis of neurotransmitter vesicles. Fenfluramine and amphetamine are both such releasers, working mostly at SERT or DAT respectively, as in papers II and IV. The increase in interstitial 5-HT levels after acute treatment with fenfluramine is around 500-900% above basal levels, peaking at 30-40 minutes, and remaining elevated for several hours (Laferrere et al. 1989; Rocher et al. 2001). The DA increase in striatum after acute amphetamine treatment is also higher than with cocaine analogues, reaching peak levels of 700-1000% above basal level, staying elevated for several hours (Hurd et al. 1989; Sharp et al. 1987).

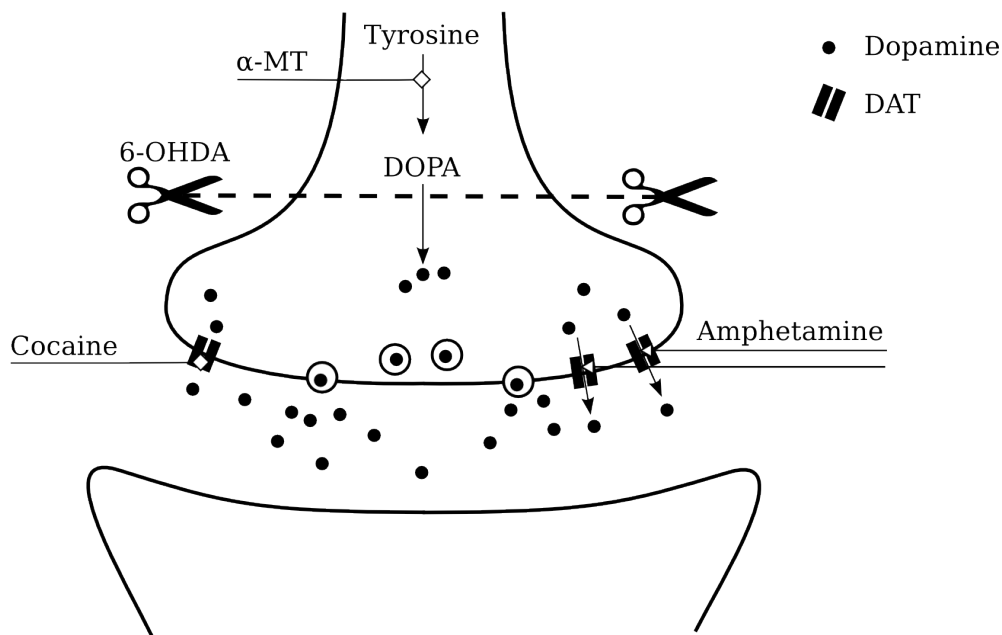


Figure 7: Sites of action for DA level increases, cocaine and amphetamine, as well as sites of action for DA level depleters, 6-OHDA and α -MT.

Endogenous Competition - Depletion

DA and 5-HT tonically occupy a fraction of their receptors; this baseline level of binding can be reduced by lowering the amount of released neurotransmitter. As with release, the pathways for synthesis are similar for the two neurotransmitters. Treatments with specific inhibitors of the enzymes synthesizing either DA or 5-HT results in

neurotransmitter depletion, and consequently decrease of the baseline occupancy. In particular, treatment with the tyrosine hydroxylase inhibitor alpha-methyl-*para*-tyrosine (α -MT) reduces the level of catecholamines (DA and noradrenaline) by 30-40% or more (Rech et al. 1968; McTavish et al. 1999). Similarly, treatment with the tryptophan hydroxylase inhibitor *para*-chloro-*D,L*-phenylalanine (pCPA) decreases the brain levels of interstitial 5-HT by 30-50% at 24 hours (Kornum et al. 2006; Steigrad et al. 1978; Datla et al. 1996). Another way to reduce the baseline level of a neurotransmitter is to destroy the projecting neurons or synaptic terminals, which leaves the postsynaptic receptors in a state of denervation. For example, the infusion of the toxin 6-OHDA to the medial forebrain bundle retrogradely destroys the dopaminergic neurons projecting to the striatum, resulting in nearly complete depletion of brain DA, paper III. This method has been extensively used to model Parkinson's disease in animals, and the relationship between depletion and behavioral impairment has been correlated (Casteels et al. 2008; Ishibashi et al. 2010). In general, DA depletions/lesions result in increased abundance of binding sites for dopamine $D_{2/3}$ -like receptor antagonists. Indeed molecular imaging has revealed a 40% increase in [^{11}C]raclopride binding in striatum of untreated patients with Parkinson's disease (Dentresangle et al. 1999).

Results & Discussion

After some work with our original pipeline it was necessary to revise it, as even good ligands *in vitro* could fail *in vivo*, as [¹¹C]2-Cl-NPA failed in paper I. We adopted the new pipeline with [¹¹C]Cimbi-5, first testing the novel agonist *in vivo* and afterwards conducting the full characterization *in vitro*. This pipeline works best if there is evidence that the chosen compound already have some of the characteristics of a good receptor ligand.

Chemical Properties of Agonist Radioligands

All the novel radioligands described in this thesis were assessed for their selectivity, either by extensive *in vitro* binding experiments or by *in vivo* blocking with well characterized ligands. For example; the *in vitro* validation showed that [¹¹C]2-Cl-NPA was slightly more selective for D₂ over D₃ than was [¹¹C]NPA. We also found [¹¹C]SKF 82547 to be highly selective for the D₁ receptor by blocking the binding with a selective antagonist SCH 23390. Following the same approach, we found that [³H]CUMI-101 bound to more than one binding site, because WAY 100635 was unable to completely block the specific binding in the striatum, this second binding site is presumably alpha₁ receptors. The *in vitro* binding properties of each radioligand is presented in table 1.

Table 1: *In vitro* binding properties (k_i values) of the radioligands used in this thesis

Radioligand	D ₁	D ₂	D ₃	5-HT _{1A}	5-HT _{2A}
[¹¹ C]NPA	-	0.12 nM	0.21 nM	-	-
[¹¹ C]2-Cl-NPA	-	4.52 nM	17.26 nM	-	-
[¹¹ C]SKF 82547	0.9 nM	-	-	-	-
[³ H]CUMI-101	>10,000 nM	>10,000 nM	>10,000 nM	0.15 nM	4980 nM
[¹¹ C]Cimbi-5	3718 nM	1600 nM	117 nM	85 nM	2.2 nM

Studying the Uptake and Distribution of Radioligands

PET is superior to *ex vivo* experiments with regard to continuous measurement of brain uptake as function of time (time activity curve, TAC) in the same animal. However, *ex vivo* experiments have the advantage of not requiring anesthesia, and also enables

investigation of a large number of animals per radioligand production. The papers included in this thesis presents *ex vivo* TACs for several of the novel agonists radioligands; [^{11}C]2-Cl-NPA and [^{11}C]NPA in paper I, [^3H]CUMI-101 in paper IV and [^{11}C]Cimbi-5 in paper V.

In paper 1, rat brain *ex vivo* TACs of the new $D_{2/3}$ agonist [^{11}C]2-Cl-NPA were compared with those of the well-established radioligand [^{11}C]NPA (figure 9). We found that [^{11}C]2-Cl-NPA had a lower SBR and a slower brain accumulation in rats than both [^{11}C]NPA and [^{11}C]PHNO. [^{11}C]PHNO has been reported to have even faster uptake and higher SBR than [^{11}C]NPA (Wilson et al. 2005). The SBR we measured *ex vivo* for [^{11}C]NPA in rats was similar to the PET-based SBR previously reported in baboons (Hwang et al. 2000).

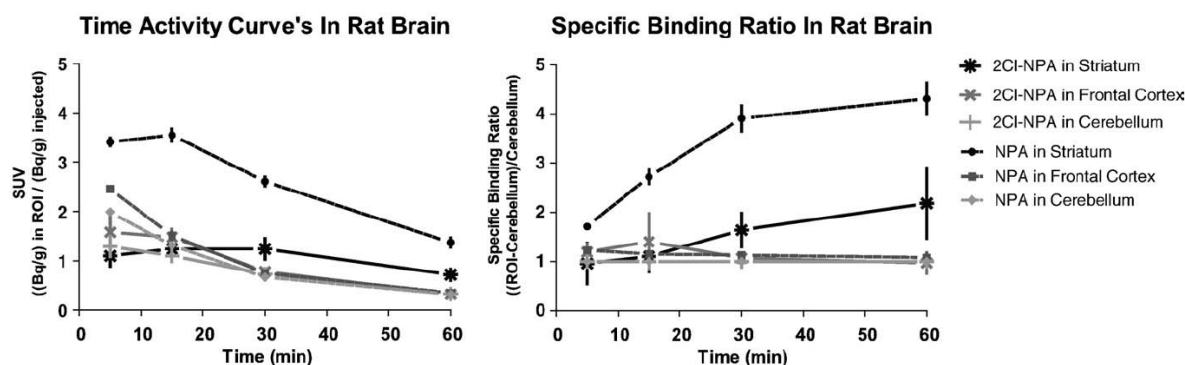


Figure 9: *Ex vivo* time activity curves (TAC) in regions of interest (ROI) of 2-Cl-[^{11}C]-(-)-NPA and [^{11}C]-(-)-NPA in awake rats. Left: Standardized Uptake Value (SUV) as a function of time. Right: Specific Binding Ratio (SBR) as a function of time. Data are shown as mean \pm SEM.

Furthermore, we evaluated the *ex vivo* TACs and SBR of the agonist [^3H]CUMI-101 in rats (figure 10, paper IV), and compared it to published results of [^{11}C]WAY 100635 (Hume et al. 1994) and [^{11}C]MPPF (Plenevaux et al. 2000), two widely used 5-HT $_{1A}$ receptor antagonist. By a direct comparison at 90 minutes we found the uptake of [^3H]CUMI-101 to be much higher than for [^3H]MPPF. [^3H]MPPF is known to be a substrate for the p-glycoprotein transporter, which greatly hinders the brain uptake of radioligands (Elsinga et al., 2005).

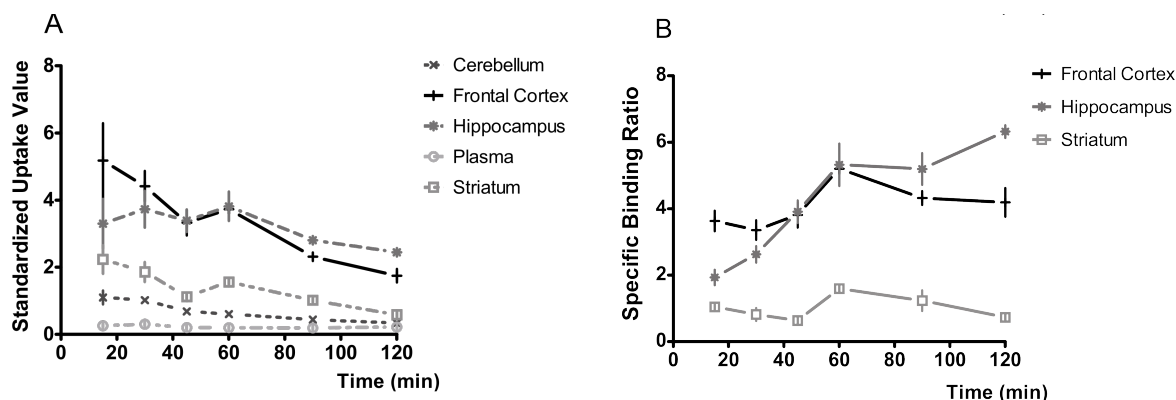


Figure 10: *Ex vivo* time activity curves (TAC) in regions of interest (ROI) of [3H]CUMI-101 in awake rats. A: Standardized Uptake Value (SUV) as a function of time. B: Specific Binding Ratio (SBR) as a function of time. Data are shown as mean \pm SEM.

Metabolism of Radioligands

The plasma metabolites were measured for several radioligands [11C]2Cl-NPA (paper I), [11C]SKF 82957 (paper II) and [11C]Cimbi-5 (paper V). The brain metabolites of [11C]SKF 82957 (paper II). Metabolites can be a huge problem in PET scanning, as explained in the methodological considerations.

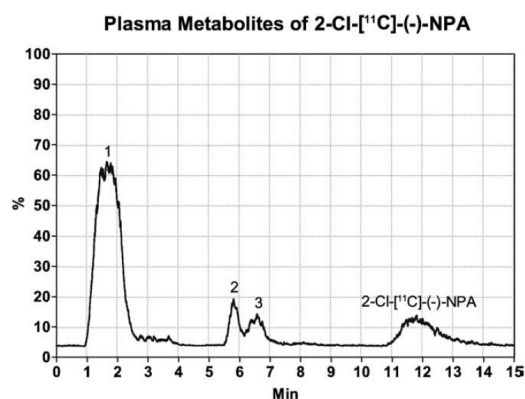


Figure 11: A representative HPLC chromatogram of plasma from a 2-Cl-[11C]-(-)-NPA-injected rat, 15 min after injection. At least three radiolabelled metabolites and the parent compound can be identified in the chromatogram.

In paper 1, [11C]2-Cl-NPA was quickly metabolized in rat, only 17% parent compound remained in plasma after 15 minutes (figure 11). At least three hydrophilic metabolites but no lipophilic metabolites were identified by HPLC analysis of plasma extracts. A very rapid metabolism can cause the radioligand to fail as a tracer, because brain uptake is limited and quantification difficult. Rapid metabolism could partly account for the lower SBR of [11C]2-Cl-NPA in comparison to [11C]NPA.

In paper II, we confirmed a prior report finding that metabolism of [11C]SKF 82957 result in a radiolabeled lipophilic metabolite in rat brain (DaSilva et al. 2003). The lipophilic metabolite accounted for 62% of the total radioactivity in the brain, at 30 min after

injection of [^{11}C]SKF 82957 (figure 12). We hypothesized that inhibition of COMT could lower the interference from the lipophilic metabolite, as it has before been demonstrated for [^{18}F]FDOPA using the first generation COMT inhibitor U-0521 (Cumming et al., 1987). As hypothesized, systemic administration of the COMT inhibitor tolcapone evoked a dose-dependent reduction of lipophilic metabolite concentration in the rat plasma and brain and a concomitant increase in the cerebral [^{11}C]SKF 82957 concentration, which favors the use of [^{11}C]SKF 82957 as a PET radioligand.

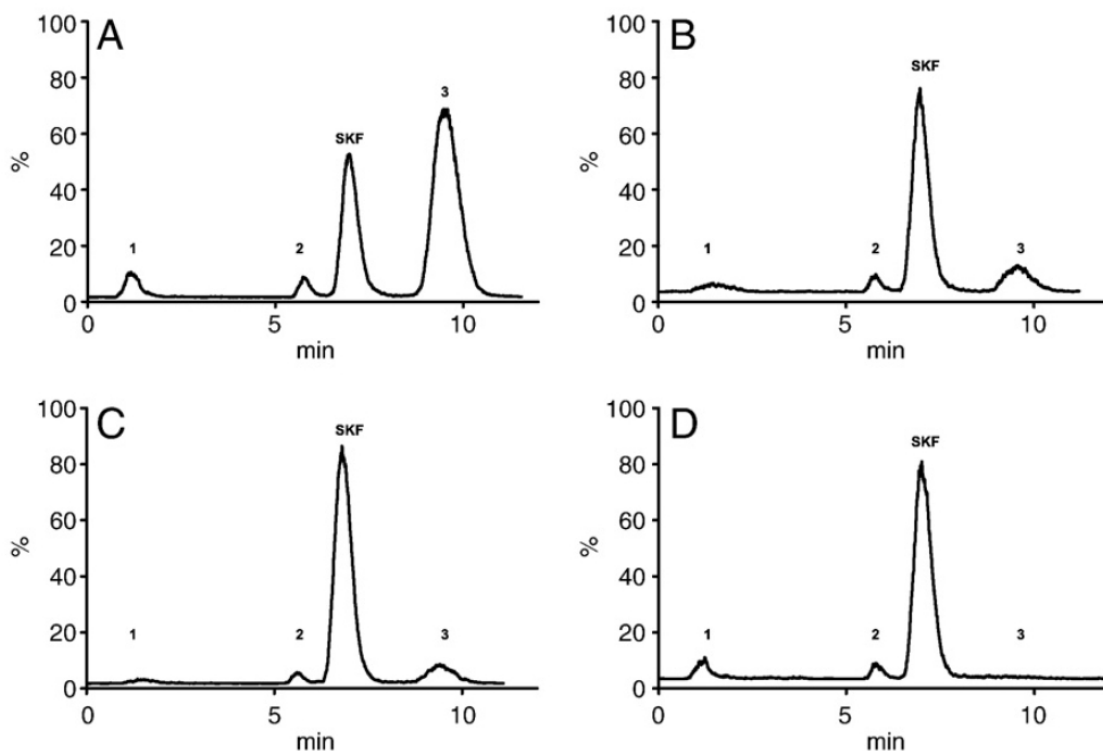


Figure 12: HPLC chromatograms of rat brain extracts 30 min post intravenous injection of [^{11}C]SKF 82957. (A) Saline treated; (B) 3 mg/kg tolcapone; (C) 10 mg/kg tolcapone; (D) 20 mg/kg tolcapone. Peaks labeled “1” and “2” are hydrophilic metabolites, SKF is R-[^{11}C]SKF 82957 and “3” is the lipophilic metabolite.

There are several ways to circumvent the metabolite problem. The method of COMT inhibition works for the special cases of [^{18}F]FDOPA, and [^{11}C]SKF 82957, but this can only be applied to a radioligand with catechol structure. Inhibition of other metabolizing enzymes might have serious effects of the general metabolism of the body, with resultant health risks. In most cases, it would be better to change the position of the radionuclide in the radioligand molecule so that the degraded radiometabolite would be hydrophobic, and thereby have restricted uptake in the brain.

In the case of the 5-HT_{2A} receptor agonist [¹¹C]Cimbi-5, a radiolabeled metabolite slightly less lipophilic than the parent compound appeared in the plasma of the pig following i.v. injection of [¹¹C]Cimbi-5. Based on previous studies describing the metabolism in rats of the 5-HT_{2A} receptor agonist compound DOI (Ewald et al. 2007), we speculated that metabolism of [¹¹C]Cimbi-5 in the pig likewise entails *O*-demethylation at one of the methoxy groups in the iodophenethylamine-moiety of the tracer. Fortunately, HPLC analysis of *ex vivo* brain extracts did not suggest that the lipophilic metabolite enters the pig brain to any large degree, and consequently the radiolabeled metabolite most likely do not contribute to the non-specific binding of [¹¹C]Cimbi-5. Radiolabeled metabolites that originate from an *O*-demethylation can be avoided by changing the labeling site to the *O*-demethylated methyl group, thereby generating a small hydrophilic compound, presumably formic acid, as the radiolabeled metabolite. However, in the present case the interference was negligible.

Binding Competition

The radioligands [¹¹C]SKF 82597 (D₁ agonist), [³H]NPA (D_{2/3} agonist) and [³H]CUMI-101 (5-HT_{1A} agonist) were all tested *ex vivo* for their susceptibility to endogenous competition, under conditions of both increased (release) and decreased (depletion) concentration of neurotransmitter. A short summary of the challenge results will follow below.

Endogenous Competition – Release

As expected, the dopamine releasing effect of amphetamine mediated competition between endogenous dopamine and the agonist [³H]NPA, lead to a decreased SBR of [³H]NPA in striatum (table 2). Indeed, the competition between amphetamine-induced DA release and a D_{2/3} receptor radioligands is the classic example that supports the competition model (Laruelle 2000). However, interpretation of the results with the other radioligands was not nearly as straightforward.

Both amphetamine and RTI-32 pre-treatment decreased the SUV of the D₁ agonist [¹¹C]SKF 82957 in rat striatum, but contrary to expectations concomitantly increased the SBR (table 2). [¹¹C]SKF 82957 has a very low non-specific binding and small changes in washout or metabolism of the radioligand induced by the pharmacological challenges

affect the concentrations of radioligand proportionally more in the non-specific region than in the binding region, where the concentration of bound ligand is high. This is believed to be the driving factor for the increase in SBR, also supported by the fact that there is a lower SUV after both treatments. However, the findings are in line with previous attempts to demonstrate *in vivo* competition using D₁ antagonists: The binding potential (BP) or ratio of bound/free ligand (B/F) of other D₁ antagonist radioligands have been found to be insensitive to, or slightly increased, after pharmacologically stimulated DA release (Abi-dargham et al. 1999; Chou et al. 1999). All in all our findings do not support the principle of agonists being more sensitive to endogenous transmitter release than antagonist.

Table 2: Percent changes in uptake (SUV) and binding (SBR) after direct release and indirect release of endogenous neurotransmitter.

	Direct Release (Amphetamine / Fenfluramine)		Indirect Release (RTI-32 / Citalopram)	
	SUV	SBR	SUV	SBR
[¹¹ C]NPA	-	-30%**	-	-
[¹¹ C]SKF 82547	-10%*	+33%**	-14%***	+12%
[³ H]CUMI-101	0%	+49%**	+5%	-11%

Direct release is compounds that directly effect the release of endogenous neurotransmitter, while indirect release is compounds that enhance the concentration of endogenous neurotransmitter in the synaptic cleft by blocking the reuptake sites. RTI-32 is a DA reuptake inhibitor. * p<0.05, ** p<0.01, *** p<0.001

We noticed a small but insignificant decline in the SBR of [³H]CUMI-101 in rat hippocampus and frontal cortex after citalopram treatment (table 2), which concurs with previous studies with the 5-HT_{1A} antagonists [¹¹C]WAY 100635 (Hume et al. 1994) and [¹⁸F]MPPF (Udo de Haes et al. 2005; Plenevaux et al. 2000), but fails to support the principle of the competition model. On the other hand, acute treatment with the potent serotonin releaser fenfluramine increased the SBR in frontal cortex and hippocampus by 30-50%, which is entirely in contrast to all other studies with 5-HT_{1A} radioligands, which report only insignificant decline or no change in binding, with [¹¹C]WAY 100635 (Maeda et al. 2001; Hume et al. 2001; Rice et al. 2001) or with [¹⁸F]MPPF (Zimmer et al. 2002; Udo de Haes et al. 2005), after fenfluramine pre-treatment. This increase in SBR is also driven by a change in the non-specific binding as with [¹¹C]SKF 82957 above. As [³H]CUMI-101 does not bind specifically in the cerebellum, the change must originate from changes in washout or metabolism induces by the fenfluramine treatment. A

combination of a high k_{off} of [^3H]CUMI-101 from the 5-HT_{1A} receptor and an increased blood-flow would increase the washout of the non-specific binding region without changing in the binding. With a low non-specific binding even a small change in this region results in larger change in the specific binding ratio, while the SUV is more resistant to these changes. In the light of our experiences, we must conclude that *ex vivo* experiments may not be the best method for evaluating competition effects from released endogenous neurotransmitter.

Endogenous Competition – Depletion

As expected from the competition model, depletion of DA by a 6-OHDA lesion resulted in a 50% increase in the SBR of the D₂ agonist [^3H]NPA (table 3), whereas it only resulted in 0-20% increase in [^3H]raclopride binding and only in the posterior ventral lateral region of the striatum. These findings can be explained with the competition model. However, the only study comparing DA agonist and antagonist binding is a [^{11}C]PHNO PET study of untreated patients with early Parkinson's disease (Boileau et al. 2009), which find equivalent 25% increases in the binding of [^{11}C]raclopride and [^{11}C]PHNO. This result is not in agreement with our findings, and do not support the competition model which would predict a proportional greater increase for the agonist, due to greater sensitivity to competition from DA.

Table 3: Percent changes in uptake (SUV) and binding (SBR) after depletion of endogenous neurotransmitter.

	Depletion (6-OHDA / α -MT / pCPA)	
	SUV	SBR
[^3H]Raclopride		+20%*
[^3H]NPA	-	+50%**
[^{11}C]SKF 82547	-29%***	-34%***
[^3H]CUMI-101	-14%	-14%

* $p < 0.05$, ** $p < 0.01$, *** $p < 0.001$

Acute α -MT treatment significantly decreased the SBR of the agonist [^{11}C]SKF 82957, by 34% (table 3). This is entirely opposite to the predictions of the competition model, but in good agreement with other D₁ studies where the binding has been either unchanged or reduced after acute DA depletion (Rice et al. 2001; Guo et al. 2003; Inoue et al. 1991). This change can not be explained by a change of the blood-flow, as we did not see a significant change in the cerebellar region after α -MT treatment, and the change was

also seen in SUV, which is unaffected by changes in the non-specific binding. Thus an explanation for these changes has yet to be established for the case of D₁ receptor ligands, both in the above conditions of increased DA release, and after depletion.

Treatment with the 5-HT synthesis inhibitor pCPA did not significantly affect the SUV or SBR of the 5-HT_{1A} partial agonist [³H]CUMI-101 as measured *ex vivo*. Contrary to this result, serotonin depletion slightly increased the [¹⁸F]MPPF binding in rat hippocampus (Zimmer et al. 2003). Again we noticed a discrepancy between our observations with agonist or partial agonist radioligands and the proposed effects by the competition model. As the competition model is a very simplified model of a single receptor in a standardized environment it is not surprising that it fail to account for all observations seen *in vivo*.

The in vivo Competition Model Expanded

Whereas the competition model may be valid for explaining observations made in simple systems, such as cell cultures and membrane preparations it seems to fails to predict the binding of receptor radioligands other than D₂/D₃. The paradoxical findings in some systems, especially with binding of D₁ radioligands under conditions of pharmacological challenge, are not completely explained. However, some alternative theories in relation to the D₁ and D₂ receptors, where the most knowledge has been obtained will be presented here. These theories could form the basis for further general competition studies, and in the future a better competition model. However, the effects of all these theories needs to be tested thoroughly.

First, it is known that D₁^{High} constitutes 15-40% of the total D₁ receptor pool, both in rat tissue and post mortem human brain (Richfield et al. 1989; Shuto et al. 2008; McCauley et al. 1995), and that D₂^{High} contributes 15-77% of the total D₂ receptors in rat and post mortem human brain (Richfield et al. 1989; Shuto et al. 2008; Leysen et al. 1993), all based on biphasic displacement of an antagonist by an agonist *in vitro*. In most reports the D₂^{High} fraction is somewhat larger than the D₁^{High} fraction. Structural studies of the location of striatal DA receptors show that D₁ receptors are mainly located extrasynaptically (Caillé et al. 1996; Dumartin et al. 1998; Smiley et al. 1994) whereas D₂ receptors are located mainly intrasynaptically. It is therefore reasonable to predict

that D₁ receptors would be activated secondly to D₂ receptors, following DA release *in vivo*, see figure 13.

Furthermore, there is evidence that D₁ and D₂ receptor responses are linked in some way. Apomorphine, a D₁ and D_{2/3} agonist, induce turning behavior in rats with hemitransection of the nigrostriatal pathway (another way to deplete striatal DA), whereas the behavioral responses to SKF 38393 (D₁ agonist) and quinpirole (D_{2/3} agonist) were much lower when given alone but equal to the apomorphine effect when given in combination (Arnt et al. 1987). In mice with severe DA depletion following reserpine + α -MT, behavioral effects of bromocriptine (D_{2/3} agonist) and CY 208-243 (D₁ agonist) were only apparent when given in combination (Robertson et al. 1986). The turning behavior in 6-OHDA lesioned rats after a caffeine induced DA release is increased with combined treatment with a D₁ agonist but not in combination with a D_{2/3} agonist (Cauli et al. 2003) supporting the idea that DA activates D₂ before activating D₁. All the above studies above agree that a combined activation of D₁ and D₂ give a stronger response than activation of only one type. It could be explained by a mechanism in which D₁ and D₂ receptor induce the high affinity state of one another, thereby reciprocally enhancing the signal of of each receptor.

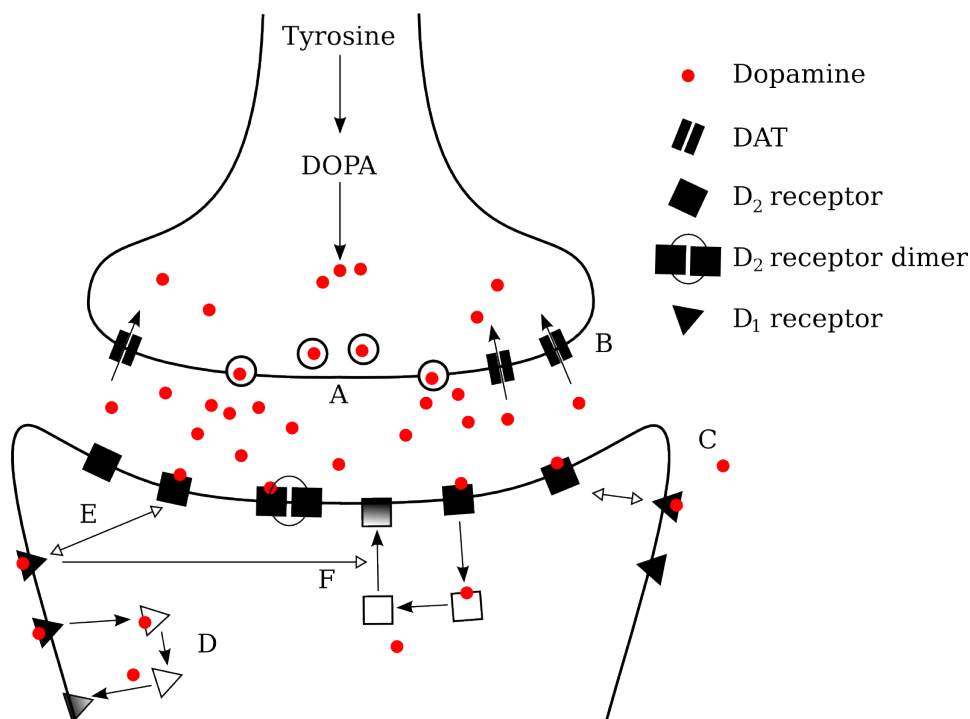


Figure 13: Receptor activation, internalization, recycling and cross-talk after DA release into the synaptic cleft.

For example: If we assume that release of DA activates the D₂ receptors first, it will evoke an increase in the D₁^{High} fraction. That would thereby lead to an increased binding of the D₁ agonist [¹¹C]SKF 82957, as seen in my experiments (table 2). Conversely, a DA depletion would lower the constitutively active D₂ signaling, leading to a decrease in D₁^{High}, thus resulting in a decreased binding of the agonist [¹¹C]SKF 82957 as seen in my experiments (table 3).

The switch between the high and low receptor affinity states might be related to internalization and recycling of the DA receptors. After DA induced activation the dendritic D₁ receptors internalize (Dumartin et al. 1998), and their overall responsiveness to further stimulation decreases (Trovero et al. 1994). However, this decrease in response is restored after only 15 minutes, and the surface expression of receptors is restored by recycling within 20-60 minutes (Martin-Negrier et al. 2006), which is within the time-frame of most experimental setups. For example; in papers II and III, amphetamine was given 50-90 minutes before decapitation, thereby leaving enough time for the D₁ and D₂ receptor respectively, to be internalized and recycle after their binding to DA. The internalization of D₁ or D₂ receptors after stimulation by [¹¹C]SKF 82957 or [³H]NPA is another matter. Different D₁ agonists have been shown to evoke internalization at very different rates. Thus, the D₁ agonist A-77636 caused seemingly permanent internalization, and the internalization evoked by the D₁ agonist dinapsoline was only slowly reversible (Ryman-Rasmussen et al. 2007). The D₁ agonist SKF 82958 evoked internalization lasting from 20 minutes to 5 hours, depending on the study (Ryman-Rasmussen et al. 2007; Martin-Negrier et al. 2006; Dumartin et al. 1998). These differences has been attributed to the kinetics of the ligand-receptor interactions, where it is the lipophilicity and dissociation constant which determine the duration of internalization. As yet, there has been no formal demonstration of internalization after [¹¹C]SKF 82957 stimulation. However, since it is structurally related to SKF 82958 but less lipophilic and with a higher efficacy, it is to be expected that [¹¹C]SKF 82957-D₁ receptor complex is likewise internalized after binding, and might retain the internalized state for longer due to the higher affinity. However, it is interesting that stimulation of the D₁ receptors with the D₁ agonist SKF 38393 seems to prime D₂ receptor surfacing (Goggi et al. 2007), which may be a contributing factor to the above theory of cross-talk between D₁ and D₂ receptors. If [¹¹C]SKF 82957 activation of the D₁ receptor leads to surfacing of D₂ receptors, it would increase the amount of the D₂ receptors. This would in turn, lead to a greater activation of D₂ receptors by the amphetamine released DA, and

thereby to a increased D_1^{High} fraction, giving an increased [^{11}C]SKF 82957 binding, as described above. The opposite experiment testing D_2 agonist activity towards D_1 receptor internalization or recycling has not been carried out, but would contribute significantly to the understanding of the D_1 and D_2 receptor interactions. Also the existence of DA receptors in multiple formations, such as D_1 - D_2 heterodimers (Grymek 2009) potentially effects the binding and behavior of these receptors. Furthermore, an additional level of complexity with the existence of GPCRs in multiple conformational states have been found by fluorescence resonance energy transfer (FRET). The alpha2a adrenergic receptor could be differential stabilized by different ligands in several different active conformations, each with different signaling profiles (Lill 2005, Ambrosio 2010).

Alternatives to the competition model has been published, the best are extending the original competition model with the internalized part of the D_2 receptors (Laruelle & Huang 2001, Narendran et al. 2004). However, in spite the additional complexity of these models, they also predicts that agonist should be more sensitive than antagonist towards endogenous neurotransmitter competition, and do not describe the results of these *ex vivo* findings better than the original competition model. A new perspective on serotonin endogenous neurotransmitter competition has also been published, which conclude that it might be a very difficult task with the current targets and available tracers, and that new tracers with higher binding potential and optimized experiment protocols are needed if this is ever going to succeed (Paterson 2010). A complete competition model with consideration of internalization, dimers and oligomers, differential agonism and multiple receptors states might ultimately help to explain the different results.

Conclusion

In the course of the work described in this thesis several novel radiolabeled agonists were evaluated as possible PET radioligands.

- The dopamine D₂ agonist [¹¹C]-2Cl-NPA failed to meet the standard of the well characterized [¹¹C]NPA, and was discarded after the *in vivo* evaluation.
- The problem of the brain-penetrating metabolite derived from the metabolism of the D₁ agonist [¹¹C]SKF 82957 was solved by inhibiting the metabolizing enzyme COMT, thereby enabling [¹¹C]SKF 82957 to be a usable PET radioligand.
- The uptake, selectivity and binding maximum of the 5-HT_{1A} agonist [³H]CUMI-101 was evaluated in rats, and found to be a good alternative to the current available 5-HT_{1A} radioligands.
- The uptake and selectivity were evaluated for the 5-HT_{2A} agonist [¹¹C]Cimbi-5, forming the basis for proceeding to testing of this radioligand for PET imaging of humans.

Methods for releasing and depleting DA and 5-HT, in particular, blocking the reuptake, promoting release, inhibition of synthesis, and neurotoxic lesioning, were used to challenge the binding of several of the agonist radioligands.

- The D_{2/3} agonist [¹¹C]NPA (and [³H]NPA) was challenged with amphetamine-induced DA release and 6-OHDA lesioning which led to changed binding in agreement with the literature.
- The D₁ agonist [¹¹C]SKF 82957 was challenged by amphetamine induced DA release and α-MT inhibition of DA synthesis. The induced challenge did not change [¹¹C]SKF 82957 binding in the hypothesized direction.
- The 5-HT_{1A} agonist [³H]CUMI-101 was challenged by re-uptake blockade with citalopram, fenfluramine-induced 5-HT release and pCPA-induced inhibition of synthesis. [³H]CUMI-101 binding did not change after any of the challenges.

Acknowledgments

This Ph.D project was supported by the Danish Agency for Science, Technology and Innovation, who gave financial support in form of an International Ph.D. Stipend, through the Graduate School of Neuroscience at the Copenhagen University. The project was performed at the Center for Integrated Molecular Brain Imaging, Department of Neurology, Rigshospitalet, and at the Centre for Addiction and Mental Health in Toronto, and Columbia University Medical Center in New York.

I would like to acknowledge the substantial help from my co-authors, collaboration partners and colleagues who have contributed to the papers in this thesis. I would like to give a special thanks to my academic advisors: Gitte Moos Knudsen, for her guidance and coaching through the scientific problems. I also thank Alan A. Wilson for my stay in his laboratory at Center for Addiction and Mental Health in Toronto, and for his great teaching in *ex vivo* experimentation and HPLC methodology. I thank Ramin V. Parsey for my stay at Columbia University Medical Center, and for giving me the opportunity and responsibility of the *ex vivo* evaluation of their novel radioligand. I would also like to thank Mark Underwood for his great humor and teaching in animal handling, and Paul Cumming for his coaching, editorial assistance, and fruitful discussions of the scientific problems.

I would also like to thank all my friends and family who supported me in the process, with special thanks to Patrick McCormick and Francesca Zanderigo for being good friends doing my visits abroad, and to my girlfriend Celia Kjærby Hansen who had to put up with my occasional frustrations, travels abroad and long hours of writing.

Copenhagen, September 2010

Mikael Palner

References

- Abbas A, Roth BL (2008) Pimavanserin tartrate: a 5-HT_{2A} inverse agonist with potential for treating various neuropsychiatric disorders. *Expert opinion on pharmacotherapy* 9:3251-9
- Abi-dargham A, Simpson N, Kegeles L, Parsey R, Hwang DR, Anjilvel S, Zea-Ponce Y, Lombardo I, Van Heertum R, Mann JJ, Foged C, Halldin C, Laruelle M (1999) PET studies of binding competition between endogenous dopamine and the D₁ radiotracer [¹¹C]NNC 756. *Synapse* 32:93-109
- Adams KH, Hansen ES, Pinborg LH, Hasselbalch SG, Svarer C, Holm S, Bolwig TG, Knudsen GM. (2005) Patients with obsessive-compulsive disorder have increased 5-HT_{2A} receptor binding in the caudate nuclei. *Int J Neuropsychopharmacol.* 8(3):391-401
- Ambrosio M, Zurn A, Lohse MJ. (2010) Sensing G protein-coupled receptor activation. *Neuropharmacology.* 1-7 In Press
- Antoni G, Långström B (2008) Radiopharmaceuticals: molecular imaging using positron emission tomography. *Handbook of experimental pharmacology*:177-201
- Arnsten AF, Cai JX, Murphy BL, Goldman-Rakic PS (1994) Dopamine D₁ receptor mechanisms in the cognitive performance of young adult and aged monkeys. *Psychopharmacology* 116:143-51
- Arnt J, Perregaard J (1987) Synergistic interaction between dopamine D-1 and D-2 receptor agonists: circling behaviour of rats with hemitranssection. *European journal of pharmacology* 143:45-53
- Bergström M, Awad R, Estrada S, Mälman J, Lu L, Lendvai G, Bergström-Pettermann E, Långström B (2003) Autoradiography with positron emitting isotopes in positron emission tomography tracer discovery. *Molecular Imaging and Biology* 5:390-6
- Besret L, Dollé F, Hérard A, Guillemier M, Demphel S, Hinnen F, Coulon C, Ottaviani M, Bottlaender M, Hantraye P, Kassiou M (2008) Dopamine D₁ receptor imaging in the rodent and primate brain using the isoquinoline +-[¹¹C]A-69024 and positron emission tomography. *Journal of pharmaceutical sciences* 97:2811-9
- Bie-Olsen LG, Kjaer TW, Pedersen-Bjergaard U, Lonsdale MN, Holst JJ, Law I, Thorsteinsson B (2009) Changes of cognition and regional cerebral activity during acute hypoglycemia in normal subjects: A H₂ ¹⁵O positron emission tomographic study. *Journal of neuroscience research* 87:1922-8
- Boileau I, Guttman M, Rusjan P, Adams JR, Houle S, Tong J, Hornykiewicz O, Furukawa Y, Wilson AA, Kapur S, Kish SJ (2009) Decreased binding of the D₃ dopamine receptor-preferring ligand [¹¹C]-(+)-PHNO in drug-naive Parkinson's disease. *Brain : a journal of neurology* 132:1366-75
- Borg J (2008) Molecular imaging of the 5-HT_{1A} receptor in relation to human cognition. *Behavioural brain research* 195:103-11
- Boyes BE, Cumming P, Martin WR, McGeer EG (1986) Determination of plasma [¹⁸F]-6-fluorodopa during positron emission tomography: elimination and metabolism in carbidopa treated subjects. *Life sciences* 39:2243-52
- Brea J, Castro M, Giraldo J, López-Giménez JF, Padín JF, Quintián F, Cadavid MI, Vilaró MT, Mengod G, Berg KA, Clarke WP, Vilardaga J, Milligan G, Loza MI (2009) Evidence for distinct antagonist-revealed functional states of 5-hydroxytryptamine(2A) receptor homodimers. *Molecular pharmacology* 75:1380-91
- Breier A, Su TP, Saunders R, Carson RE, Kolachana BS, de Bartolomeis A, Weinberger DR, Weisenfeld N, Malhotra AK, Eckelman WC, Pickar D (1997) Schizophrenia is associated with elevated amphetamine-induced synaptic dopamine concentrations: evidence from a novel positron
-

- emission tomography method. *Proceedings of the National Academy of Sciences of the United States of America* 94:2569-74
- Briand LA, Flagel SB, Seeman P, Robinson TE (2008) Cocaine self-administration produces a persistent increase in dopamine D2 High receptors. *European Neuropsychopharmacology* 18:551-6
- Brunelli SA, Aviles JA, Gannon KS, Branscomb A, Shacham S (2009) PRX-00023, a selective serotonin 1A receptor agonist, reduces ultrasonic vocalizations in infant rats bred for high infantile anxiety. *Pharmacology, biochemistry, and behavior* 94:8-15
- Caillé I, Dumartin B, Bloch B (1996) Ultrastructural localization of D1 dopamine receptor immunoreactivity in rat striatonigral neurons and its relation with dopaminergic innervation. *Brain research* 730:17-31
- Carrasco GA, Van de Kar LD, Sullivan NR, Landry M, Garcia F, Muma NA, Battaglia G (2006) Cocaine-mediated supersensitivity of 5-HT_{2A} receptors in hypothalamic paraventricular nucleus is a withdrawal-induced phenomenon. *Neuroscience* 143:7-13
- Casteels C, Lauwers E, Bormans G, Baekelandt V, Van Laere K (2008) Metabolic-dopaminergic mapping of the 6-hydroxydopamine rat model for Parkinson's disease. *European journal of nuclear medicine and molecular imaging* 35:124-34
- Cauli O, Pinna A, Valentini V, Morelli M (2003) Subchronic caffeine exposure induces sensitization to caffeine and cross-sensitization to amphetamine ipsilateral turning behavior independent from dopamine release. *Neuropsychopharmacology : official publication of the American College of Neuropsychopharmacology* 28:1752-9
- Ceglia I, Acconcia S, Fracasso C, Colovic M, Caccia S, Invernizzi RW (2004) Effects of chronic treatment with escitalopram or citalopram on extracellular 5-HT in the prefrontal cortex of rats: role of 5-HT_{1A} receptors. *British journal of pharmacology* 142:469-78
- Chou YH, Karlsson P, Halldin C, Olsson H, Farde L (1999) A PET study of D(1)-like dopamine receptor ligand binding during altered endogenous dopamine levels in the primate brain. *Psychopharmacology* 146:220-7
- Church WH, Jr J, J.b, Byrd LD (1987) Extracellular dopamine in rat striatum following uptake inhibition by cocaine, nomifensine and bsztoprine. *Eur. J. Pharmacol* 139:345-348
- Clawges HM, Depree KM, Parker EM, Graber SG (1997) Human 5-HT₁ receptor subtypes exhibit distinct G protein coupling behaviors in membranes from Sf9 cells. *Biochemistry* 36:12930-8
- Cumming P, Boyes BE, Martin WR, Adam M, Ruth TJ, McGeer EG (1987) Altered metabolism of [18F]-6-fluorodopa in the hooded rat following inhibition of catechol-O-methyltransferase with U-0521. *Biochemical pharmacology* 36:2527-31
- Cumming P, Wong DF, Dannals RF, Gillings N, Hilton J, Scheffel U, Gjedde A (2002) The competition between endogenous dopamine and radioligands for specific binding to dopamine receptors. *Annals of the New York Academy of Sciences* 965:440-50
- Cumming P, Wong DF, Gillings N, Hilton J, Scheffel U, Gjedde A (2002) Specific binding of [(11)C]raclopride and N-[(3)H]propyl-norapomorphine to dopamine receptors in living mouse striatum: occupancy by endogenous dopamine and guanosine triphosphate-free G protein. *Journal of cerebral blood flow and metabolism : official journal of the International Society of Cerebral Blood Flow and Metabolism* 22:596-604
- Dahlström A, Fuxe K, (1964) Localization of monoamines in the lower brain stem. *Experientia* 15 20(7):398-9
- DaSilva J, Cheung H, Wilson A, Houle S (2003) Metabolism of dopamine D1 agonist R-(+)-[11C]SKF 82957 produces a radiolabeled metabolite in rat brain. *Journal of Labelled Compounds and Radiopharmaceuticals* 46:S365-S382
- DaSilva JN, Schwartz RA, Greenwald ER, Lourenco CM, Wilson AA, Houle S (1999) Dopamine D1 agonist R-[11C]SKF 82957: synthesis and in vivo characterization in rats. *Nuclear medicine and biology* 26:537-42

- Datla KP, Curzon G (1996) Effect of p-chlorophenylalanine at moderate dosage on 5-HT and 5-HIAA concentrations in brain regions of control and p-chloroamphetamine treated rats. *Neuropharmacology* 35:315-20
- De Boer SF, Koolhaas JM (2005) 5-HT_{1A} and 5-HT_{1B} receptor agonists and aggression: a pharmacological challenge of the serotonin deficiency hypothesis. *European journal of pharmacology* 526:125-39
- De Camilli P, Macconi D and Spada A (1979) Dopamine inhibits adenylate cyclase in human prolactin-secreting pituitary adenomas. *Nature* 278:252-4.
- De Lean A, Stadel JM, Lefkowitz RJ (1980) A ternary complex model explains the agonist-specific binding properties of the adenylate cyclase-coupled beta-adrenergic receptor. *The Journal of biological chemistry* 255:7108-17
- Dentresangle C, Veyre L, Le Bars D, Pierre C, Lavenne F, Pollak P, Guerin J, Froment JC, Brousolle E (1999) Striatal D₂ dopamine receptor status in Parkinson's disease: an [¹⁸F]dopa and [¹¹C]raclopride PET study. *Movement disorders* 14:1025-30
- Dumartin B, Caillé I, Gonon F, Bloch B (1998) Internalization of D₁ dopamine receptor in striatal neurons in vivo as evidence of activation by dopamine agonists. *The Journal of Neuroscience* 18:1650-61
- Ebenezer IS, Arkle MJ, Tite RM (2007) 8-Hydroxy-2-(di-n-propylamino)-tetralin inhibits food intake in fasted rats by an action at 5-HT_{1A} receptors. *Methods and findings in experimental and clinical pharmacology* 29:269-72
- Egan C, Roth BL, Grinde E, Dupre A, Roth BL, Hake M, Teitler M, Herrick-Davis K (2000) Agonist high and low affinity state ratios predict drug intrinsic activity and a revised ternary complex mechanism at serotonin 5-HT_{2A} and 5-HT_{2C} receptors. *Synapse* 35:144-50
- Elsinga PH, Hendrikse NH, Bart J, van Waarde A, Vaalburg W (2005) Positron emission tomography studies on binding of central nervous system drugs and P-glycoprotein function in the rodent brain. *Mol Imaging Biol.* 7(1):37-44.
- Ewald AH, Fritschi G, Maurer HH (2007) Metabolism and toxicological detection of the designer drug 4-iodo-2,5-dimethoxy-amphetamine (DOI) in rat urine using gas chromatography-mass spectrometry. *Journal of chromatography. B, Analytical technologies in the biomedical and life sciences* 857:170-4
- Farde L, Halldin C, Stone-Elander S, Sedvall G (1987) PET analysis of human dopamine receptor subtypes using ¹¹C-SCH 23390 and ¹¹C-raclopride. *Psychopharmacology* 92:278-84
- Farrell CB, O'Boyle KM (1994) The kinetics of [³H]SCH 23390 dissociation from rat striatal dopamine D₁ receptors: effect of dopamine. *European journal of pharmacology* 268:79-88
- Finnema SJ, Seneca N, Farde L, Shchukin E, Sóvágó J, Gulyás B, Wikström HV, Innis RB, Neumeier JL, Halldin C (2005) A preliminary PET evaluation of the new dopamine D₂ receptor agonist [¹¹C]MNPA in cynomolgus monkey. *Nuclear medicine and biology* 32:353-60
- Frøkjær VG, Mortensen EL, Nielsen FÅ, Haugbøl S, Pinborg LH, Adams KH, Svarer C, Hasselbalch SG, Holm S, Paulson OB, Knudsen GM (2008) Frontolimbic serotonin 2A receptor binding in healthy subjects is associated with personality risk factors for affective disorder. *Biological psychiatry* 63:569-76
- Fuxe K., Hillarp N., Dahlström A., (1996) Demonstration and mapping of central neurons containing dopamine, noradrenaline and 5-hydroxytryptamine and their reactions to psychopharmaca. *Pharmacological Reviews* 18:727
- Ginovart N, Galineau L, Willeit M, Mizrahi R, Bloomfield PM, Seeman P, Houle S, Kapur S, Wilson Aa (2006) Binding characteristics and sensitivity to endogenous dopamine of [¹¹C]-(+)-PHNO, a new agonist radiotracer for imaging the high-affinity state of D₂ receptors in vivo using positron emission tomography. *Journal of neurochemistry* 97:1089-103

- Goggi JL, Sardini A, Egerton A, Strange PG, Grasby PM (2007) Agonist-dependent internalization of D2 receptors: Imaging quantification by confocal microscopy. *Synapse (New York, N.Y.)* 61:231-41
- Goldman-Rakic PS, Castner SA, Svensson TH, Siever LJ, Williams GV (2004) Targeting the dopamine D1 receptor in schizophrenia: insights for cognitive dysfunction. *Psychopharmacology* 174:3-16
- González-Maeso J, Weisstaub NV, Zhou M, Chan P, Ivic L, Ang R, Lira A, Bradley-Moore M, Ge Y, Zhou Q, Sealfon SC, Gingrich JA (2007) Hallucinogens recruit specific cortical 5-HT(2A) receptor-mediated signaling pathways to affect behavior. *Neuron* 53:439-52
- Gozlan H, Thibault S, Laporte AM, Lima L, Hamon M (1995) The selective 5-HT1A antagonist radioligand [3H]WAY 100635 labels both G-protein-coupled and free 5-HT1A receptors in rat brain membranes. *European journal of pharmacology* 288:173-86
- Grigoriadis D, Seeman P (1985) Complete Conversion of Brain D2 Dopamine Receptors from the High- to the Low-Affinity State for Dopamine Agonists, Using Sodium Ions and Guanine Nucleotide. *Journal of Neurochemistry* 44:1925-1935
- Grymek K, Lukasz S, Faron-Gorecka, Tworzydło M, Polit A, Dziedzicka-Wasylewska M. (2009) Role of silent polymorphisms within the dopamine D1 receptor associated with schizophrenia on D1-D2 receptor hetero-dimerization, *Pharmacological Reports* 61:1024-1033
- Gunn RN, Sargent PA, Bench CJ, Rabiner EA, Osman S, Pike VW, Hume SP, Grasby PM, Lammertsma AA (1998) Tracer kinetic modeling of the 5-HT1A receptor ligand [carbonyl-11C]WAY-100635 for PET. *NeuroImage* 8:426-40
- Guo N, Hwang D, Lo E, Huang Y, Laruelle M, Abi-Dargham A (2003) Dopamine depletion and in vivo binding of PET D1 receptor radioligands: implications for imaging studies in schizophrenia. *Neuropsychopharmacology* 28:1703-11
- Halldin C, Foged C, Chou YH, Karlsson P, Swahn CG, Sandell J, Sedvall G, Farde L (1998) Carbon-11-NNC 112: a radioligand for PET examination of striatal and neocortical D1-dopamine receptors. *Journal of Nuclear Medicine* 39:2061-8
- Halldin C, Foged C, Farde L, Karlsson P, Hansen K, Grønvald F, Swahn CG, Hall H, Sedvall G (1993) [11C]NNC 687 and [11C]NNC 756, dopamine D-1 receptor ligands. Preparation, autoradiography and PET investigation in monkey. *Nuclear medicine and biology* 20:945-53
- Hartvig P, Bergström M, Långström B (2001) Use of positron emission tomography in analysing receptor function in vivo. *Toxicology letters* 120:243-51
- Hirvonen J, van Erp TG, Huttunen J, Aalto S, Någren K, Huttunen M, Lönngqvist J, Kaprio J, Cannon TD, Hietala J (2006) Brain dopamine d1 receptors in twins discordant for schizophrenia. *The American journal of psychiatry* 163:1747-53
- Huang M, Ichikawa J, Li Z, Dai J, Meltzer HY (2006) Augmentation by citalopram of risperidone-induced monoamine release in rat prefrontal cortex. *Psychopharmacology* 185:274-81
- Hume S, Hirani E, Opacka-Juffry J, Myers R, Townsend C, Pike V, Grasby P (2001) Effect of 5-HT on Binding of WAY 100635 to receptors in rat brain, assessed using in vivo microdialysis. *Synapse* 41:150-159
- Hume SP, Ashworth S, Opacka-Juffry J, Ahier RG, Lammertsma AA, Pike VW, Cliffe IA, Fletcher A, White AC (1994) Evaluation of [O-methyl-3H]WAY-100635 as an in vivo radioligand for 5-HT1A receptors in rat brain. *European journal of pharmacology* 271:515-23
- Hurd YL, Ungerstedt U (1989) Cocaine: an in vivo microdialysis evaluation of its acute action on dopamine transmission in rat striatum. *Synapse (New York, N.Y.)* 3:48-54
- Hwang DR, Kegeles LS, Laruelle M (2000) (-)-N-[11C]propyl-norapomorphine: a positron-labeled dopamine agonist for PET imaging of D(2) receptors. *Nuclear medicine and biology* 27:533-9

- Innis RB et al. (2007) Consensus nomenclature for in vivo imaging of reversibly binding radioligands. *Journal of cerebral blood flow and metabolism : official journal of the International Society of Cerebral Blood Flow and Metabolism* 27:1533-9
- Inoue O, Tsukada H, Yonezawa H, Suhara T, Langstrom B (1991) Reserpine-induced reduction of in vivo binding of SCH 23390 and N-methylspiperone and its reversal by d-amphetamine. *European journal of pharmacology* 197:143-9
- Ishibashi K, Ishii K, Oda K, Mizusawa H, Ishiwata K (2010) Competition between ¹¹C-raclopride and endogenous dopamine in Parkinson's disease. *Nuclear medicine communications* 31:159-66
- Ito H, Nyberg S, Halldin C, Lundkvist C, Farde L (1998) PET imaging of central 5-HT_{2A} receptors with carbon-11-MDL 100,907. *Journal of nuclear medicine : official publication, Society of Nuclear Medicine* 39:208-14
- Jaber M, Robinson SW, Missale C and Caron MG (1996) Dopamine receptors and brain function. *Neuropharmacology* 35:1503-19.
- Kahlig KM, Binda F, Khoshbouei H, Blakely RD, McMahon DG, Javitch JA, Galli A (2005) Amphetamine induces dopamine efflux through a dopamine transporter channel. *Proceedings of the National Academy of Sciences of the United States of America* 102:3495-500
- Karlin A (1967) On the application of "a plausible model" of allosteric proteins to the receptor for acetylcholine. *Journal of theoretical biology* 16:306-20
- Kassiou M, Scheffel U, Ravert HT, Mathews WB, Musachio JL, Lambrecht RM, Dannals RF (1995) [¹¹C]A-69024: a potent and selective non-benzazepine radiotracer for in vivo studies of dopamine D₁ receptors. *Nuclear medicine and biology* 22:221-6
- Kenakin T (2004) Principles: receptor theory in pharmacology. *Trends in pharmacological sciences* 25:186-92
- Kim S, Shin I, Kim J, Youn T, Yang S, Hwang MY, Yoon J (2009) The 5-HT₂ receptor profiles of antipsychotics in the pathogenesis of obsessive-compulsive symptoms in schizophrenia. *Clinical neuropharmacology* 32:224-6
- Kleven MS, Barret-Grévoz C, Bruins Slot L, Newman-Tancredi A (2005) Novel antipsychotic agents with 5-HT_{1A} agonist properties: role of 5-HT_{1A} receptor activation in attenuation of catalepsy induction in rats. *Neuropharmacology* 49:135-43
- Kornum BR, Licht CL, Weikop P, Knudsen GM, Aznar S (2006) Central serotonin depletion affects rat brain areas differently: a qualitative and quantitative comparison between different treatment schemes. *Neuroscience letters* 392:129-34
- Kornum BR, Lind NM, Gillings N, Marner L, Andersen F, Knudsen GM (2009) Evaluation of the novel 5-HT₄ receptor PET ligand [¹¹C]SB207145 in the Göttingen minipig. *Journal of cerebral blood flow and metabolism : official journal of the International Society of Cerebral Blood Flow and Metabolism* 29:186-96
- Kortekaas R, Maguire RP, Cremers TI, Dijkstra D, van Waarde A, Leenders KL (2004) In vivo binding behavior of dopamine receptor agonist (+)-PD 128907 and implications for the "ceiling effect" in endogenous competition studies with [¹¹C]raclopride—a positron emission tomography study in *Macaca mulatta*. *Journal of Cerebral Blood Flow and Metabolism* 24:531-5
- Kumar JS, Prabhakaran J, Majo VJ, Milak MS, Hsiung S, Tamir H, Simpson NR, Van Heertum RL, Mann JJ, Parsey RV (2007) Synthesis and in vivo evaluation of a novel 5-HT_{1A} receptor agonist radioligand [O-methyl- ¹¹C]2-(4-(4-(2-methoxyphenyl)piperazin-1-yl)butyl)-4-methyl-1,2,4-triazine-3,5(2H,4H)dione in nonhuman primates. *European journal of nuclear medicine and molecular imaging* 34:1050-60
- Kurrasch-Orbaugh DM, Parrish JC, Watts VJ, Nichols DE (2003a) A complex signaling cascade links the serotonin_{2A} receptor to phospholipase A₂ activation: the involvement of MAP kinases. *Journal of Neurochemistry* 86:980-991

-
- Kurrasch-Orbaugh DM, Watts VJ, Barker EL, Nichols DE (2003b) Serotonin 5-hydroxytryptamine 2A receptor-coupled phospholipase C and phospholipase A2 signaling pathways have different receptor reserves. *The Journal of pharmacology and experimental therapeutics* 304:229-37
- Laferrere B, Wurtman RJ (1989) Effect of D-fenfluramine on serotonin release in brains of anaesthetized rats. *Brain research* 504:258-63
- Laihinen AO, Rinne JO, Ruottinen HM, Någren KA, Lehtikainen PK, Oikonen VJ, Ruotsalainen UH, Rinne UK (1994) PET studies on dopamine D1 receptors in the human brain with carbon-11-SCH 39166 and carbon-11-NNC 756. *Journal of Nuclear Medicine* 35:1916-20
- Lanfumeij L and Hamon M (2004) 5-HT₁ receptors, *Curr Drug Targets CNS Neurol Disord* 3(1):1-10
- Langer O, Halldin C, Dollé F, Swahn CG, Olsson H, Karlsson P, Hall H, Sandell J, Lundkvist C, Vaufray F, Loc'h C, Crouzel C, Mazière B, Farde L (1999) Carbon-11 epidepride: a suitable radioligand for PET investigation of striatal and extrastriatal dopamine D2 receptors. *Nuclear medicine and biology* 26:509-18
- Langley K and Grant NJ (1997) Are exocytosis mechanisms neurotransmitter specific? *Neurochem Int* 31:739-57.
- Laruelle M, Abi-Dargham A, van Dyck CH, Rosenblatt W, Zea-Ponce Y, Zoghbi SS, Baldwin RM, Charney DS, Hoffer PB, Kung HF (1995) SPECT imaging of striatal dopamine release after amphetamine challenge. *Journal of nuclear medicine : official publication, Society of Nuclear Medicine* 36:1182-90
- Laruelle M, D'Souza CD, Baldwin RM, Abi-Dargham A, Kanes SJ, Fingado CL, Seibyl JP, Zoghbi SS, Bowers MB, Jatlow P, Charney DS, Innis RB (1997) Imaging D2 receptor occupancy by endogenous dopamine in humans. *Neuropsychopharmacology : official publication of the American College of Neuropsychopharmacology* 17:162-74
- Laruelle M (2000) Imaging synaptic neurotransmission with in vivo binding competition techniques: a critical review. *Journal of cerebral blood flow and metabolism* 20:423-51
- Laruelle M, Huang Y (2001) Vulnerability of Positron Emission Tomography radiotracers to endogeneous competition. *New insights. Q J Nucl Med.* 45(2):124-38.
- Lee C, Farde L (2006) Using positron emission tomography to facilitate CNS drug development. *Trends in pharmacological sciences* 27:310-6
- Leff P (1995) The two-state model of receptor activation. *Trends in Pharmacological Sciences* 16:89-97
- Leff SE, Hamblin MW, Creese I (1985) Interactions of dopamine agonists with brain D1 receptors labeled by 3H-antagonists. Evidence for the presence of high and low affinity agonist-binding states. *Molecular pharmacology* 27:171-83
- Lledo PM, Legendre P, Israel JM and Vincent JD (1990a) Dopamine inhibits two characterized voltage-dependent calcium currents in identified rat lactotroph cells. *Endocrinology* 127:990-1001.
- Lledo PM, Legendre P, Zhang J, Israel JM and Vincent JD (1990b) Effects of dopamine on voltage-dependent potassium currents in identified rat lactotroph cells. *Neuroendocrinology* 52:545-55.
- Leysen JE, Gommeren W, Mertens J, Luyten WH, Pauwels PJ, Ewert M, Seeburg P (1993) Comparison of in vitro binding properties of a series of dopamine antagonists and agonists for cloned human dopamine D_{2S} and D_{2L} receptors and for D₂ receptors in rat striatal and mesolimbic tissues, using [¹²⁵I] 2'-iodospiperone. *Psychopharmacology* 110:27-36
- Lill Y, Martinez KL, Lill MA, Meyer BH, Vogel H, Hecht B (2005) Kinetics of the Initial Steps of g protein coupled receptor-mediated cellular signaling revealed by single-molecular imaging *ChemPhysChem* 6:1633-1640
- Lind NM, Olsen AK, Moustgaard A, Jensen SB, Jakobsen S, Hansen AK, Arnfred SM, Hemmingsen RP, Gjedde A, Cumming P (2005) Mapping the amphetamine-evoked dopamine release in the brain of the Göttingen minipig. *Brain research bulletin* 65:1-9
-

- Maeda J, Suhara T, Ogawa M, Okauchi T, Kawabe K, Zhang MR, Semba J, Suzuki K (2001) In vivo binding properties of [carbonyl-11C]WAY-100635: effect of endogenous serotonin. *Synapse* (New York, N.Y.) 40:122-9
- Marner L, Gillings N, Comley RA, Baaré WF, Rabiner EA, Wilson AA, Houle S, Hasselbalch SG, Svarer C, Gunn RN, Laruelle M, Knudsen GM (2009) Kinetic modeling of 11C-SB207145 binding to 5-HT₄ receptors in the human brain in vivo. *Journal of Nuclear Medicine* 50:900-8
- Marner L, Frokjaer VG, Kalbitzer J, Lehel S, Madsen K, Baaré WF, Knudsen GM, Hasselbalch SG. (2010) Loss of serotonin 2A receptors exceeds loss of serotonergic projections in early Alzheimer's disease: a combined [(11C)DASB and [(18F]altanserin-PET study. *Neurobiol Aging*. Epub Ahead of Print
- Martin-Negrier M, Charron G, Bloch B (2006) Receptor recycling mediates plasma membrane recovery of dopamine D1 receptors in dendrites and axons after agonist-induced endocytosis in primary cultures of striatal neurons. *Synapse* 60:194-204
- Martinez D, Greene K, Broft A, Kumar D, Liu F, Narendran R, Slifstein M, Van Heertum R, Kleber HD (2009) Lower level of endogenous dopamine in patients with cocaine dependence: findings from PET imaging of D(2)/D(3) receptors following acute dopamine depletion. *The American journal of psychiatry* 166:1170-7
- McCauley PG, O'Boyle KM, Waddington JL (1995) Dopamine-induced reduction in the density of guanine nucleotide-sensitive D1 receptors in human postmortem brain in the absence of apparent D1: D2 interactions. *Neuropharmacology* 34:777-83
- McCormick PN, Wilson AA, Kapur S, Seeman P (2008) Dopamine D2 receptor radiotracers [(11C) (+)-PHNO and [(3H]raclopride are indistinguishably inhibited by D2 agonists and antagonists ex vivo. *Nuclear medicine and biology* 35:11-7
- McTavish SF, Callado L, Cowen PJ, Sharp T (1999) Comparison of the effects of α -methyl-p-tyrosine and a tyrosine-free amino acid load on extracellular noradrenaline in the rat hippocampus in vivo. *Journal of Psychopharmacology* 13:379-384
- Mintun MA, Raichle ME, Kilbourn MR, Wooten GF, Welch MJ (1984) A quantitative model for the in vivo assessment of drug binding sites with positron emission tomography. *Ann Neurol*. 15(3):217-227
- Missale C, Nash SR, Robinson SW, Jaber M and Caron MG (1998) Dopamine receptors: from structure to function. *Physiol Rev* 78:189-225.
- Mongeau R, Welner SA, Quirion R, Suranyi-Cadotte BE (1992) Further evidence for differential affinity states of the serotonin1A receptor in rat hippocampus. *Brain research* 590:229-38
- Monod J, Wyman J, Changeux JP (1965) On the nature of allosteric transitions: A plausible model. *Journal of molecular biology* 12:88-118
- Mukherjee J, Christian BT, Dunigan KA, Shi B, NaraMc Cormic 2010yanan TK, Satter M, Mantil J (2002) Brain imaging of 18F-fallypride in normal volunteers: blood analysis, distribution, test-retest studies, and preliminary assessment of sensitivity to aging effects on dopamine D-2/D-3 receptors. *Synapse* (New York, N.Y.) 46:170-88
- Mukherjee J, Christian BT, Narayanan TK, Shi B, Collins D (2005) Measurement of d-amphetamine-induced effects on the binding of dopamine D-2/D-3 receptor radioligand, 18F-fallypride in extrastriatal brain regions in non-human primates using PET. *Brain research* 1032:77-84 McCormick
- Männistö PT, Kaakkola S (1999) Catechol-O-methyltransferase (COMT): biochemistry, molecular biology, pharmacology, and clinical efficacy of the new selective COMT inhibitors. *Pharmacological reviews* 51:593-628
- Mørk A, Kreilgaard M, Sánchez C (2003) The R-enantiomer of citalopram counteracts escitalopram-induced increase in extracellular 5-HT in the frontal cortex of freely moving rats. *Neuropharmacology* 45:167-73

- Narendran R, Hwang D, Slifstein M, Hwang Y, Huang Y, Ekelund J, Guillin O, Scher E, Martinez D, Laruelle M (2005) Measurement of the Proportion of D2 Receptors Configured in State of High Affinity for Agonists in Vivo: A Positron Emission Tomography Study Using [11 C]N-Propyl-norapomorphine and [11 C]Raclopride in Baboons. *Pharmacology* 315:80-90
- Oikonen V, Allonen T, Nägren K, Kajander J, Hietala J (2000) Quantification of [Carbonyl-(11)C]WAY-100635 binding: considerations on the cerebellum. *Nuclear medicine and biology* 27:483-6
- Olivier B, Soudijn W and van Wijngaarden I (2000) Serotonin, dopamine and norepinephrine transporters in the central nervous system and their inhibitors. *Prog Drug Res* 54:59-119.
- Pakkenberg B, Gundersen H (1997) Neocortical neuron number in humans: effect of sex and age. *The Journal of Comparative Neurology* 384:312-320
- Pakkenberg B, Pelvig D, Marner L, Bundgaard MJ, Gundersen HJ, Nyengaard JR, Regeur L (2003) Aging and the human neocortex. *Experimental gerontology* 38:95-9
- Paterson LM, Tyacke RJ, Nutt DJ, Knudsen GM (2010) Measuring endogenous 5-HT release by emission tomography: promises and pitfalls. *Journal of Cerebral Blood Flow & Metabolism* 1-25
- Pedersen K, Simonsen M, Østergaard SD, Munk OL, Rosa-Neto P, Olsen AK, Jensen SB, Møller A, Cumming P (2007) Mapping the amphetamine-evoked changes in [11C]raclopride binding in living rat using small animal PET: modulation by MAO-inhibition. *NeuroImage* 35:38-46
- Piomelli D, Pilon C, Giros B, Sokoloff P, Martres MP and Schwartz JC (1991) Dopamine activation of the arachidonic acid cascade as a basis for D1/D2 receptor synergism. *Nature* 353:164-7.
- Plenevaux A, Lemaire C, Aerts J, Lacan G, Rubins D, Melega WP, Brihaye C, Degueldre C, Fuchs S, Salmon E, Maquet P, Laureys S, Damhaut P, Weissmann D, Le Bars D, Pujol JF, Luxen A (2000) [(18)F]p-MPPF: aA radiolabeled antagonist for the study of 5-HT(1A) receptors with PET. *Nuclear medicine and biology* 27:467-71
- Rabinovici GD, Furst AJ, O'Neil JP, Racine CA, Mormino EC, Baker SL, Chetty S, Patel P, Pagliaro TA, Klunk WE, Mathis CA, Rosen HJ, Miller BL, Jagust WJ (2007) 11C-PIB PET imaging in Alzheimer disease and frontotemporal lobar degeneration. *Neurology* 68:1205-12
- Rech RH, Carr LA, Moore KE (1968) Behavioral effects of alpha-methyltyrosine after prior depletion of brain catecholamines. *The Journal of pharmacology and experimental therapeutics* 160:326-35
- Rice O, Gatley S, Shen J, Huemmer C, Rogoz R, DeJesus O, Volkow N, Gifford A (2001) Effects of endogenous neurotransmitters on the in vivo binding of dopamine and 5-HT radiotracers in mice. *Neuropsychopharmacology* 25:679-689
- Rice OV, Gatley SJ, Shen J, Huemmer CL, Rogoz R, DeJesus OT, Volkow ND, Gifford AN (2001) Effects of endogenous neurotransmitters on the in vivo binding of dopamine and 5-HT radiotracers in mice. *Neuropsychopharmacology* : official publication of the American College of Neuropsychopharmacology 25:679-89
- Richfield EK, Penney JB, Young AB (1989) Anatomical and affinity state comparisons between dopamine D1 and D2 receptors in the rat central nervous system. *Neuroscience* 30:767-77
- Richfield EK, Young AB, Penney JB, Arbor A (1986) Properties of D2 Dopamine Receptor Autoradiography: High Percentage of High-Affinity Agonist Sites and Increased Nucleotide Sensitivity in Tissue Sections. *Brain Research* 383:121-128
- Robertson GS, Robertson HA (1986) Synergistic effects of D1 and D2 dopamine agonists on turning behaviour in rats. *Brain research* 384:387-90
- Rocher C, Gardier AM (2001) Effects of repeated systemic administration of d-Fenfluramine on serotonin and glutamate release in rat ventral hippocampus: comparison with methamphetamine using in vivo microdialysis. *Naunyn-Schmiedeberg's archives of pharmacology* 363:422-8
- Rominger A, Wagner E, Mille E, Böning G, Esmailzadeh M, Wängler B, Gildehaus F, Nowak S, Bruche A, Tatsch K, Bartenstein P, Cumming P (2009) Endogenous competition against binding of

- [(18)F]DMFP and [(18)F]fallypride to dopamine D(2/3) receptors in brain of living mouse. *Synapse* 64:313-322
- Roth BL, Choudhary MS, Khan N, Uluer AZ (1997) High-affinity agonist binding is not sufficient for agonist efficacy at 5-hydroxytryptamine_{2A} receptors: evidence in favor of a modified ternary complex model. *The Journal of pharmacology and experimental therapeutics* 280:576-83
- Roth BL, Egan C, Grinde E, Dupre a, Hake M, Teitler M, Herrick-Davis K (2000) Agonist high and low affinity state ratios predict drug intrinsic activity and a revised ternary complex mechanism at serotonin 5-HT(2A) and 5-HT(2C) receptors. *Synapse* 35:144-50
- Roth BL, Willins DL, Kristiansen K, Kroeze WK (1998) 5-Hydroxytryptamine₂-family receptors (5-hydroxytryptamine_{2A}, 5-hydroxytryptamine_{2B}, 5-hydroxytryptamine_{2C}): where structure meets function. *Pharmacology & therapeutics* 79:231-57
- Ryman-Rasmussen JP, Griffith A, Oloff S, Vaidehi N, Brown JT, Goddard WA, Mailman RB (2007) Functional selectivity of dopamine D1 receptor agonists in regulating the fate of internalized receptors. *Neuropharmacology* 52:562-75
- Sadzot B, Lemaire C, Maquet P, Salmon E, Plenevaux A, Degueldre C, Hermanne JP, Guillaume M, Cantineau R, Comar D (1995) Serotonin 5HT₂ receptor imaging in the human brain using positron emission tomography and a new radioligand, [18F]altanserin: results in young normal controls. *Journal of cerebral blood flow and metabolism : official journal of the International Society of Cerebral Blood Flow and Metabolism* 15:787-97
- Sanabria-Bohórquez SM, Biver F, Damhaut P, Wikler D, Veraart C, Goldman S (2002) Quantification of 5-HT(1A) receptors in human brain using p-MPPF kinetic modelling and PET. *European journal of nuclear medicine and molecular imaging* 29:76-81
- Seamans JK, Floresco SB, Phillips AG (1998) D1 receptor modulation of hippocampal-prefrontal cortical circuits integrating spatial memory with executive functions in the rat. *The Journal of Neuroscience* 18:1613-21
- Seeman P, Schwarz J, Chen J, Szechtman H, Perreault M, McKnight GS, Roder JC, Quirion R, Boksa P, Srivastava LK, Yanai K, Weinshenker D, Sumiyoshi T (2006) Psychosis pathways converge via D₂high dopamine receptors. *Synapse (New York, N.Y.)* 60:319-46
- Seneca N, Finnema SJ, Farde L, Gulyás B, Wikström HV, Halldin C, Innis RB (2006) Effect of amphetamine on dopamine D₂ receptor binding in nonhuman primate brain: a comparison of the agonist radioligand [11C]MNPA and antagonist [11C]raclopride. *Synapse* 59:260-9
- Serdons K, Verbruggen A, Bormans GM (2009) Developing new molecular imaging probes for PET. *Methods* 48:104-11
- Sharp T, Zetterström T, Ljungberg T, Ungerstedt U (1987) A direct comparison of amphetamine-induced behaviours and regional brain dopamine release in the rat using intracerebral dialysis. *Brain research* 401:322-30
- Shi B, Narayanan TK, Christian BT, Chattopadhyay S, Mukherjee J (2004) Synthesis and biological evaluation of the binding of dopamine D₂/D₃ receptor agonist, (R,S)-5-hydroxy-2-(N-propyl-N-(5'-(18)F-fluoropentyl)aminotetralin ((18)F-5-OH-FPPAT) in rodents and nonhuman primates. *Nuclear medicine and biology* 31:303-11
- Shi J, Damjanoska KJ, Singh RK, Carrasco GA, Garcia F, Grippo AJ, Landry M, Sullivan NR, Battaglia G, Muma NA (2007) Agonist induced-phosphorylation of Galpha11 protein reduces coupling to 5-HT_{2A} receptors. *The Journal of pharmacology and experimental therapeutics* 323:248-56
- Shi J, Landry M, Carrasco Ga, Battaglia G, Muma Na (2008) Sustained treatment with a 5-HT(2A) receptor agonist causes functional desensitization and reductions in agonist-labeled 5-HT(2A) receptors despite increases in receptor protein levels in rats. *Neuropharmacology* 55:687-92
- Shuto T, Seeman P, Kuroiwa M, Nishi A (2008) Repeated administration of a dopamine D₁ receptor agonist reverses the increased proportions of striatal dopamine D₁High and D₂High receptors in methamphetamine-sensitized rats. *The European journal of neuroscience* 27:2551-7

- Sibley D, Creese I (1979) Guanine nucleotides regulate anterior pituitary dopamine receptors. *European journal of pharmacology* 55:341-343
- Sibley DR, De Lean A, Creese I (1982) Anterior pituitary dopamine receptors. Demonstration of interconvertible high and low affinity states of the D-2 dopamine receptor. *The Journal of biological chemistry* 257:6351-61
- Sidhu A, Vachvanichsanong P, Jose PA, Felder RA (1992) Persistent Defective Coupling of Dopamine-1 Receptors to G Proteins after Solubilization from Kidney Proximal Tubules of Hypertensive Rats. *The Journal of Clinical Investigation* 89:789-793
- Sjostrom R, Ekstedt J and Anggard E (1975) Concentration gradients of monoamine metabolites in human cerebrospinal fluid. *J Neurol Neurosurg Psychiatry* 38:666-8.
- Smiley JF, Levey AI, Ciliax BJ, Goldman-Rakic PS (1994) D1 dopamine receptor immunoreactivity in human and monkey cerebral cortex: predominant and extrasynaptic localization in dendritic spines. *Proceedings of the National Academy of Sciences of the United States of America* 91:5720-4
- Sokoloff, P., Giros, B., Martres, M.P., Bouthenet, M.L. and Schwartz, J.C. (1990) Molecular cloning and characterization of a novel dopamine receptor (D3) as a target for neuroleptics. *Nature* 347, 146-51.
- Song J, Hanniford D, Doucette C, Graham E, Poole MF, Ting A, Sherf B, Harrington J, Brunden K, Stricker-Krongrad A (2005) Development of homogeneous high-affinity agonist binding assays for 5-HT₂ receptor subtypes. *Assay and drug development technologies* 3:649-59
- Stathis M, Scheffel U, Lever SZ, Boja JW, Carroll FI, Kuhar MJ (1995) Rate of binding of various inhibitors at the dopamine transporter in vivo. *Psychopharmacology* 119:376-84
- Steigrad P, Tobler I, Waser PG, Borbély AA (1978) Effect of p-chlorophenylalanine on cerebral serotonin binding, serotonin concentration and motor activity in the rat. *Naunyn-Schmiedeberg's archives of pharmacology* 305:143-8
- Stoof JC and Kebabian JW (1984) Two dopamine receptors: Biochemistry, Physiology and Pharmacology. *Life Science* 35:2281-96.
- Sumiyoshi T, Seeman P, Uehara T, Itoh H, Tsunoda M, Kurachi M (2005) Increased proportion of high-affinity dopamine D2 receptors in rats with excitotoxic damage of the entorhinal cortex, an animal model of schizophrenia. *Brain Research* 140:116-9
- Sunahara RK, Niznik HB, Weiner DM, Stormann TM, Brann MR, Kennedy JL, Gelernter JE, Rozmahel R, Yang YL, Israel Y, Seeman P and O'Dowd BF (1990) Human dopamine D1 receptor encoded by an intronless gene on chromosome 5. *Nature* 347:80-3.
- Syvänen S, Lindhe O, Palner M, Kornum BR, Rahman O, Långström B, Knudsen GM, Hammarlund-Udenaes M (2009) Species differences in blood-brain barrier transport of three positron emission tomography radioligands with emphasis on P-glycoprotein transport. *Drug metabolism and disposition* 37:635-43
- Syvänen S (2008) Blood-Brain Barrier Transport, investigation of active efflux using positron emission tomography and modelling studies. :15-17
- Trouvin JH, Prioux-Guyonneau M, Cohen Y and Jacquot C (1986) Rat brain monoamine metabolism and hypobaric hypoxia: a new approach. *Gen Pharmacol* 17:69-73.
- Trovero F, Marin P, Tassin JP, Premont J, Glowinski J (1994) Accelerated resensitization of the D1 dopamine receptor-mediated response in cultured cortical and striatal neurons from the rat: respective role of alpha 1-adrenergic and N-methyl-D-aspartate receptors. *The Journal of Neuroscience* 14:6280-8
- Udo De Haes JI, Cremers TI, Bosker F, Postema F, Tiemersma-Wegman TD, den Boer JA (2005) Effect of increased serotonin levels on [18F]MPPF binding in rat brain: fenfluramine vs the combination of citalopram and ketanserin. *Neuropsychopharmacology : official publication of the American College of Neuropsychopharmacology* 30:1624-31

-
- Vallone D, Picetti R and Borrelli E (2000) Structure and function of dopamine receptors. *Neurosci Biobehav Rev* 24:125-32.
- Van Tol HH, Bunzow JR, Guan HC, Sunahara RK, Seeman P, Niznik HB and Civelli O (1991) Cloning of the gene for a human dopamine D4 receptor with high affinity for the antipsychotic clozapine. *Nature* 350:610-4.
- Williams GV, Goldman-Rakic PS (1995) Modulation of memory fields by dopamine D1 receptors in prefrontal cortex. *Nature* 376:572-5
- Wilson AA, McCormick P, Kapur S, Willeit M, Garcia A, Hussey D, Houle S, Seeman P, Ginovart N (2005) Radiosynthesis and evaluation of [¹¹C]-(+)-4-propyl-3,4,4a,5,6,10b-hexahydro-2H-naphtho[1,2-b][1,4]oxazin-9-ol as a potential radiotracer for in vivo imaging of the dopamine D2 high-affinity state with positron emission tomography. *Journal of medicinal chemistry* 48:4153-60
- Wilson SJ, Bailey JE, Rich AS, Nash J, Adrover M, Tournoux A, Nutt DJ (2005) The use of sleep measures to compare a new 5HT1A agonist with buspirone in humans. *Journal of Psychopharmacology* 19:609-13
- Yang ZY, Perry B, Mukherjee J (1996) Fluorinated benzazepines: 1. Synthesis, radiosynthesis and biological evaluation of a series of substituted benzazepines as potential radiotracers for positron emission tomographic studies of dopamine D-1 receptors. *Nuclear medicine and biology* 23:793-805
- Zahniser NR, Molinoff PB (1978) Effect of guanine nucleotides on striatal dopamine receptors. *Nature* 275:453-5
- Zimmer L, Le Bars D, Mauger G, Luxen A, Bonmarchand G, Pujol J (2002) Effect of endogenous serotonin on the binding of the 5-HT1A PET ligand 18F-MPPF in the rat hippocampus: kinetic beta measurements combined with microdialysis. *Journal of neurochemistry* 80:278-86
- Zimmer L, Rbuh L, Giacomelli F, Le Bars D, Renaud B (2003) A reduced extracellular serotonin level increases the 5-HT1A PET ligand 18F-MPPF binding in the rat hippocampus. *Journal of nuclear medicine : official publication, Society of Nuclear Medicine* 44:1495-501
-

Appendices

- I **Mikael Palner**, Patrick McCormick, Nic Gillings, Mikael Begtrup, Alan A. Wilson, Gitte M. Knudsen (2010) Radiosynthesis and *ex vivo* evaluation of (*R*)-(-)-2-chloro-*N*-[1-¹¹C-propyl]*n*-propylnorapomorphine. Nucl Med Biol 37(1):35-40 Page 59
- II **Mikael Palner**, Patrick McCormick, Jun Parkes, Gitte M Knudsen, Alan A. Wilson (2010) Systemic catechol-O-methyl transferase inhibition enables the D₁ agonist radiotracer *R*-[¹¹C]SKF 82957. Nucl Med Biol 37(7): 837-843 Page 65
- III **Mikael Palner**, Celia Kjaerby, Gitte M Knudsen, Paul Cumming (2011) Effects of unilateral 6-OHDA lesion on [3H]NPA binding in striatum *ex vivo*, and vulnerability to amphetamine-evoked dopamine release in rat. Neurochem International 58: 243-247 Page 72
- IV **Mikael Palner**, Mark Underwood, Dileep Kumar, Victoria Arango, Gitte M Knudsen, J. John Mann, Ramin V. Parsey (2010) *Ex vivo* binding and pharmacological challenges of the serotonin 1A receptor agonist [³H]CUMI-101 in awake rats. In Press Synapse Page 77
- V Anders Ettrup, **Mikael Palner**, Nic Gillings, Martin A. Santini, Martin Hansen, Birgitte R. Kornum, Lars K. Rasmussen, Kjell Någren, Jacob Madsen, Mikael Begtrup, Gitte M Knudsen (2010) Radiosynthesis and evaluation of [¹¹C]Cimbi-5 as a 5-HT_{2A} receptor agonist radioligand for positron emission tomography. Journal of Nuclear Medicine 51:1-8 Page 86
-

Radiosynthesis and ex vivo evaluation of (*R*)-(-)-2-chloro-*N*-[1-¹¹C-propyl]*n*-propylnorapomorphine[☆]

Mikael Palner^{a,b,*}, Patrick McCormick^c, Nic Gillings^{b,d}, Mikael Begtrup^{b,e}, Alan A. Wilson^c, Gitte M. Knudsen^{a,b}

^aNeurobiology Research Unit, Rigshospitalet, University of Copenhagen, DK-2300, Copenhagen, Denmark

^bCenter for Integrated Molecular Brain Imaging, Copenhagen, Denmark

^cPET Centre, Centre for Addiction and Mental Health, M5T 1R8, Toronto, ON, Canada

^dPET and Cyclotron Unit, Rigshospitalet, DK-2300, Copenhagen, Denmark

^eInstitute for Medicinal Chemistry, Pharmaceutical Faculty, University of Copenhagen, DK-2300, Copenhagen, Denmark

Received 13 March 2009; received in revised form 4 August 2009; accepted 23 August 2009

Abstract

Introduction: Several dopamine D₂ agonist radioligands have been used with positron emission tomography (PET), including [¹¹C]-(-)-MNPA, [¹¹C]-(-)-NPA and [¹¹C]-(+)-PHNO. These radioligands are considered particularly powerful for detection of endogenous dopamine release, but they either provide PET brain images with limited contrast or have affinity for both D₂ and D₃ receptors. We here present the carbon-11 radiolabeling and ex vivo evaluation of 2-Cl-(-)-NPA, a novel PET-tracer candidate with high in vitro D₂/D₃ selectivity.

Methods: 2-Cl-[¹¹C]-(-)-NPA and [¹¹C]-(-)-NPA were synthesized by a two step *N*-acylation-reduction process using [¹¹C]-propionyl chloride. Awake rats were injected with either tracer, via the tail vein. The rats were decapitated at various times, the brains were removed and quickly dissected, and plasma metabolites were measured. Radioligand specificity, and P-glycoprotein involvement in brain uptake, was also assessed.

Results: 2-Cl-[¹¹C]-(-)-NPA and [¹¹C]-(-)-NPA were produced in high specific activity and purity. 2-Cl-[¹¹C]-(-)-NPA accumulated slower in the striatum than [¹¹C]-(-)-NPA, reaching maximum concentrations after 30 min. The maximal striatal uptake of 2-Cl-[¹¹C]-(-)-NPA (standard uptake value 0.72±0.24) was approximately half that of [¹¹C]-(-)-NPA (standard uptake value 1.37±0.18). Nonspecific uptake was similar for the two compounds. 2-Cl-[¹¹C]-(-)-NPA was metabolized quickly, leaving only 17% of the parent compound in the plasma after 30 min. The specific binding of 2-Cl-[¹¹C]-(-)-NPA was completely blocked and inhibition of P-glycoprotein did not alter the brain uptake.

Conclusion: Ex vivo experiments showed, despite a favorable D₂/D₃ selectivity, that 2-Cl-[¹¹C]-(-)-NPA is inferior to [¹¹C]-(-)-NPA as a PET tracer in rat, because of slower brain uptake and lower specific to nonspecific binding ratio.

© 2010 Elsevier Inc. All rights reserved.

Keywords: PET; Agonist; D₂; D₃; Dopamine; Apomorphine; 2-Cl-[¹¹C]-(-)-NPA; [¹¹C]-(-)-NPA; Radioligand; P-glycoprotein; Amphetamine

[☆] This work was supported by the Danish Agency for Science, Technology and Innovation; Rigshospitalet; the EC-FP6-project DiMI, LSHB-CT-2005-512146; the Centre of Addiction and Mental Health in Toronto, Canada; and the Lundbeck Foundation, Denmark. *K_i* determinations were generously performed by the National Institute of Mental Health's Psychoactive Drug Screening Program (NIMH PDSP), contract no. NO1MH32004.

* Corresponding author. Neurobiology Research Unit, Rigshospitalet, DK-2100 Copenhagen, Denmark. Tel.: +45 3545 6704; fax: +45 3545 6713.

E-mail address: mikael.palner@nru.dk (M. Palner).

1. Introduction

Dopamine receptors are implicated in numerous neuropharmacological functions and in diseases such as schizophrenia [1] and Parkinson's disease [2]. Also, increased dopamine release is implicated in the pathology of psychosis [3]. In order to understand these functions fully, it is fundamental to expand our knowledge of the interactions and implications of the dopaminergic system. Based on their intracellular secondary messengers, the G protein-coupled

dopamine receptors can be divided into two major classes: D₁-like receptors (D₁ and D₅) linked to activation of adenylate cyclase, and D₂-like receptors (D₂, D₃ and D₄) linked to inhibition of adenylate cyclase [4].

Based on the results from in vitro competition between agonist and antagonists, D₂ receptors are believed to exist in two affinity states: a functional state coupled to G-protein with high affinity for endogenous dopamine and exogenous agonists (D₂^{high}), and a state not coupled to G-protein with lower affinity to endogenous dopamine and exogenous agonists (D₂^{low}). While the presence of these different affinity states is clearly identified in vitro [5], the in vivo relevance of this model is still debated. Recent studies have cast some doubt on the in vivo applicability of the two affinity state model (two-state model). For example, rather than a biphasic displacement of [¹¹C]raclopride from striatum in nonhuman primate by the D₂/D₃ agonist (+)-PD 128907, expected on the basis of the two-state model [6], the displacement was monophasic and complete [7]. Furthermore, in an ex vivo dual-tracer rat study, agonist and antagonist drugs were equally efficient in displacement of the D₂/D₃ agonist [¹¹C]-(+)-PHNO and the D₂/D₃ antagonist [³H]raclopride [8]. On the other hand, in a study in awake mouse the D₂/D₃ agonist [³H]-(-)-NPA was found to be 60% more sensitive to an amphetamine challenge than [¹¹C]raclopride [9], and similar findings were seen in anaesthetized nonhuman primates with [¹¹C]-(-)-NPA [10] and [¹¹C]-(-)-MNPA [11]. The existence of two distinguishable affinity states in vivo is therefore still debatable and more investigations are needed.

Recently, several suitable dopamine D₂ agonist radioligands have been developed for positron emission tomography (PET) scanning, including the ¹¹C-labeled apomorphines [¹¹C]-(-)-NPA [12] and [¹¹C]-(-)-MNPA [13], and the naphthoxazine [¹¹C]-(+)-PHNO [14]. Another newly developed agonist is the fluorinated tetralin analogue [¹⁸F]-5-OH-FPPAT [15]. As agonists, these radioligands are considered particularly suitable for detection of endogenous dopamine release, but their properties are not optimal, for two reasons. Firstly, they display affinity for both D₂ and D₃ receptors; in vivo [¹¹C]-(+)-PHNO is even a D₃ receptor preferring agonist [16], and, secondly, the apomorphine derivatives provide PET brain images with limited contrast which is of particular concern if these radiotracers are to be utilized as markers of endogenously increased dopamine levels.

The presence of electron-withdrawing groups at the 2-position was shown to considerably enhance the affinity of apomorphines to the dopamine D₂ receptor [17]. Recently, we developed a new synthesis route for the preparation of 2-substituted apomorphines [18] and used this method to make a series of 2-substituted apomorphines (unpublished work). One of the promising candidates, 2-Cl(-)-NPA, showed a higher D₂ over D₃ selectivity (D₂/D₃ 0.26) than (-)-NPA (D₂/D₃ 0.56). Here, we present the radiolabelling of 2-Cl(-)-NPA with carbon-11 and the ex vivo evaluation of this compound in conscious rats.

2. Material and methods

2.1. Synthesis of (R)-(-)-2-chloro-N-[1-¹¹C-propyl]n-propylnorapomorphine (2-Cl-[¹¹C]-(-)-NPA)

[¹¹C]Propionyl chloride/THF (prepared as described previously) [14] was distilled into a 5-ml V-vial containing (-)-2-chloronorapomorphine hydrobromide (2 mg), *N,N*-diisopropylethylamine (100 μl) and THF (100 μl) at -30°C. When levels of radioactivity in the vial peaked, the vial was immersed in an oil bath at 85°C until the internal temperature reached 60°C (about 2.5 min). Two minutes later, the vial was cooled in an ethanol/dry ice bath until the internal temperature was below -30°C, at which point LiAlH₄ in THF (0.2 M, 0.6 ml) was added. The vial was then reimmersed in the oil bath and THF was removed by a flow of N₂ (80 ml/min) through the vial. When THF removal was complete, 0.6 M aqueous HCl (0.8 ml) was added, followed, after 30 s, by 1 ml of the HPLC eluent. The reaction mixture was purified by reverse-phase HPLC using Phenomenex Luna C18(2) (250×10 mm), eluting with 30% CH₃CN 70% H₂O+0.1 M aqueous ammonium formate at pH 4 (6 ml/min) and monitoring by UV (280 nm) and radioactivity detectors. The desired fraction (R_t 10 min) was collected in a flask containing 4% aqueous L-ascorbic acid (0.25 ml), evaporated to dryness under vacuum at 70°C, and the residue taken up in 10 ml of sterile saline. The saline solution of 2-Cl-[¹¹C]-(-)-NPA was passed through a sterile 0.22-μm filter into a sterile, pyrogen-free bottle containing 8.4% aqueous sodium bicarbonate (1 ml). Aliquots of the formulated solution were used to establish the chemical and radiochemical purity and the specific activity of the final solution by analytical HPLC on Phenomenex Prodigy C18 10 μm (250×4.5 mm), eluting with 30% CH₃CN 70% H₂O+0.1 M ammonium formate at pH 4 (3 ml/min). The radiosynthesis is summarized in Fig. 1.

2.2. Synthesis of (R)-(-)-[1-¹¹Cpropyl]n-propylnorapomorphine ([¹¹C]-(-)-NPA)

[¹¹C]-(-)-NPA was prepared in an identical fashion to 2-Cl-[¹¹C]-(-)-NPA using (-)-norapomorphine hydrobromide as precursor.

2.3. Animal studies

Rats (male, Sprague-Dawley) weighing 340±35 g were used in the study. Animal experiments were conducted in accordance with the guidelines of the Canadian Council on Animal Care and with approval from the Animal Care Committee at the Center of Addiction and Mental Health. Rats were kept on a 12-h light/dark cycle with free access to food and water.

2.4. Time-activity curve and plasma metabolites

Rats were injected in the tail vein with 2-Cl-[¹¹C]-(-)-NPA or [¹¹C]-(-)-NPA (37 MBq per rat, corrected to the time of the first injection on the day of the experiment; specific activity around 30 GBq/μmol). The rats were

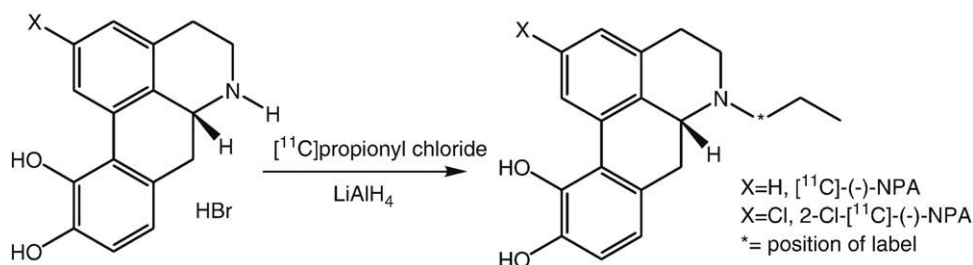


Fig. 1. Radiosynthesis of 2-Cl- $[^{11}\text{C}]\text{-}(-)\text{-NPA}$ and $[^{11}\text{C}]\text{-}(-)\text{-NPA}$.

decapitated at different time points (5, 15, 30 and 60 min, $n=4$ for each time point); the brain was removed, placed on ice and quickly dissected into striatum, frontal cortex (anterior 3 mm of the brain) and cerebellum. Blood from the trunk was collected and the plasma obtained by centrifugation. Then, glacial acetic acid was added to the plasma (10 vol%) and the plasma sample was directly analyzed with HPLC using an OASIS capture column and 1% CH_3CN in water (2 ml/min) and C18 Luna 10 μm (250 \times 4.6 mm), 2 ml/min, 30% $\text{CH}_3\text{CN}/70\%$ $\text{H}_2\text{O}+0.1\text{N}$ ammonium formate+1% formic acid, as described previously [19]. All brain tissue samples were collected in tared counting vials and counted in a gamma counter. The injected dose was corrected for remaining activity in the syringe and the tail of the rat. Time–activity curves (TACs) and standard uptake values [SUVs=(Activity in region of interest/Brain mass)/(Activity injected/Rat weight)] were subsequently calculated using diluted aliquots of the injected dose as standards, and the specific binding ratio [SBR=((Activity in region of interest – Activity in cerebellum)/Activity in cerebellum)] calculated from the SUV values.

2.5. Competition and P-glycoprotein inhibition studies

Rats were divided into four groups ($n=4$ per group): haloperidol treated (A), cyclosporin A treated (B), haloperidol and cyclosporin A treated (C), and untreated controls (D). Group A rats were injected with haloperidol (5 mg/kg sc in 0.3 ml of saline) 30 min prior to 2-Cl- $[^{11}\text{C}]\text{-}(-)\text{-NPA}$ administration; Group B were injected with cyclosporin A (50 mg/kg iv in 0.3 ml of saline) 40 min prior to radiotracer injection; Group C were injected with both haloperidol and

cyclosporin A as described above. 2-Cl- $[^{11}\text{C}]\text{-}(-)\text{-NPA}$ (15 \pm 5 MBq) was injected in the tail vein and the rats were decapitated 40 min after. The brains and blood samples were treated as described above. Plasma and brain tissue samples were collected in tared counting vials and counted in a gamma counter. Tails and syringes were counted and the SUV was calculated as described above.

2.6. Statistics and calculations

SUVs and SBRs were calculated in Excel, and TACs were calculated using GraphPad Prism version 5. Significant blocking of 2-Cl- $[^{11}\text{C}]\text{-}(-)\text{-NPA}$ by haloperidol was assessed by a one-tailed unpaired t test. Log D was calculated using Pallas 3.5 (CompuDrug International, Inc., Sedona, AZ, USA).

3. Results

Thirty-five gigabecquerel of $[^{11}\text{C}]\text{CO}_2$ afforded 2–2.9 GBq of 2-Cl- $[^{11}\text{C}]\text{-}(-)\text{-NPA}$ and 2.5–3.5 GBq of $[^{11}\text{C}]\text{-}(-)\text{-NPA}$ in 40 min. The specific activities of the radioligands were 28–45 GBq/ μmol at end of synthesis and the radiochemical purities exceeded 97%. In the absence of ascorbic acid, both radioligands underwent extensive radiolysis during the formulation process.

Table 1 summarizes the pharmacological and binding characteristics of 2-Cl- $[^{11}\text{C}]\text{-}(-)\text{-NPA}$ and $[^{11}\text{C}]\text{-}(-)\text{-NPA}$.

The brain 2-Cl- $[^{11}\text{C}]\text{-}(-)\text{-NPA}$ and $[^{11}\text{C}]\text{-}(-)\text{-NPA}$ TACs and SBRs are presented in Fig. 2. 2-Cl- $[^{11}\text{C}]\text{-}(-)\text{-NPA}$ was found to be highest in the dopamine D_2 -rich striatum, whereas uptake in frontal cortex was very similar to that in the cerebellum. In striatum, maximum uptake was seen

Table 1
Lipophilicity (Log P), K_i values of $[^{11}\text{C}]\text{-}(-)\text{-NPA}$ and 2-Cl- $[^{11}\text{C}]\text{-}(-)\text{-NPA}$ for D_2 and D_3 , SUV and SBR

	cLog D^*	D_2K_i (nM)**	D_3K_i (nM)**	D_2/D_3	SUV		SBR (60 min)
					Striatum (60 min)	Cerebellum (60 min)	
2-Cl- $[^{11}\text{C}]\text{-}(-)\text{-NPA}$	2.25	4.52 \pm 0.98	17.26 \pm 2.88	0.26	0.72 \pm 0.24	0.33 \pm 0.02	1.18 \pm 0.78
$[^{11}\text{C}]\text{-}(-)\text{-NPA}$	0.79	0.12 \pm 0.04	0.21 \pm 0.09	0.57	1.37 \pm 0.18	0.32 \pm 0.04	3.31 0.32

Values are given as means \pm S.E.M.

* cLog $D_{7,4}$ (Pallas 3.5).

** NIMH PDSP and Ref. [20].

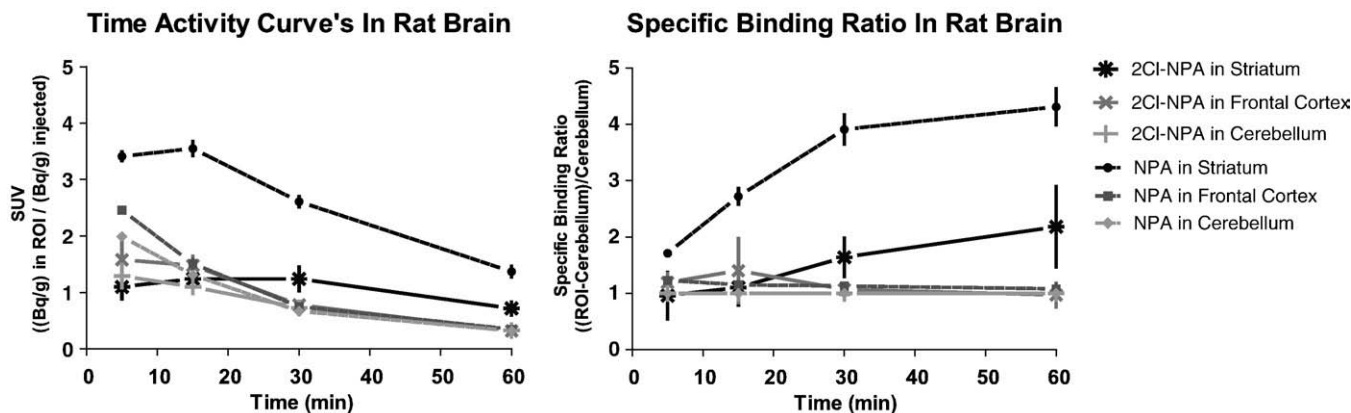


Fig. 2. Ex vivo TACs of 2-Cl-[¹¹C]-(-)-NPA and [¹¹C]-(-)-NPA in rat striatum, frontal cortex and cerebellum. Specific binding ratios at different time points are calculated for striatum and frontal cortex using the cerebellum as the reference region.

30 min after injection of 2-Cl-[¹¹C]-(-)-NPA, whereas the maximum uptake of [¹¹C]-(-)-NPA was found at 15 min after injection. At 60 min, the SUV in striatum was 0.72 ± 0.24 for 2-Cl-[¹¹C]-(-)-NPA, around half of the 1.37 ± 0.18 found for [¹¹C]-(-)-NPA. Cerebellum uptake (equivalent to nonspecific uptake) at early time points was higher for [¹¹C]-(-)-NPA than for 2-Cl-[¹¹C]-(-)-NPA, but by 30 min the cerebellum uptake was similar with both radiotracers; at 60 min, the SUV in cerebellum was 0.33 ± 0.02 for 2-Cl-[¹¹C]-(-)-NPA and 0.32 ± 0.04 for [¹¹C]-(-)-NPA. The SBR in the striatum was 1.18 ± 0.78 for 2-Cl-[¹¹C]-(-)-NPA and 3.31 ± 0.32 for [¹¹C]-(-)-NPA at 60 min, reflecting the SUV values reported above.

HPLC measurements of plasma taken 15 min after injection showed that only 17% of the parent compound (2-Cl-[¹¹C]-(-)-NPA) remained and that at least three hydrophilic metabolites were present. No lipophilic metabolites were identified in the plasma. A typical HPLC chromatogram is shown in Fig. 3.

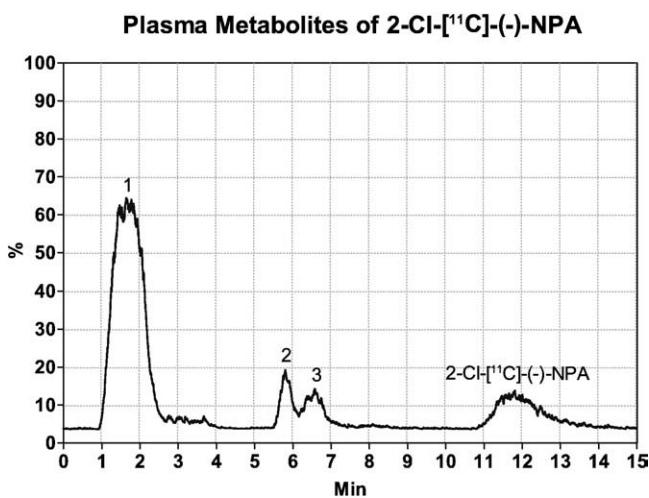


Fig. 3. A representative HPLC chromatogram of plasma from a 2-Cl-[¹¹C]-(-)-NPA-injected rat, 15 min after injection. At least three radiolabelled metabolites and the parent compound can be identified in the chromatogram.

The specific binding of 2-Cl-[¹¹C]-(-)-NPA could be blocked by pretreatment with haloperidol (Fig. 4) (*T* test, $P < .0001$). Pretreatment with cyclosporine A to inhibit the P-glycoprotein efflux transporter did not alter the brain uptake of 2-Cl-[¹¹C]-(-)-NPA.

4. Discussion

We successfully radiolabelled 2-Cl-[¹¹C]-(-)-NPA and [¹¹C]-(-)-NPA in good yields by modifications of the *N*-acylation-reduction method first described by Hwang et al. [12] for labeling [¹¹C]-(-)-NPA.

In ex vivo experiments in the rat, we found that a new selective agonist PET tracer for the dopamine D₂ receptor, 2-Cl-[¹¹C]-(-)-NPA, had a lower signal-to-noise ratio and a slower brain accumulation than did [¹¹C]-(-)-NPA. After 60 min, the SBR was 1.18 for 2-Cl-[¹¹C]-(-)-NPA as compared to 3.31 for [¹¹C]-(-)-NPA. [¹¹C]-(+)-PHNO has been reported to have even faster uptake than [¹¹C]-(-)-NPA and a higher SBR of 4.6 at 60 min [14]. In vivo, [¹¹C]-(+)-PHNO is a D₃ preferring tracer and for that reason

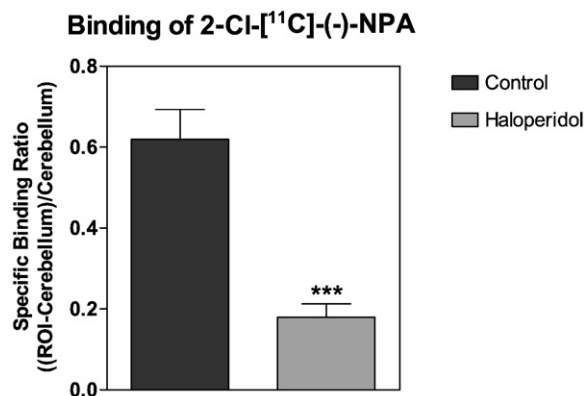


Fig. 4. Specific binding ratios after pretreatment with the dopamine D₂ antagonist haloperidol.

we chose not to compare it to 2-Cl-[¹¹C]-(-)-NPA. It is worth mentioning that the SBR of 3.31 from our [¹¹C]-(-)-NPA experiments closely resembles the SBR of 3.4 reported by Hwang et al. [12] in the same species.

The D₂/D₃ agonist [¹¹C]-(-)-MNPA shows a SBR of 1.23 (at 78 min) in cynomolgus monkeys [13]. This is similar to [¹¹C]-(-)-NPA which has a SBR of 1.8 at 45 min in baboons [12], but with slower kinetics. Generally, the SBR of apomorphines seems lower in nonhuman primates than in rats, and for that reason it is considered unlikely that 2-Cl-[¹¹C]-(-)-NPA would have a better outcome as a radiotracer in higher species.

We found that after systemic injection, 2-Cl-[¹¹C]-(-)-NPA was metabolized fairly rapidly with only 17% unchanged compound in plasma after 15 min. The metabolites were composed of at least three polar metabolites, but no lipophilic metabolites were observed. Forty to 45 min after intravenous injection of [¹¹C]-(-)-NPA, 20% of the compound is unchanged in the plasma of pigs [9] and 30% in that of baboon [12]. Similarly, 40 min after [¹¹C]-(+)-PHNO injection in rats, 26% remains unchanged in the plasma [14]. For [¹¹C]-(-)-MNPA, the fraction is 20% in the cynomolgus monkey at 45 min after injection. It is likely that this rapid systemic metabolism contributes to the overall relatively low brain uptake of 2-Cl-[¹¹C]-(-)-NPA. The calculated lipophilicity of 2-Cl-[¹¹C]-(-)-NPA (cLogD_{7,4}=2.25) is much higher than that of [¹¹C]-(-)-NPA (cLogD_{7,4}=0.79). This could be one of the contributing factors to the lower SBR. We did not measure protein binding of any of the radiotracers, but it is possible that a lower plasma free fraction of 2-Cl-[¹¹C]-(-)-NPA associated with its higher lipophilicity counteracted the anticipated increase in brain uptake. Alternatively, 2-Cl-[¹¹C]-(-)-NPA could be a substrate for the efflux transporter P-glycoprotein [21] and, therefore, we investigated whether inhibition of P-glycoprotein with cyclosporine A could enhance the brain uptake of 2-Cl-[¹¹C]-(-)-NPA. We found no evidence that P-glycoprotein activity is the cause of the relatively limited brain uptake of 2-Cl-[¹¹C]-(-)-NPA. We cannot exclude that the superior characteristics of [¹¹C]-(-)-NPA as a PET tracer as compared to 2-Cl-[¹¹C]-(-)-NPA could be reverted in primates. Based on these rodent data, however, a more viable approach would be to test other analogues. We suggest that better D₂ receptor agonist PET tracers may be developed by 2-substitution of apomorphine derivatives with, e.g., fluorine or hydroxy, with the aim of lowering lipophilicity and nonspecific binding and increasing brain penetration.

5. Conclusion

We have described an efficient radiosynthesis of [¹¹C]-(-)-2-Cl-NPA, a novel in vitro selective D₂ agonist. Ex vivo studies in the rat showed that 2-Cl-[¹¹C]-(-)-NPA in comparison to other commonly used D₂/D₃ radiotracers had a relatively high systemic metabolism, a slower brain

uptake and a lower target-to-background ratio. Based on studies of [¹¹C]-(-)-NPA, it is considered unlikely that the radiotracer would show improved pharmacokinetic properties in nonhuman primates or humans.

Acknowledgments

The NIMH PDSP is directed by Bryan L. Roth, M.D., Ph.D., at the University of North Carolina at Chapel Hill and Project Officer Jamie Driscoll at NIMH, Bethesda, MD, USA.

References

- [1] Seeman P, Schwarz J, Chen JF, Szechtman H, Perreault M, McKnight GS, et al. Psychosis pathways converge via D₂ high dopamine receptors. *Synapse* 2006;60(4):319–46.
- [2] Dentresangle C, Veyre L, Le BD, Pierre C, Lavenne F, Pollak P, et al. Striatal D₂ dopamine receptor status in Parkinson's disease: an [¹⁸F]dopa and [¹¹C]raclopride PET study. *Mov Disord* 1999;14(6):1025–30.
- [3] Toda M, bi-Dargham A. Dopamine hypothesis of schizophrenia: making sense of it all. *Curr Psychiatry Rep* 2007;9(4):329–36.
- [4] Stoof JC, Kebebian JW. Two dopamine receptors: biochemistry, physiology and pharmacology. *Life Sci* 1984;35(23):2281–96.
- [5] Sibley DR, De LA, Creese I. Anterior pituitary dopamine receptors. Demonstration of interconvertible high and low affinity states of the D-2 dopamine receptor. *J Biol Chem* 1982;257(11):6351–61.
- [6] Seeman P, Tallerico T, Ko F. Dopamine displaces [³H]domperidone from high-affinity sites of the dopamine D₂ receptor, but not [³H]raclopride or [³H]spiperone in isotonic medium: implications for human positron emission tomography. *Synapse* 2003;49(4):209–15.
- [7] Kortekaas R, Maguire RP, Cremers TI, Dijkstra D, Van WA, Leenders KL. In vivo binding behavior of dopamine receptor agonist (+)-PD 128907 and implications for the “ceiling effect” in endogenous competition studies with [(11)C]raclopride—a positron emission tomography study in *Macaca mulatta*. *J Cereb Blood Flow Metab* 2004;24(5):531–5.
- [8] McCormick PN, Kapur S, Seeman P, Wilson AA. Dopamine D₂ receptor radiotracer [¹¹C](+)-PHNO and [³H]raclopride are indistinguishably inhibited by D₂ agonists and antagonists ex vivo. *Nucl Med Biol* 2008;35(1):11–7.
- [9] Cumming P, Wong DF, Gillings N, Hilton J, Scheffel U, Gjedde A. Specific binding of [(11)C]raclopride and *N*-[(3)H]propyl-norapomorphine to dopamine receptors in living mouse striatum: occupancy by endogenous dopamine and guanosine triphosphate-free G protein. *J Cereb Blood Flow Metab* 2002;22(5):596–604.
- [10] Narendran R, Hwang DR, Slifstein M, Talbot PS, Erritzoe D, Huang Y, et al. In vivo vulnerability to competition by endogenous dopamine: comparison of the D₂ receptor agonist radiotracer (-)-*N*-[¹¹C]propyl-norapomorphine ([¹¹C]NPA) with the D₂ receptor antagonist radiotracer [¹¹C]-raclopride. *Synapse* 2004;52(3):188–208.
- [11] Seneca N, Finnema SJ, Farde L, Gulyas B, Wikstrom HV, Halldin C, et al. Effect of amphetamine on dopamine D₂ receptor binding in nonhuman primate brain: a comparison of the agonist radioligand [¹¹C]MNPA and antagonist [¹¹C]raclopride. *Synapse* 2006;59(5):260–9.
- [12] Hwang DR, Kegeles LS, Laruelle M. (-)-*N*-[(11)C]Propyl-norapomorphine: a positron-labeled dopamine agonist for PET imaging of D (2) receptors. *Nucl Med Biol* 2000;27(6):533–9.
- [13] Finnema SJ, Seneca N, Farde L, Shchukin E, Sovago J, Gulyas B, et al. A preliminary PET evaluation of the new dopamine D₂ receptor agonist [¹¹C]MNPA in cynomolgus monkey. *Nucl Med Biol* 2005;32(4):353–60.
- [14] Wilson AA, McCormick P, Kapur S, Willeit M, Garcia A, Hussey D, et al. Radiosynthesis and evaluation of [¹¹C]-(+)-4-propyl-3,4,4a,5,6,10b-hexahydro-2H-naphtho[1,2-*b*][1,4]oxazin-9-ol as a

- potential radiotracer for in vivo imaging of the dopamine D₂ high-affinity state with positron emission tomography. *J Med Chem* 2005;48(12):4153–60.
- [15] Shi B, Narayanan TK, Christian BT, Chattopadhyay S, Mukherjee J. Synthesis and biological evaluation of the binding of dopamine D₂/D₃ receptor agonist, (*R,S*)-5-hydroxy-2-(*N*-propyl-*N*-(5'-(18)F-fluoropentyl)aminotetralin ((18)F-5-OH-FPPAT) in rodents and nonhuman primates. *Nucl Med Biol* 2004;31(3):303–11.
- [16] Narendran R, Slifstein M, Guillin O, Hwang Y, Hwang DR, Scher E, et al. Dopamine (D_{2/3}) receptor agonist positron emission tomography radiotracer [¹¹C]-(+)-PHNO is a D₃ receptor preferring agonist in vivo. *Synapse* 2006;60(7):485–95.
- [17] Ramsby S, Neumeyer JL, Grigoriadis D, Seeman P. 2-Haloaporphines as potent dopamine agonists. *J Med Chem* 1989;32(6):1198–201.
- [18] Sondergaard K, Kristensen JL, Palner M, Gillings N, Knudsen GM, Roth BL, et al. Synthesis and binding studies of 2-aryl aporphines. *Org Biomol Chem* 2005;3(22):4077–81.
- [19] Hilton J, Yokoi F, Dannals RF, Ravert HT, Szabo Z, Wong DF. Column-switching HPLC for the analysis of plasma in PET imaging studies. *Nucl Med Biol* 2000;27(6):627–30.
- [20] Freedman SB, Patel S, Marwood R, Emms F, Seabrook GR, Knowles MR, et al. Expression and pharmacological characterization of the human D₃ dopamine receptor. *J Pharmacol Exp Ther* 1994;268(1):417–26.
- [21] Palner M, Syvanen S, Kristoffersen US, Gillings N, Kjaer A, Knudsen GM. The Effect of a P-glycoprotein inhibitor on rat brain uptake and binding of [¹⁸F]altanserin; a micro-PET study. *J Cereb Blood Flow Metab* 2007;27(Suppl 1).



ELSEVIER

Available online at www.sciencedirect.com

Nuclear Medicine and Biology xx (2010) xxx – xxx

NUCLEAR
MEDICINE
— AND —
BIOLOGY

www.elsevier.com/locate/nucmedbio

Systemic catechol-*O*-methyl transferase inhibition enables the D₁ agonist radiotracer *R*-[¹¹C]SKF 82957[☆]

Mikael Palner^{a,b,*}, Patrick McCormick^c, Jun Parkes^c, Gitte M. Knudsen^{a,b}, Alan A. Wilson^{c,d}

^aNeurobiology Research Unit, Rigshospitalet and University of Copenhagen, Copenhagen, Denmark

^bCenter for Integrated Molecular Brain Imaging, Rigshospitalet, Denmark

^cPET Center, Center for Addiction and Mental Health, Toronto, Ontario, Canada

^dDepartment of Psychiatry, University of Toronto, Toronto, Ontario, Canada

Received 3 February 2010; received in revised form 4 March 2010; accepted 28 April 2010

Abstract

Introduction: *R*-[¹¹C]-SKF 82957 is a high-affinity and potent dopamine D₁ receptor agonist radioligand, which gives rise to a brain-penetrant lipophilic metabolite. In this study, we demonstrate that systemic administration of catechol-*O*-methyl transferase (COMT) inhibitors blocks this metabolic pathway, facilitating the use of *R*-[¹¹C]-SKF 82957 to image the high-affinity state of the dopamine D₁ receptor with PET.

Methods: *R*-[¹¹C]SKF 82957 was administered to untreated and COMT inhibitor-treated conscious rats, and the radioactive metabolites present in the brain and plasma were quantified by HPLC. Under optimal conditions, cerebral uptake and dopamine D₁ binding of *R*-[¹¹C]SKF 82957 were measured ex vivo. In addition, pharmacological challenges with the receptor antagonist SCH 23390, amphetamine, the dopamine reuptake inhibitor RTI-32 and the dopamine hydroxylase inhibitor α -methyl-*p*-tyrosine were performed to study the specificity and sensitivity of *R*-[¹¹C]-SKF 82957 dopamine D₁ binding in COMT-inhibited animals.

Results: Treatment with the COMT inhibitor tolcapone was associated with a dose-dependent (EC₉₀ 5.3±4.3 mg/kg) reduction in the lipophilic metabolite. Tolcapone treatment (20 mg/kg) also resulted in a significant increase in the striatum/cerebellum ratio of *R*-[¹¹C]SKF 82957, from 15 (controls) to 24. Treatment with the dopamine D₁ antagonist SCH 23390 reduced the striatal binding to the levels of the cerebellum, demonstrating a high specificity and selectivity of *R*-[¹¹C]SKF 82957 binding.

Conclusions: Pre-treatment with the COMT inhibitor tolcapone inhibits formation of an interfering metabolite of *R*-[¹¹C]SKF 82957. Under such conditions, *R*-[¹¹C]SKF 82957 demonstrates high potential as the first agonist radiotracer for imaging the dopamine D₁ receptor by PET.

© 2010 Elsevier Inc. All rights reserved.

Keywords: Agonist; Dopamine D₁ receptor; *R*-[¹¹C]SKF 82957; Metabolites; Catechol-*O*-methyltransferase; Tolcapone; Entacapone; Ex vivo; PET Tracer

1. Introduction

Dopamine D₁ receptors are implicated in numerous neuropharmacological and neurobiological functions. For

example, D₁ receptors are involved in different types of memory function [1–3] and in the cognitive deficits of schizophrenic patients [4,5]. Brain imaging with positron emission tomography (PET) is an important tool to elucidate the significance of D₁-receptor signaling, and improving the selectivity of PET tracers will facilitate this pursuit. The hitherto most widely used radiotracers for D₁-receptor brain imaging include [¹¹C]SCH 23390 [6,7] and [¹¹C]NNC 112 [7]. Other but less widely used tracers are [¹¹C]NNC 756 [8,9], [¹¹C]A-69024 [10,11] and the ¹⁸F-labeled compound (*R*)-*N*-(3-¹⁸F-fluoropropyl)SCH 38548 [12]. However, all of these tracers are antagonists at the D₁ receptor, and an agonist would potentially give more functional knowledge

[☆] This work was supported by the Danish Agency for Science, Technology and Innovation, Rigshospitalet; the EC-FP6-project DiMI, LSHB-CT-2005-512146; the Centre of Addiction and Mental Health in Toronto, Canada; and the Lundbeck Foundation, Denmark.

* Corresponding author. Neurobiology Research Unit, Juliane Maries Vej 24 Rigshospitalet, Building 9201, DK-2100 Copenhagen, Denmark. Tel.: +45 3545 6704; fax: +45 3545 6713.

E-mail address: mikael.palner@nru.dk (M. Palner).

about the receptor by binding only to the functional active (G-protein-coupled, high-affinity) subset of receptors, as shown with in vitro experiments [13].

The benzazepine R - $[^{11}\text{C}]$ SKF 82957 (R -(+)-3- $[^{11}\text{C}]$ methyl-6-chloro-7,8-dihydroxy-1-phenyl-2,3,4,5-tetrahydro-1H-3-benzazepine) is a high-affinity ($K_i=0.9$ nM [14]) D_1 receptor agonist. In vitro autoradiography and ex vivo studies in rats have shown that R - $[^{11}\text{C}]$ SKF 82957 has an excellent signal-to-noise ratio above 10 [15–17]. Unfortunately, data from our laboratory has revealed that when administered systemically in rats, the radiotracer generates a lipophilic metabolite which crosses the blood–brain barrier resulting in about 50–60% of the activity in the brain emanating from the metabolite [18]. The lipophilic metabolite, which has not been structurally identified, is generated not only in rats but also, although to a lesser extent, in humans. Systemic or cerebral production of radiolabeled metabolites, particularly those with affinity to relevant receptors in the brain, hampers the quantification of the radiotracer binding. Therefore, the lipophilic metabolite of R - $[^{11}\text{C}]$ SKF 82957 constitutes a major confound in interpreting PET or ex vivo animal experiments.

Given the catecholamine structure of the radiotracer (Scheme 1) and that >95% of specific binding in the rat striatum can be blocked by D_1 antagonists, such as SCH 23390, we hypothesized that the lipophilic metabolite resulted from methylation of R - $[^{11}\text{C}]$ SKF 82957 by the enzyme catechol- O -methyl transferase (COMT), as has been described for other related catechols [19]. Methylation of one of the phenol groups would produce a radiotracer which almost certainly has D_1 affinity and acts as antagonist, as the presence of 7,8-cathechol hydroxyl has been shown to be essential for agonist activity, while other 7,8 substitutions result in antagonists [20].

In patients with Parkinson's disease treated with L-DOPA, COMT inhibition minimizes the methylation of dopamine (99% efficiency), thus enhancing the L-DOPA treatment effect. In a preliminary report, COMT inhibition was able to inhibit the peripheral in vivo formation of the lipophilic radiometabolite of the partial D_1 receptor agonist (S)- $[^{11}\text{C}]$ N -methyl-NNC 01-0259 [21]. However, direct analysis of brain tissue was not carried out.

In this study, we investigated the effect of tolcapone and entacapone (two widely used COMT inhibitors) on the formation of lipophilic radiometabolites of R - $[^{11}\text{C}]$ SKF

82957 in rat. We examined the relationship between brain and plasma levels, and the effects of COMT inhibition on the brain uptake and binding of R - $[^{11}\text{C}]$ SKF 82957. We investigated the selectivity of R - $[^{11}\text{C}]$ SKF 82957 binding to dopamine D_1 receptors after COMT inhibition by blockade with SCH 23390, a selective D_1 antagonist, and the binding ratio and uptake after treatment with amphetamine, RTI-32 (a dopamine reuptake inhibitor) and inhibition of dopamine formation by use of α -methyl- p -tyrosine (α -MT), a tyrosine hydroxylase inhibitor.

2. Material and methods

2.1. General

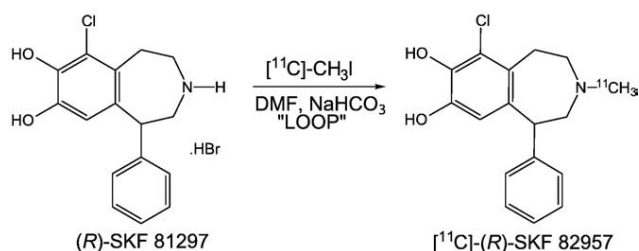
Male Sprague-Dawley rats, weighing 282 ± 5 g on the day of the experiments, were used. Rats were maintained on a 12-h light/dark cycle with free access to food and water for at least 1 week prior to the experiments. Experiments were conducted in accordance with the guidelines of the Canadian Council on Animal Care and with approval from the Animal Care Committee at the Center of Addiction and Mental Health. RTI-32 was prepared in-house [22]. All other chemicals were from commercial sources.

2.2. Radiosynthesis of R - $[^{11}\text{C}]$ SKF 82957

$[^{11}\text{C}]$ -Iodomethane (produced as previously described [23]) was swept into a 2-ml HPLC loop [24,25] by a stream of N_2 gas (8 ml/min). The loop had been precoated with a solution of SKF 81297 hydrochloride (1 mg) in DMF (70 μl) and 1N NaHCO_3 (10 μl). Upon maximal trapping of radioactivity in the loop (3–4 min), the flow of N_2 was stopped and the reaction allowed to proceed (3.5 min). The contents of the loop were then injected onto the HPLC purification column and purified by HPLC using a Phenomenex Gemini C18 10- μm column eluted with THF/ H_2O (13:87)+0.1N NaOAc (pH 5) at 8 ml/min. The desired fraction (reaction time 7–8 min) was collected, evaporated to dryness under vacuum at 70°C and the residue taken up in 10 ml of sterile saline. The saline solution of R - $[^{11}\text{C}]$ SKF 82957 was passed through a sterile 0.22- μm filter into a sterile, pyrogen-free bottle containing aqueous sodium bicarbonate (1 ml, 8.4%). Aliquots of the formulated solution were used to establish the chemical and radiochemical purity and specific activity of the final solution by analytical HPLC.

2.3. Initial comparison of tolcapone and entacapone

The metabolites of R - $[^{11}\text{C}]$ SKF 82957 were examined in plasma and brain homogenate of male rats after pretreatment of either entacapone or tolcapone. Awake rats (male, Sprague-Dawley, 260 g) were pretreated intraperitoneally with either entacapone (5 mg/kg, $n=1$), tolcapone (5 mg/kg, $n=1$) or vehicle (5% Tween 80 in saline, $n=3$) 30 min before injection of 50 MBq high specific activity R - $[^{11}\text{C}]$ SKF 82957 (2.5 nmol) in 0.5 ml of buffered saline via the tail



Scheme 1. Radiochemical synthesis of R - $[^{11}\text{C}]$ SKF 82957.

vein. Rats were killed by decapitation after 30 min and their brains were quickly removed and placed on ice; blood from the trunk was collected in heparinized tubes. Control animals ($n=2$), which received no radiotracer, were also killed, blood was collected and the brain excised and stored on ice. One megabecquerel of R -[^{11}C]SKF 82957 in 10 μl of buffered saline was added to the control brain and control blood only. All brains were homogenized (Polytron, setting 7) in 4 ml of ice-cold 70% aqueous ethanol and centrifuged (17,000 rpm, 15 min). Aliquots of the supernatants and the pellets were counted for radioactivity, and the supernatants were then diluted 4:1 (v/v) with water for HPLC analysis. Blood was centrifuged to separate the plasma which was then used directly for HPLC analysis. HPLC analyses of plasma and brain extracts were performed by minor modifications of the method described by Hilton et al. [26]. Briefly, samples were loaded onto a 5-ml HPLC injector loop (Valco Texas) and injected onto a small capture column (4.6 \times 20 mm) packed in-house with OASIS HLB 30 μm (Waters, New Jersey, USA). The capture column was eluted with 1% aqueous acetonitrile (2 ml/min) for 4 min, then back-flushed (25% acetonitrile/75% H_2O +0.1N ammonium formate) onto a Phenomenex Prodigy 10- μm C18 column (250 \times 4.6 mm). Both column effluents were monitored through a flow detector (Bioscan Flow-Count) operated in coincidence mode. After 14 min, the HPLC eluent was changed to 60% acetonitrile/40% H_2O +0.1N ammonium formate, pH 4, 2 ml/min to monitor for strongly retained (lipophilic) metabolites. All radioactivity data were corrected for physical decay and integrated using a PC. Hold-up of radioactivity in the HPLC system was less than 2% of applied radioactivity, while the pellet had less than 10%.

2.4. Tolcapone inhibition of R -[^{11}C]SKF 82957 metabolism

The dose–response relationship for tolcapone on the brain and plasma metabolites of R -[^{11}C]SKF 82957 was examined. Awake rats were divided into different groups as noted

in Table 1. Rats were pretreated intraperitoneally with tolcapone or vehicle (5% Tween 80 in saline) 30 min before injection of 50 MBq high specific activity R -[^{11}C]SKF 82957 (2.5 nmol) in 0.5 ml of buffered saline via the tail vein. Rats were killed by decapitation after 30 min and their brains were quickly removed and placed on ice; blood from the trunk was collected in heparinized tubes. Brain and blood samples were processed and measured as described above.

2.5. Pharmacological challenges

The cerebral binding of R -[^{11}C]SKF 82957 after pharmacological challenges was examined.¹ Rats were divided into different groups as noted in Table 1. All groups received an intraperitoneal injection of tolcapone (20 mg/kg in 5% Tween 80 in saline) 30 min before injection of 37 MBq R -[^{11}C]SKF 82957 and were killed by decapitation 60 min postinjection of the radiotracer. Brains were quickly removed and placed on ice, blood from the trunk was collected in heparinized tubes and the blood (collected from the trunk) was centrifuged to isolate plasma. The brain regions of the striatum and cerebellum were dissected. All tissue and plasma samples were collected in tarred counting vials and counted in a gamma counter. Used syringes and rat tails were counted in a dose calibrator, and the injected dose was corrected for activity left in the syringe and tail. Standard uptake value [$\text{SUV}=(\text{Bq/g in ROI})/(\text{Bq/g injected})$] was calculated using aliquots of the injected dose as standards. Plasma from each group was pooled and examined for radioactive metabolites as described above.

2.6. Calculations and statistics

Tolcapone effective concentration (EC_{90}) was calculated based on the effect of tolcapone on the concentration of unmetabolised R -[^{11}C]SKF 82957 in the rat brain. A linear regression between R -[^{11}C]SKF 82957 levels in the brain vs. plasma was performed. A Student's unpaired t test was used to compare the groups in the pharmacological experiment. All results are given as mean \pm S.E.M.

3. Results

3.1. Radiosynthesis of R -[^{11}C]SKF 82957

R -[^{11}C]SKF 82957 was efficiently prepared by N -methylation of the precursor R -SKF 81297 with [^{11}C]-iodomethane (Scheme 1) using a captive solvent or “loop” technique [24,25]. Uncorrected radiochemical yields of the final formulated product from [^{11}C]- CO_2 were 13–17% in a synthesis time of 25 min. Radiochemical purities were >97% and specific activities (at end of synthesis) were 50–80 GBq/ μmol .

¹ It should be noted that inhibition of COMT potentiated the physiological effects of amphetamine on the animals, possibly as a result of inhibition of dopamine metabolism. We advise future investigators to be vigilant when combining the two drugs.

Table 1
Group conditions

Tolcapone COMT inhibition			
Group	Pretreatment	Amount	n
Control	5% Tween in saline	300 μl	6
Tolcapone-1	Tolcapone ip 30 min	3 mg/kg	6
Tolcapone-2	Tolcapone ip 30 min	10 mg/kg	6
Tolcapone-3	Tolcapone ip 30 min	20 mg/kg	6
Ex vivo binding			
Group	Time	Amount	n
Control	Saline coinjected with tolcapone	300 μl	12
SCH 23390	Coinjected with R -[^{11}C]SKF 82957	2 mg/kg	5
Amphetamine	Coinjected with tolcapone	1 mg/kg	9
RTI-32	Coinjected with tolcapone	2 mg/kg	6
α -MP	30 min before tolcapone	250 mg/kg	6

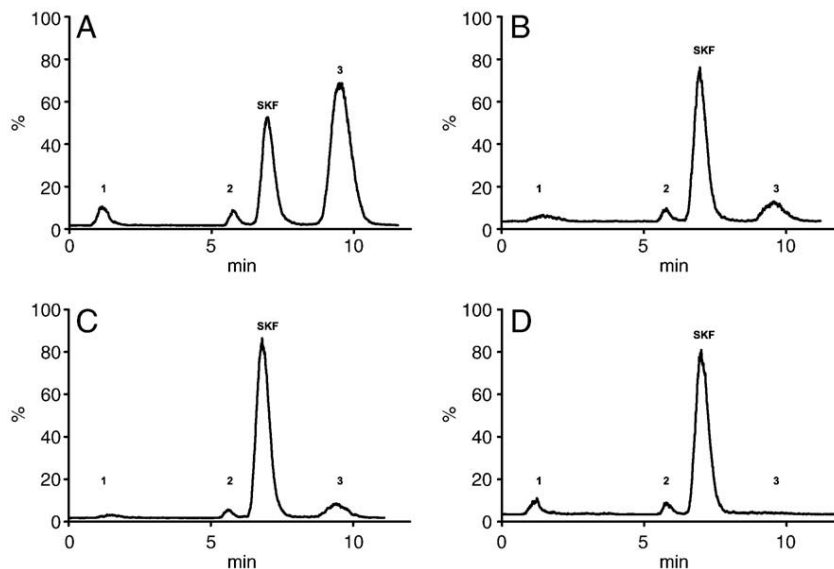


Fig. 1. HPLC chromatograms of rat brain extracts 30 min post intravenous injection of $[^{11}\text{C}]$ -SKF 82957. (A) Saline treated; (B) 3 mg/kg tolcapone; (C) 10 mg/kg tolcapone; (D) 20 mg/kg tolcapone. Peaks labeled “1” and “2” are hydrophilic metabolites, SKF is R - $[^{11}\text{C}]$ SKF 82957 and “3” is the lipophilic metabolite.

3.2. Initial comparison of tolcapone and entacapone

Greater than 90% of radioactivity could be extracted from homogenized brain tissue. HPLC chromatograms from brain extracts of untreated animals 30 min after injection of R - $[^{11}\text{C}]$ SKF 82957 confirm the previous finding [18] that three metabolites are present: two small hydrophilic and one large lipophilic one (Fig. 1A). The lipophilic metabolite constituted 62% of the radioactivity in the brain, with 32% R - $[^{11}\text{C}]$ SKF 82957 and low levels of hydrophilic metabolites. Treatment with 5 mg/kg entacapone intravenously reduced the concentration of lipophilic metabolite in the brain to 35% (59% R - $[^{11}\text{C}]$ SKF 82957 and 35% lipophilic metabolite), while treatment with 5 mg/kg tolcapone intravenously reduced the concentration of the lipophilic metabolite in the brain even further to 22% (73% R - $[^{11}\text{C}]$ SKF 82957 and 22% lipophilic metabolite). There was only a very limited formation of 2% lipophilic metabolite in the

brain used as in vitro controls (92% R - $[^{11}\text{C}]$ SKF 82957, 2% lipophilic metabolite and 6% hydrophilic metabolite).

3.3. Tolcapone inhibition of R - $[^{11}\text{C}]$ SKF 82957 metabolism

The composition of radioactive metabolites of R - $[^{11}\text{C}]$ SKF 82957 in the brain and plasma after intraperitoneally injected tolcapone was examined with HPLC (Fig. 2). In saline-treated animals, we found similar results as reported in the initial experiments above, again confirming the formation of 20.4% lipophilic metabolite in plasma and 61.5% lipophilic metabolite in the brain (plasma: 12.5%±6.5 Metabolite 1, 47.7%±2.7 Metabolite 2, 20.1% R - $[^{11}\text{C}]$ SKF 82957 and 20.4%±3.3 lipophilic metabolite; brain: 3.6%±0.1 Metabolite 1, 2.20%±0.54 Metabolite 2, 32.3%±4.0 R - $[^{11}\text{C}]$ SKF 82957 and 61.5%±3.4 lipophilic metabolite). Treatment with tolcapone intraperitoneally reduced the formation of lipophilic metabolite in a dose-dependent manner (brain: log

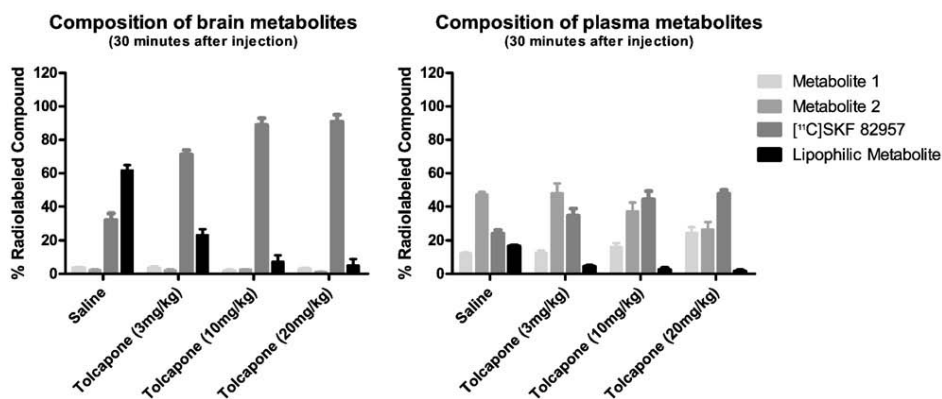


Fig. 2. Composition of radiolabeled compounds in the brain and plasma from rats, 30 min after injection of R - $[^{11}\text{C}]$ SKF 82957.

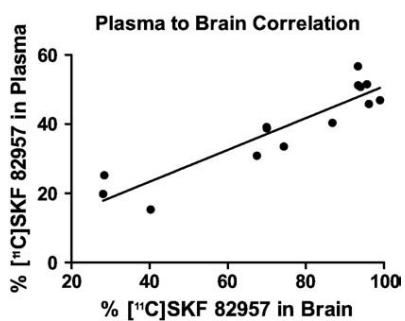


Fig. 3. Correlation between plasma and brain concentration of R - $[^{11}\text{C}]$ SKF 82957 and the lipophilic metabolite in rats, 30 min after injection of R - $[^{11}\text{C}]$ SKF 82957.

$\text{EC}_{90} -1.273 \pm 0.149$, $\text{EC}_{90} 5.3 \pm 4.3$ mg/kg) to a negligible level of 2.6% in plasma and 5.1% in the brain at the highest (20 mg/kg) dosage. Tolcapone also induces a reduction in plasma levels of Metabolite 2 from 47% to 37% (Fig. 2). (Plasma: $15.5\% \pm 0.5$ Metabolite 1, $37.0\% \pm 4.3$ Metabolite 2, $45.0\% \pm 5.8$ R - $[^{11}\text{C}]$ SKF 82957, $2.6\% \pm 2.0$ lipophilic metabolite; brain: $2.7\% \pm 0.6$ Metabolite 1, $1.2\% \pm 0.2$ Metabolite 2, $90.8\% \pm 4.2$ R - $[^{11}\text{C}]$ SKF 82957 and $5.1\% \pm 3.8$ lipophilic metabolite.) There is a linear correlation between plasma and brain levels of R - $[^{11}\text{C}]$ SKF 82957 ($r^2=0.84$; Fig. 3), and between plasma and brain levels of the lipophilic metabolite ($r^2=0.91$; Fig. 3).

3.4. Effect of COMT treatment on ex vivo binding of R - $[^{11}\text{C}]$ SKF 82957

The striatal and cerebellar uptake of R - $[^{11}\text{C}]$ SKF 82957 in rats treated with 20 mg/kg tolcapone intraperitoneally was compared to saline-treated controls (Table 2). Inhibition of COMT by tolcapone resulted in a highly significant increase in striatal SUV ($77\%***$) and a highly significant increase in the striatum-to-cerebellum ratio (S/C ratio) ($57\%***$) compared to the saline-treated controls to a remarkable ratio of 24. There was no significant change in the SUV of

the cerebellum. Treatment of tolcapone-treated animals with the D_1 selective antagonist SCH 23390 prior to radiotracer injection reduced the striatal binding to the levels of the cerebellum (Table 2), demonstrating that, under COMT inhibition conditions, R - $[^{11}\text{C}]$ -SKF 82957 uptake in rat striatum reflects binding to dopamine D_1 receptors.

3.5. Effect of endogenous dopamine manipulations on $[^{11}\text{C}]$ -SKF 82957 binding

Under COMT inhibition conditions, the effects of pharmacological challenges with dopaminergic drugs on ex vivo R - $[^{11}\text{C}]$ SKF 82957 binding were examined (Table 2). The amphetamine-induced release of dopamine resulted in reduced striatal SUV ($-10\%*$) and cerebellum SUV ($-29\%**$), resulting in a significant increase in the S/C ratio ($+33\%***$). Treatment with the dopamine reuptake inhibitor RTI-32 also resulted in decreased striatal SUV ($-14\%***$) and cerebellum SUV ($-21\%**$) with a nonsignificant increase in the S/C ratio ($+12\%$). Treatment with the dopamine hydroxylase inhibitor α -MT caused a significant decrease in striatal SUV ($-29\%***$) and unchanged cerebellum SUV ($+7\%$) and a corresponding decrease in the S/C ratio ($-34\%***$).

4. Discussion

We confirmed the prior-reported finding [18] that intravenous injection of R - $[^{11}\text{C}]$ SKF 82957 results in a radiolabeled lipophilic metabolite in rat brain. The lipophilic metabolite accounted for 62% of the total radioactivity in the brain, 30 min after injection of R - $[^{11}\text{C}]$ SKF 82957. Both COMT inhibitors, entacapone and tolcapone, inhibited the formation of lipophilic metabolite; however, tolcapone (22% lipophilic metabolite in the brain after treatment) proved to be more efficient than entacapone (35% lipophilic metabolite in the brain after treatment) at the same dose. This may be a consequence of tolcapone's better brain-penetrating abilities

Table 2
Results from pharmacological challenges

	Saline	Tolcapone	Tolcapone+				% Difference			
			SCH 23390	Amphetamine	RTI-32	α -MP	Tolcapone/ saline	Amphetamine/ tolcapone	RTI/ Tolcapone	α -MT/ Tolcapone
Striatum	1.87±0.09	3.31±0.06	0.17±0.01	3.00±0.44	2.85±0.18	2.36±0.21	+77%***	-10%*	-14%***	-29%***
Cerebellum	0.12±0.01	0.14±0.02	0.10±0.01	0.10±0.04	0.11±0.01	0.15±0.01	+16%	-29%**	-21%*	+7%
Plasma	0.47±0.02	0.72±0.06	0.56±0.13	0.90±0.18	0.53±0.09	0.68±0.04	+53%*	+25%	-26%	-6%
Striatum/ cerebellum ratio	15.44±0.59	24.28±0.62	1.64±0.08	32.41±2.64	27.08±1.84	16.26±1.42	+57%***	+33%**	+12%	-34%***

Standard uptake value [SUV=(Bq/g in ROI)/(Bq/g injected)] and striatum-to-cerebellum ratio of R - $[^{11}\text{C}]$ SKF 82957 in rats treated with saline or the COMT inhibitor tolcapone. The tolcapone group serves as control for the tolcapone+pharmacological challenges with the D_1 antagonist SCH23390, the dopamine releaser amphetamine, the dopamine transporter antagonist RTI-32 and the dopamine hydroxylase inhibitor α -MT.

* $P < 0.05$.

** $P < 0.01$.

*** $P < 0.001$.

[27,28]. On this basis, we chose tolcapone as the COMT inhibitor for a full dose–response experiment.

After systemic administration of the COMT inhibitor tolcapone, there was a dose–response correlated reduction of lipophilic metabolite concentration in the rat brain and concomitant increase in R -[^{11}C]SKF 82957 concentration (Table 2). The effective dose of tolcapone to have more than 90% of the parent compound present in the brain was 5.3 ± 4.3 mg/kg. A tolcapone dose four times higher than the calculated ED90 (20 mg/kg) reduced the lipophilic metabolite to acceptable levels ($5.1\% \pm 3.8$) of the total radioactivity in the brain. Since the measurement of the extent of metabolism of R -[^{11}C]SKF 82957 in human brain is not possible, we investigated the correlation between plasma concentration and brain concentration of both lipophilic metabolite and parent compound. There was a good correlation (Fig. 3), suggesting that the concentration of lipophilic metabolite in plasma can be used with some confidence to predict the concentration of lipophilic metabolite in the brain.

Pretreatment of rats with tolcapone (30 mg/kg) effectively eliminated the presence of interfering radioactive metabolites in brain tissue (see above), thus allowing a fresh evaluation of the potential of R -[^{11}C]SKF 82957 as a radiotracer for the PET imaging of the high-affinity state of dopamine D_1 receptors. Under full COMT inhibition, the uptake of R -[^{11}C]SKF 82957 in rat striatum increased substantially with a concomitant increase in the S/C ratio from 15 to 24. This high value bodes well for future PET imaging with R -[^{11}C]SKF 82957 in humans. In addition, pretreatment of tolcapone-treated rats with a D_1 receptor antagonist, SCH 23390, blocked the striatal uptake of R -[^{11}C]SKF 82957, lowering the S/C ratio from 24.28 to 1.64. This supports that R -[^{11}C]SKF 82957 is a selective D_1 receptor ligand as shown before [15].

We found that acute α -MT treatment (dopamine depletion) significantly decreases the SUV of R -[^{11}C]SKF 82957 and at the same time significantly decreases the S/C ratio by about 30%; this is in good agreement with other D_1 studies where the binding has been either unchanged or reduced. For example, the S/C ratio of [^3H]A69024 in awake mice was not affected by the acute depletion with 4-hydroxybutyrate [29], and the S/C ratio of [^{11}C]SCH 23390 was found to be decreased after both acute and chronic depletion of dopamine in anaesthetized rats [30] and in awake mice [31]. Both amphetamine and RTI-32 pretreatment (leading to dopamine release) decreased the SUV of R -[^{11}C]SKF 82957, but concomitantly increased the S/C ratio. These results are also in line with other D_1 studies. For example, the binding potential (BP) or ratio of bound/free ligand (B/F) of D_1 radiotracers has been found to be insensitive or slightly increased after dopamine release (BP [^{11}C]NNC 756 [32], B/F [^{11}C]NNC 112 and [^{11}C]SCH 23390 [33]). It was never the aim of this article to definitely conclude what causes these increases and decreases in R -[^{11}C]SKF 82957 SUV and S/C ratio after pharmacological challenges, but even

though still unexplained they do concur with the results of other D_1 receptor binding studies in relation to dopamine release and depletion. A limitation of our study is the single time point S/C ratio; a detailed full kinetic analysis will be required to explore the dopamine manipulation on binding.

In principle, COMT inhibition could be done in conjunction with D_1 receptor PET studies in humans. There could be a concern about the safety of such an approach, since some clinical studies have found that repeated tolcapone treatment induces hepatotoxicity. The frequency of severe hepatic side effects, however, has been greatly overestimated [34], and, therefore, tolcapone has now been reinstated on the European market as a treatment for Parkinson's disease patients together with L-DOPA. Single-dose tolcapone treatment in association with a PET scan using [^{11}C]SKF 82957 may be a feasible procedure for future PET studies of the D_1 high-affinity state in humans.

5. Conclusion

Systemic inhibition of catechol- O -methyl transferase by tolcapone lowers the levels of the lipophilic metabolite of R -[^{11}C]SKF 82957 in rat brain by 95% with a concomitant increase in the S/C ratio from 15 to 24. The combination of tolcapone and R -[^{11}C]SKF 82957 provides a tool to interrogate, for the first time, the high-affinity state of the D_1 dopamine receptor in vivo using PET imaging. It also raises the possibility of human PET studies of the high-affinity state of the dopamine D_1 receptor.

References

- [1] Williams GV, Goldman-Rakic PS. Modulation of memory fields by dopamine D_1 receptors in prefrontal cortex. *Nature* 1995;376:572–5.
- [2] Arnsten AF, Cai JX, Murphy BL, Goldman-Rakic PS. Dopamine D_1 receptor mechanisms in the cognitive performance of young adult and aged monkeys. *Psychopharmacology* 1994;116:143–51.
- [3] Seamans JK, Floresco SB, Phillips AG. D_1 receptor modulation of hippocampal–prefrontal cortical circuits integrating spatial memory with executive functions in the rat. *J Neurosci* 1998;18:1613–21.
- [4] Goldman-Rakic PS, Castner SA, Svensson TH, Siever LJ, Williams GV. Targeting the dopamine D_1 receptor in schizophrenia: insights for cognitive dysfunction. *Psychopharmacology* 2004;174:3–16.
- [5] Hirvonen J, van Erp TG, Huttunen J, Aalto S, Nägren K, Huttunen M, et al. Brain dopamine D_1 receptors in twins discordant for schizophrenia. *Am J Psychiatr* 2006;163:1747–53.
- [6] Farde L, Halldin C, Stone-Elander S, Sedvall G. PET analysis of human dopamine receptor subtypes using [^{11}C]SCH 23390 and [^{11}C]raclopride. *Psychopharmacology* 1987;92:278–84.
- [7] Halldin C, Foged C, Chou YH, Karlsson P, Swahn CG, Sandell J, et al. Carbon-11-NNC 112: a radioligand for PET examination of striatal and neocortical D_1 -dopamine receptors. *J Nucl Med* 1998;39:2061–8.
- [8] Halldin C, Foged C, Farde L, Karlsson P, Hansen K, Grönvald F, et al. [^{11}C]NNC 687 and [^{11}C]NNC 756, dopamine D_1 receptor ligands. Preparation, autoradiography and PET investigation in monkey. *Nucl Med Biol* 1993;20:945–53.
- [9] Laihinne AO, Rinne JO, Ruottinen HM, Nägren KA, Lehtikoinen PK, Oikonen VJ, et al. *J Nucl Med* 1994;35:1916–20.
- [10] Besret L, Dollé F, Hérard A, Guillemier M, Demphel S, Hinnen F, et al. *J Pharm Sci* 2008;97:2811–9.

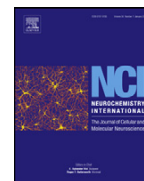
- [11] Kassiou M, Scheffel U, Ravert HT, Mathews WB, Musachio JL, Lambrecht RM, et al. [¹¹C]A-69024: a potent and selective non-benzazepine radiotracer for in vivo studies of dopamine D₁ receptors. *Nucl Med Biol* 1995;22:221–6.
- [12] Yang ZY, Perry B, Mukherjee J. Fluorinated benzazepines: 1. Synthesis, radiosynthesis and biological evaluation of a series of substituted benzazepines as potential radiotracers for positron emission tomographic studies of dopamine D-1 receptors. *Nucl Med Biol* 1996; 23:793–805.
- [13] Farrell CB, O'Boyle KM. The kinetics of [³H]SCH 23390 dissociation from rat striatal dopamine D₁ receptors: effect of dopamine. *Eur J Pharm* 1994;268:79–88.
- [14] Seeman P, Neumeyer JL, Baidur N, Niznik HB, Guan HC. (+/-)-3-Allyl-6-bromo-7,8-dihydroxy-1-phenyl-2,3,4,5-tetrahydro-1H-3-benzazepin, a new high-affinity D₁ dopamine receptor ligand: synthesis and structure–activity relationship. *J Med Chem* 1991;34:3366–71.
- [15] DaSilva JN, Schwartz RA, Greenwald ER, Lourenco CM, Wilson AA, Houle S. Dopamine D₁ agonist *R*-[¹¹C]SKF 82957: synthesis and in vivo characterization in rats. *Nucl Med Biol* 1999;26:537–42.
- [16] DaSilva JN, Wilson AA, Nobrega JN, Jiwa D, Houle S. Synthesis and autoradiographic localization of the dopamine D-1 agonists [¹¹C]SKF 75670 and [¹¹C]SKF 82957 as potential PET radioligands. *Appl Radiat Isotopes* 1996;47:279–84.
- [17] DaSilva JN, Wilson AA, Valente CM, Hussey D, Wilson D, Houle S. In vivo binding of [¹¹C]SKF 75670 and [¹¹C]SKF 82957 in rat brain: two dopamine D-1 receptor agonist ligands. *Life Sci* 1996;58: 1661–70.
- [18] DaSilva JN, Cheung H, Wilson AA, Houle S. Metabolism of dopamine D₁ agonist *R*-(+)-[¹¹C]SKF 82957 produces a radiolabeled metabolite in rat brain. *J Label Compd Radiopharm* 2003;46:S365–82.
- [19] Männistö PT, Kaakkola S. Catechol-*O*-methyltransferase (COMT): biochemistry, molecular biology, pharmacology, and clinical efficacy of the new selective COMT inhibitors. *Pharmacol Rev* 1999;51: 593–628.
- [20] Pfeiffer FR, Wilson JW, Weinstock J, Kuo GY, Chambers PA, Holden KG, et al. Dopaminergic activity of substituted 6-chloro-1-phenyl-2,3,4,5-tetrahydro-1H-3-benzazepines. *J Med Chem* 1982;25:352–8.
- [21] Finnema S, Bang Andersen B, Jorgensen M, Gulyas B, Farde L, Wikstrom H, et al. COMT inhibition prevents the formation of lipophilic radiometabolites of catechols — An example with (*S*)-[¹¹C] *N*-methyl-NNC 01-0259. *NeuroImage* 2008;41:T–T91.
- [22] Wilson AA, DaSilva JN, Houle S. Facile radiolabelling and purification of 2β-[¹¹C]CH₃-carbomethoxy-3β-aryltropanes: radiotracers for the dopamine transporter. *J Label Compd Radiopharm* 1994;34: 759–65.
- [23] Wilson AA, DaSilva JN, Houle S. In vivo evaluation of [¹¹C]- and [¹⁸F]-labelled cocaine analogues as potential dopamine transporter ligands for positron emission tomography. *Nucl Med Biol* 1996;23: 141–6.
- [24] Wilson AA, Garcia A, Jin L, Houle S. Radiotracer synthesis from [(11) C]-iodomethane: a remarkably simple captive solvent method. *Nucl Med Biol* 2000;27:529–32.
- [25] Wilson AA, Garcia A, Houle S, Vasdev N. Utility of commercial radiosynthetic modules in captive solvent [¹¹C]-methylation reactions. *J Label Compd Radiopharm* 2009;52:490–2.
- [26] Hilton J, Yokoi F, Dannals RF, Ravert HT, Szabo Z, Wong DF. *Nucl Med Biol* 2000;27:627–30.
- [27] Forsberg M, Lehtonen M, Heikkinen M, Savolainen J, Järvinen T, Männistö PT. Pharmacokinetics and pharmacodynamics of entacapone and tolcapone after acute and repeated administration: a comparative study in the rat. *J Pharmacol Exp Ther* 2003;304:498–506.
- [28] Kaakkola S, Gordin A, Männistö PT. General properties and clinical possibilities of new selective inhibitors of catechol *O*-methyltransferase. *Gen Pharmacol* 1994;25:813–24.
- [29] Rice O, Gatley S, Shen J, Huemmer C, Rogoz R, Dejesus O, et al. Effects of endogenous neurotransmitters on the in vivo binding of dopamine and 5-HT radiotracers in mice. *Neuropsychopharmacology* 2001;25:679–89.
- [30] Guo N, Hwang DR, Lo E, Huang Y, Laruelle M, Abi-Dargham A. Dopamine depletion and in vivo binding of PET D₁ receptor radioligands: implications for imaging studies in schizophrenia. *Neuropsychopharmacology* 2003;28:1703–11.
- [31] Inoue O, Tsukada H, Yonezawa H, Suhara T, Langstrom B. Reserpine-induced reduction of in vivo binding of SCH 23390 and *N*-methylspiperone and its reversal by *d*-amphetamine. *Eur J Pharmacol* 1991;197:143–9.
- [32] Abi-Dargham A, Simpson N, Kegeles L, Parsey R, Hwang DR, Anjilvel S, et al. PET studies of binding competition between endogenous dopamine and the D₁ radiotracer [¹¹C]NNC 756. *Synapse* 1999;32:93–109.
- [33] Chou YH, Karlsson P, Halldin C, Olsson H, Farde L. A PET study of D (1)-like dopamine receptor ligand binding during altered endogenous dopamine levels in the primate brain. *Psychopharmacology* 1999;146: 220–7.
- [34] Olanow CW, Watkins PB. Tolcapone: an efficacy and safety review. *Clin Neuropharmacol* 2007;30:287–94.



Contents lists available at ScienceDirect

Neurochemistry International

journal homepage: www.elsevier.com/locate/neuint



Rapid communication

Effects of unilateral 6-OHDA lesions on [³H]-N-propylnorapomorphine binding in striatum ex vivo and vulnerability to amphetamine-evoked dopamine release in rat

Mikael Palner^{a,b,*}, Celia Kjaerby^b, Gitte M. Knudsen^{a,b}, Paul Cumming^c

^a Neurobiology Research Unit, Rigshospitalet, Juliane Maries Vej 24, Rigshospitalet, Building 9201, DK-2100 Copenhagen, Denmark

^b Center for Integrated Molecular Brain Imaging, Rigshospitalet, Juliane Maries Vej 24, Rigshospitalet, Building 9201, DK-2100 Copenhagen, Denmark

^c Department of Nuclear Medicine, Ludwig-Maximilians-Universität München, Geschwister-Scholl-Platz 1, 80539 Munich, Germany

ARTICLE INFO

Article history:

Received 23 June 2010

Received in revised form 1 December 2010

Accepted 6 December 2010

Available online xxx

Keywords:

Dopamine lesion

6-OHDA

Dopamine D₂ receptor

Amphetamine

[³H]NPA

[³H]raclopride

ABSTRACT

It has been argued that agonist ligands for dopamine D_{2/3} receptors recognize a privileged subset of the receptors in living striatum, those which are functionally coupled to intracellular G-proteins. In support of this claim, the D_{2/3} agonist [³H]-N-propylnorapomorphine ([³H]NPA) proved to be more vulnerable to competition from endogenous dopamine than was the antagonist ligand [¹¹C]raclopride, measured ex vivo in mouse striatum, and subsequently in multi-tracer PET studies of analogous design. Based on these results, we predicted that prolonged dopamine depletion would result in a preferential increase in agonist binding, and a lesser competition from residual dopamine to the agonist binding. To test this hypothesis we used autoradiography to measure [³H]NPA and [³H]raclopride binding sites in hemiparkinsonian rats with unilateral 6-OHDA lesions, with and without amphetamine challenge. Unilateral lesions were associated with a more distinct increase in [³H]NPA binding ex vivo than was seen for [³H]raclopride binding in vitro. Furthermore, this preferential asymmetry in [³H]NPA binding was more pronounced in amphetamine treated rats. We consequently predict that agonist ligands should likewise be fitter than antagonists for detecting responses to denervation in positron emission tomography studies of idiopathic Parkinson's disease. Agonist binding increases in vivo are likely to reflect the composite of a sensitization-like phenomenon, and relatively less competition from endogenous dopamine, as seen in the lesioned side of 6-OHDA induced hemi-parkinsonism.

© 2010 Elsevier Ltd. All rights reserved.

1. Introduction

In molecular imaging studies employing a competition paradigm, in vivo changes in the availability of binding sites for benzamide antagonists of dopamine D_{2/3} receptors are interpreted to reveal altered competition from endogenous dopamine (Laruelle, 2000). However, dopamine receptors can exist in distinct affinity states with respect to dopamine and exogenous agonist ligands, with perhaps 50% of the receptors, designated D₂^{High}, naturally occurring in a state with high affinity for agonists, and coupled with intracellular G-proteins. As such, the fractional abundance of D₂^{High}

sites would limit the possible extent of occupancy by endogenous dopamine, and therefore should also represent the upper limit of the vulnerability of the in vivo binding of benzamide dopamine antagonists to competition from endogenous dopamine or exogenous agonists. In support of this notion, the dopamine D_{2/3} agonist [³H]-N-propylnorapomorphine [³H]NPA proven to be considerably more sensitive than was the antagonist [¹¹C]raclopride to pharmacologically evoked changes in dopamine tonus in striatum of living mice (Cumming et al., 2002) and likewise in positron emission tomography (PET) agonist studies of non-human primate (Narendran et al., 2005). However, the potential utility of agonist ligands for PET investigations of the pathophysiology of Parkinson's disease has scarcely been investigated.

Parkinson's disease can be modeled in rats, which have undergone substantial depletions of the dopamine innervation in striatum following unilateral infusion of the toxin 6-OHDA to the medial forebrain bundle. In general, these dopamine depletions eventually result in increased abundance of binding sites for dopamine D₂-like receptor antagonists, as in untreated cases of

Abbreviations: NSB, non specific binding; ROI, region of interest; SBR, specific binding ratio.

* Corresponding author at: Center for Integrated Molecular Brain Imaging, Neurobiology Research Unit, Rigshospitalet, Juliane Maries Vej 24, Rigshospitalet, Building 9201, DK-2100 Copenhagen, Denmark. Tel.: +3545 6704; fax: +45 3545 6713.

E-mail address: mikael.palner@gmail.com (M. Palner).

0197-0186/\$ – see front matter © 2010 Elsevier Ltd. All rights reserved.

doi:10.1016/j.neuint.2010.12.007

Please cite this article in press as: Palner, M., et al., Effects of unilateral 6-OHDA lesions on [³H]-N-propylnorapomorphine binding in striatum ex vivo and vulnerability to amphetamine-evoked dopamine release in rat. *Neurochem. Int.* (2011), doi:10.1016/j.neuint.2010.12.007

idiopathic Parkinson's disease. Thus, molecular imaging has revealed a 40% increase in [^{11}C]raclopride binding in striatum of untreated patients with Parkinson's disease (Dentresangle et al., 1999). The response of agonist binding sites to dopamine depletion is less well-established. The specific binding of [^3H]NPA was 50–100% increased in rat striatum ipsilateral to extensive 6-OHDA lesions (Van der Werf et al., 1984). However, in untreated patients with early Parkinson's disease, the binding in striatum (more exactly the putamen) of the D_3 -preferring agonist [^{11}C]PHNO was elevated by 25%, as was likewise the binding of [^{11}C]raclopride (Boileau et al., 2009). Furthermore, the vulnerability of [^{11}C]PHNO binding in intact striatum does not differ from that of [^3H]raclopride in an amphetamine challenge study ex vivo (McCormick et al., 2008), which might likewise predict a comparable responsiveness of agonist sites to 6-OHDA lesions as well. Thus, it has not been clearly established that agonist binding sites are up-regulated to a greater extent than antagonist sites in a condition of dopamine depletion. Furthermore, the studies have hitherto considered whole striatum, or large divisions such as the putamen. Therefore, in order to compare the responsiveness of agonist and antagonist binding sites to prolonged dopamine depletion, we used quantitative autoradiography to measure ex vivo the availability of binding sites for [^3H]NPA in five divisions of the extended striatum of rats with unilateral 6-OHDA lesions. These results were directly contrasted with the density of binding sites measured with [^3H]raclopride in vitro from the same animals. We also tested the hypothesis that [^3H]NPA binding ex vivo should be asymmetrically responsive to amphetamine challenge, in analogy to a pharmacological activation study in early Parkinson's disease, which is usually characterized by asymmetric nigrostriatal degeneration. The [^3H]raclopride autoradiography in vitro was conducted in order to quantify the up-regulation of antagonist binding sites in divisions of the denervated striatum.

2. Materials and methods

2.1. Materials

Chemicals was obtained from Sigma–Aldrich except in the following cases: zoletil (Virbac), xylazine (Intervet), butorphanol tartrate (Scan Vet), d-amphetamine (Lipomed), [^3H]NPA (Vitrox), [^3H]raclopride (PerkinElmer) and [^{125}I]PE2I (MAP Medical Technologies).

2.2. Animals

Sixteen male Sprague–Dawley rats (Charles River, Germany) weighing between 250 and 300 g were used in this study. The animals were held under standard laboratory conditions with a 12-h light/12-h dark cycle and ad libitum access to food and water. After arrival, the animals were allowed to acclimatize for at least five days before use. All efforts were made to minimize animal suffering, to reduce the number of animals used. All animal experiments were carried out in accordance with the European Communities Council Resolves of 24 November 1986 (86-609/ECC) and approved by the Danish State Research Inspectorate (J. No. 2002/561-527).

2.3. 6-OHDA lesion

The rats were anesthetized with 1 mL/kg i.m. of a mixture containing zoletil (6.25 mg/mL), xylazine (5 mg/mL) and butorphanol tartrate (0.25 mg/mL). Animals then received desmethylimipramine (DMI) (25 mg/kg, i.p.) to protect noradrenergic neurons, and were placed in a stereotaxic apparatus (David Kopf Instruments) with the incisor bar set 3.3 mm below the level of the ear bars. A solution of 6-OHDA hydrobromide (8 μg dissolved in 4 μL saline containing 0.05% ascorbic acid) was drawn into a 10 μL syringe, and infused into the medial forebrain bundle at coordinates (AP: -4.4 mm, ML: 2 mm, DV: 8 mm) according to the coordinates given by Paxinos and Watson. The infusion was delivered at 1 $\mu\text{L}/\text{min}$ driven by an infusion pump, followed by a 5 min pause prior to slow withdrawal of the syringe needle. The burr hole was closed with bone wax and the wound was sutured. After recovery from anesthesia, rats were returned to the home cage for recovery for 14 days, so as to allow development of the lesions, and the attainment of stable changes in post-synaptic dopamine $\text{D}_{2/3}$ receptors in response to prolonged denervation.

2.4. Ex vivo [^3H]NPA autoradiography and response to amphetamine

Rats were randomly assigned to saline or amphetamine groups. During acute immobilization, saline ($n = 9$) or d-amphetamine ($n = 7$) (3 mg/kg, in a total of 500 μL saline) was administered i.p. 5 min prior to tracer injection. The [^3H]NPA (specific activity >50 Ci/mmol) was administered through the tail vein as a single bolus in 300 μL saline containing 0.1% ascorbic acid. Rats were returned to their cage, and killed by decapitation 45 min later, doing a state of pseudo-equilibrium of the specific [^3H]NPA binding (Cumming et al., 2002). Brains were quickly removed, rinsed in ice-cold water, and placed on ice until frozen by immersion in isopentane at -40 $^{\circ}\text{C}$. After storage at -80 $^{\circ}\text{C}$, brains were cut with a cryostat (Microme HM 500 OM), and 20 μm sections, collected from the anterior striatum (+1.56 to +1.36 AP) and posterior striatum (-1.08 to -1.28 AP), were mounted on glass slides. Those slides for autoradiography ex vivo were dehydrated and fixed overnight by exposure to para-formaldehyde vapor. The following day, they were placed along with tritium standard strips (Amersham) on phosphor imaging plates (BAS-TR2040, Fujifilm), which were exposed for three weeks. We calculated the specific binding ratio (SBR) in each region of interests (ROI), as defined in Fig. 1. Non-specific binding (NSB) was determined by the binding in cortex on the same section. $\text{SBR} = (\text{total activity in ROI} - \text{total activity in NSB ROI}) / \text{total activity in NSB ROI}$. The binding in the lesioned side was reported (Fig. 2) as a percentage of the SBR in the lesion side to the corresponding SBR in the intact side.

2.5. In vitro [^3H]raclopride autoradiography

Sections collected from the ex vivo experiment were washed 2×15 min in assay buffer (Tris-HCl 50 mM, NaCl 150 mM, KCl 5 mM, CaCl_2 1 mM, MgCl_2 1 mM, 0.1% ascorbic acid, pH 7.4, 21 $^{\circ}\text{C}$) to remove [^3H]NPA and endogenous dopamine. Sections was then incubated for 60 min at room temperature in assay buffer modified by the addition of [^3H]raclopride to a final concentration of 2 nM. For every second section, butaclamol (10 μM) was added to determine the non-specific binding. After 60 min the incubation was terminated by washing 3×5 min in ice cold assay buffer. The sections was dehydrated, fixed in para-formaldehyde vapor and exposed to an imaging plate (BAS-TR2040, Fujifilm) for 14 days, and the binding in lesioned vs. intact sides was calculated as above.

2.6. Dopamine transporter [^{125}I]PE2I autoradiography

In order to verify the 6-OHDA lesions, selected brain sections from anterior and posterior levels were incubated at room temperature in Tris buffer (pH 7.4) containing 200 mM NaCl for 10 min prior to addition of the dopamine transporter ligand, [^{125}I]PE2I (8.8 TBq/ μmol) to a final concentration of 2 nM. After 60 min incubation at room temperature, the slides were washed in ice-cold buffer (3×5 min), rapidly dried, and then exposed to an imaging plate (BAS-MS 2040, Fujifilm) for 14 h, and the binding in lesioned vs. intact sides was calculated as above.

2.7. Statistics

ImageJ v1.37 was used for image analysis. A paired two-tailed t -test was used to compare lesion vs. healthy side on the same section, an unpaired two-tailed t -test was used to compare across sections and an unpaired one tailed t -test was used to calculate the significance of a % increase. A two-tailed ANOVA was used to calculate the significance of the gradient in striatum. Significant differences was marked as * $p < 0.05$, ** $p < 0.01$ and *** $p < 0.001$. A few significant outliers were removed after a Grubb's test with confidence interval of 99%. All deviations are shown as standard errors of the mean (SEM).

3. Results

Representative autoradiograms for [^{125}I]PE2I, [^3H]NPA and [^3H]raclopride are shown in Fig. 1. [^{125}I]PE2I specific binding was 90% abolished in striatum on the ipsilateral side of the lesion, whereas the extent of the lesion was less consistent in the nucleus accumbens ($30 \pm 81\%$). The binding (SBR) of [^3H]NPA was increased by approximately 50% in the lesioned anterior striatum (anterior dorsal medial and anterior ventral lateral) of the saline treated rats and by 100% in the same regions of the amphetamine-treated rats (Fig. 2). Lesser, but not significant, increases in binding (SBR) were seen in lesioned nucleus accumbens and posterior striatum (posterior dorsal medial and posterior ventral lateral). Increases in the binding (SBR) of [^3H]raclopride on the lesioned side were in the range of 0–20% in both saline and amphetamine groups, reaching significance only in the posterior ventral lateral region of striatum.

The overall percentage increases in binding were greater with [^3H]NPA than [^3H]raclopride, a difference reaching significance in

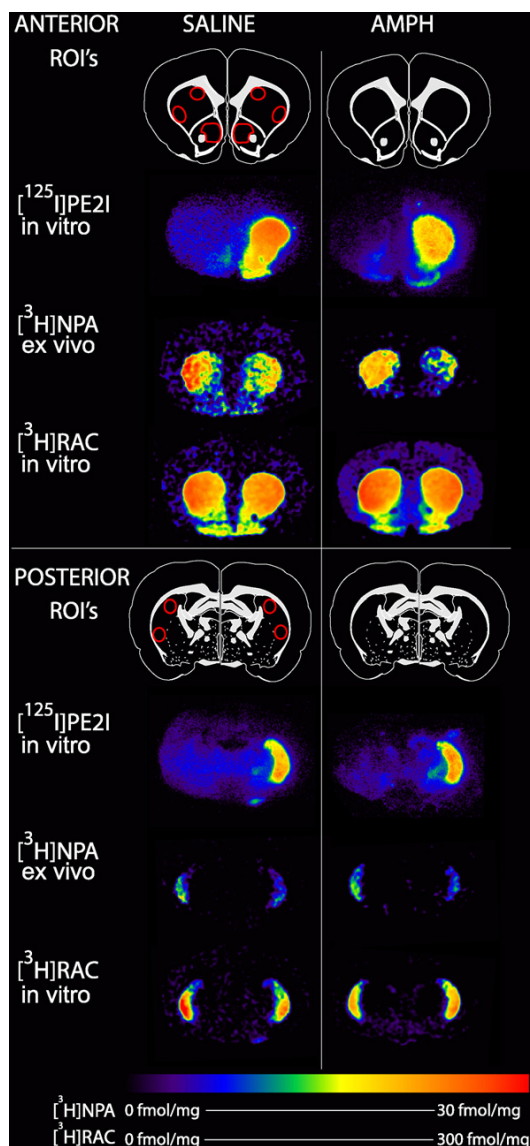


Fig. 1. Representative autoradiograms of [^{125}I]PE2I, [^3H]NPA and [^3H]raclopride binding in unilateral 6-OHDA lesioned rats. This figure shows the anterior and posterior regions of interest (ROIs) projected upon representative autoradiograms from a representative saline-treated (left column) and an amphetamine-treated (AMPH) (right column) rat. Autoradiograms show binding of the dopamine transporter ligand [^{125}I]PE2I in vitro, dopamine $\text{D}_{2/3}$ agonist ligand [^3H]NPA ex vivo, and the dopamine $\text{D}_{2/3}$ antagonist ligand [^3H]raclopride ([^3H]RAC) in vitro.

both anterior regions of striatum in the saline-treated group (anterior dorsal medial $p = 0.0135$ and anterior ventral-lateral striatum $p = 0.0085$) and which was highly significance in the anterior striatal regions of the amphetamine treated group (anterior dorsal media $p = 0.0038$, and anterior ventral lateral striatum $p = 0.0001$). Bound [^3H]NPA on the lesioned side was not substantially displaced in the amphetamine treated group, presumably due to the 90% dopamine depletion. As expected, there was no evidence for acute amphetamine effects on [^3H]raclopride binding in vitro, given the rigorous washing of the brain sections to removed bound [^3H]NPA and endogenous dopamine.

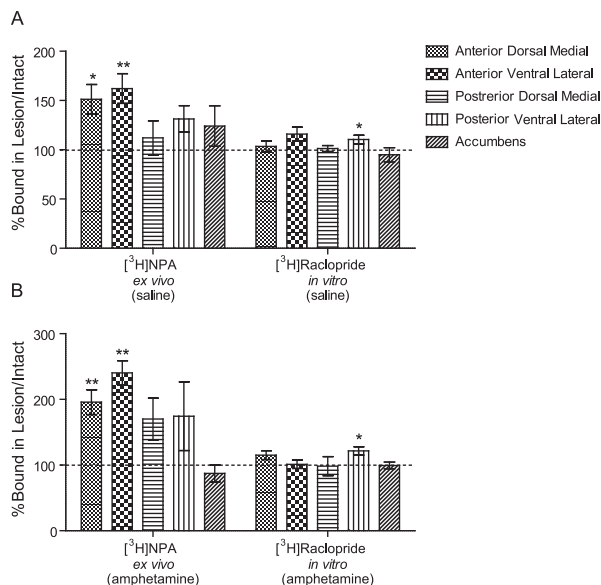


Fig. 2. Percentage differences in specific binding in unilateral 6-OHDA lesioned rats. This figure shows the percentage difference in specific binding ratio of lesion vs. intact side in several striatal regions of interest of 6-OHDA lesioned rats. The figure illustrates (A) the saline-treated rats and (B) the corresponding observations in rats with amphetamine challenge.

4. Discussion

We found that the unilateral 6-OHDA lesions produced the expected 90% decrease in the concentrations of dopamine reuptake sites in dorsal striatum, indicative of a substantial loss of ascending dopaminergic fibres, leading to dopamine depletion. The main emphasis of this study concerns the consequences of prolonged dopamine depletion on the abundance and affinity state of dopamine D_2 -like receptors in rat striatum, and by extension the predicted changes which might be expected in PET studies of Parkinson's disease patients. We noted a latero-medial gradient of increased binding of the D_2 -antagonist [^3H]raclopride in the 6-OHDA-lesioned rat striatum in vitro (after removal of endogenous dopamine), as described previously in a study with [^3H]spiperone (Cadet et al., 1991). However, others reported no difference between the increase in dopamine $\text{D}_{2/3}$ receptor antagonist binding in the dorsal and ventral lateral striatal areas following similar lesions (LaHoste and Marshall, 1989). In our hands, the maximal magnitude of the observed increases in [^3H]raclopride binding in the dopamine depleted striatum was about 15%, in comparison to the 50% increases reported in another rat study (Ishida et al., 2004), and in a PET study of untreated patients with Parkinson's disease (Dentresangle et al., 1999). Discrepancies in the extent of striatal dopamine D_2 receptor up-regulation are likely due to regional differences in the completeness of the dopamine lesion. In previous 6-OHDA-lesion studies, there was a triple relationship between (1) the extent of loss of dopamine transporters, (2) the turning behaviour evoked by pharmacological challenges with apomorphine or methamphetamine (Liu et al., 2009), and (3) the increase in striatal [^{11}C]raclopride binding in vivo (Inaji et al., 2005). In the latter study, asymmetric motor behaviour and increased dopamine D_2 receptor availability in striatum was evident only in animals with more than 90% loss of dopamine transporters on the side of the lesion. As such, the lesions in the present study, as verified by autoradiographic [^{125}I]PE2I binding, were just at the threshold required for upregulation of dopamine receptors in dorsal lateral striatum,

thus emulating the condition of early Parkinson's disease, rather than complete denervation.

Qualitatively, the autoradiographic distribution of [³H]NPA binding is highest in ventral lateral and dorsal medial regions of the striatum (Minuzzi and Cumming, 2010; Dubois and Scatton, 1985). Quantitative analysis in the latter study revealed near equivalence of the maximal binding of [³H]NPA and [³H]raclopride in dorsal striatum, but a certain predominance of [³H]raclopride binding sites in the ventral striatum and olfactory tubercle. However, the present study was not designed to test the relative absolute abundances (B_{\max}) of agonist and antagonist sites, but rather to establish the sensitivity of [³H]NPA binding (at a tracer dose) measured ex vivo to a 90% dopamine depletion, and the relative vulnerability of [³H]NPA binding in the unlesioned striatum to amphetamine-evoked dopamine release.

The [³H]NPA binding results ex vivo in the saline-treated rats showed a 50% increase in receptor availability in the 6-OHDA lesioned anterior regions of striatum, and a non-significant 20% increase in the posterior regions of striatum and nucleus accumbens. Thus, findings with [³H]NPA binding ex vivo show greater responsiveness to the dopamine depletion as compared to the [³H]raclopride findings in vitro, where there was only a slight up-regulation in antagonist binding sites. The preferential increase in [³H]NPA binding likely results from two phenomena, which cannot be entirely disentangled in the present study: reduced competition from endogenous dopamine in the side of the 6-OHDA lesion, and actual increases in the abundance of dopamine receptors. Since the effects of the 90% dopamine depletion on [³H]raclopride binding site up-regulation were slight, and since washing should have removed any competition from endogenous dopamine in vitro, it may be that altered competition effects predominantly explain the increased [³H]NPA binding ex vivo. Indeed, this would be expected from the earlier result that the vulnerability of [³H]NPA binding measured ex vivo to altered dopamine release exceeds that of the antagonist [¹¹C]raclopride in the same intact animals (Cumming et al., 2002). The present regional analysis suggests that this effect favoring agonist binding is less marked in the posterior regions of the rat striatum. It should be noted that comparing the bindings of [³H]NPA ex vivo and of [¹¹C]raclopride in vitro presents a limitation of the study in that the response of agonist and antagonist sites to the asymmetric dopamine lesion are not compared directly. However, the present preliminary study was intended only to characterize the extent of altered [³H]NPA binding in vivo in association with a 10–20% upregulation of antagonist sites, as documented with [³H]raclopride in vitro.

The only other study comparing agonist and antagonist binding in a condition of dopamine depletion is a [¹¹C]PHNO PET study of untreated patients with early Parkinson's disease (Boileau et al., 2009). In that report, there were roughly equivalent 25% increases in the availability of binding sites for the D₃-preferring agonist [¹¹C]PHNO and the D_{2/3} antagonist [¹¹C]raclopride. Our study suggests that the D_{2/3} agonist [¹¹C]NPA would be superior to [¹¹C]raclopride for detecting increases in receptor availability in PET studies of early Parkinson's disease. Present results also suggest that this difference might be greater in a condition of challenge with indirect agonists such as levodopa or amphetamine, as used in the present rat study. Indeed, we found that the amphetamine challenge nearly doubled the asymmetric distribution of [³H]NPA measured in striatum ex vivo; most likely the challenge treatment increased the endogenous competition mainly on the intact side, without substantially increasing the competition on the 6-OHDA lesioned side. Likewise, a methylphenidate (Ritalin) challenge failed to evoke any reduction in putamenal [¹¹C]raclopride binding in a PET study of Parkinson's

disease patients (Koochesfahani et al., 2006), nor did amphetamine challenge alter the apparent affinity of [¹¹C]raclopride binding in striatum of parkinsonian monkeys (Doudet et al., 2002). However, further experiments are required to verify that the residual dopamine innervation in the 6-OHDA lesion model is completely insufficient to subserve amphetamine-evoked [³H]NPA binding changes.

5. Conclusion

Our study shows that the D_{2/3} agonist [³H]NPA binding increase in the lesioned side of unilateral 6-OHDA lesioned rats was greater than the increase of [³H]raclopride. Furthermore, amphetamine challenge nearly doubled this asymmetric distribution of [³H]NPA measured in striatum ex vivo. Our results suggest that [¹¹C]NPA will be superior to [¹¹C]raclopride for detecting increases in receptor availability in PET studies of early Parkinson's disease.

Acknowledgements

This work was supported by the Danish Agency for Science, Technology and Innovation, Rigshospitalet, the EC-FP6-project DiMI, LSHB-CT-2005-512146 and the Lundbeck Foundation.

References

- Boileau, I., Guttman, M., Rusjan, P., Adams, J.R., Houle, S., Tong, J., Hornykiewicz, O., Yoshiaki, F., Wilson, A.A., Kapur, S., Kish, S.J., 2009. Decreased binding of the D₂ dopamine receptor-preferring ligand [¹¹C]-(+)-PHNO in drug-naïve Parkinson's disease. *Brain* 132 (5), 1366–1375.
- Cadet, J.L., Last, R., Kostic, V., Przedborski, S., Jackson-Lewis, V., 1991. Long-term behavioral and biochemical effects of 6-hydroxydopamine injections in rat caudate-putamen. *Brain Research Bulletin* 26 (5), 707–713.
- Cumming, P., Wong, D.F., Gillings, N., Hilton, J., Scheffel, U., Gjedde, A., 2002. Specific binding of [¹¹C]raclopride and N-[³H]propyl-norapomorphine to dopamine receptors in living mouse striatum: occupancy by endogenous dopamine and guanosine triphosphate-free G protein. *Journal of Cerebral Blood Flow and Metabolism* 22 (5), 596–604.
- Dentresangle, C.L., Veyre, D., Bars, L., Pierre, C., Lavenne, F., Pollak, P., Guerin, J., Froment, J.C., Brousolle, E., 1999. Striatal D₂ dopamine receptor status in Parkinson's disease: an [¹⁸F]dopa and [¹¹C]raclopride PET study. *Movement Disorders* 14 (6), 1025–1030.
- Doudet, D.J., Jivan, S., Ruth, T.J., Holden, J.E., 2002. Density and affinity of the dopamine D₂ receptors in aged symptomatic and asymptomatic MPTP-treated monkeys: PET studies with [¹¹C]raclopride. *Synapse* 44 (3), 198–202.
- Dubois, A., Scatton, B., 1985. Heterogeneous distribution of dopamine D₂ receptors within the rat striatum as revealed by autoradiography of [³H]N-n-propyl-norapomorphine binding sites. *Neuroscience Letters* 57 (1), 7–12.
- Inaji, M., Okouchi, T., Ando, K., Maeda, J., Nagai, Y., Yoshizaki, T., Okano, H., Nariai, T., Ohno, K., Obayashi, S., Higuchi, M., Suhara, T., 2005. Correlation between quantitative imaging and behavior in unilaterally 6-OHDA-lesioned rats. *Brain Research* 1064 (1–2), 136–145.
- Ishida, Y., Keiichi, K., Magata, Y., Takeda, R., Hashiguchi, H., Abe, H., Mukai, T., Hideo, S., 2004. Changes in dopamine D₂ receptors and 6-[¹⁸F]fluoro-L-3,4-dihydroxyphenylalanine uptake in the brain of 6-hydroxydopamine-lesioned rats. *Neurodegenerative Diseases* 1 (2–3), 109–112.
- Koochesfahani, K.M., de la Fuente-Fernández, R., Sossi, V., Schulzer, M., Yatham, L.N., Ruth, T.J., Blinder, S., Stoessl, A.J., 2006. Oral methylphenidate fails to elicit significant changes in extracellular putamenal dopamine levels in Parkinson's disease patients: positron emission tomographic studies. *Movement Disorders* 21 (7), 970–975.
- LaHoste, G.J., Marshall, J.F., 1989. Non-additivity of D₂ receptor proliferation induced by dopamine denervation and chronic selective antagonist administration: evidence from quantitative autoradiography indicates a single mechanism of action. *Brain Research* 502 (2), 223–232.
- Laruelle, M., 2000. Imaging synaptic neurotransmission with in vivo binding competition techniques: a critical review. *Journal of Cerebral Blood Flow and Metabolism* 20, 423–451.
- Liu, L., Wang, Y., Li, B., Jia, J., Sun, Z., Zhang, J., Tian, J., Wang, X., 2009. Evaluation of nigrostriatal damage and its change over weeks in a rat model of Parkinson's disease: small animal positron emission tomography studies with [¹¹C]beta-CFT. *Nuclear Medicine and Biology* 36 (8), 941–947.
- McCormick, P.N., Wilson, A.A., Kapur, S., Seeman, P., 2008. Dopamine D₂ receptor radiotracers [¹¹C](+)-PHNO and [³H]raclopride are indistinguishably inhibited by D₂ agonists and antagonists ex vivo. *Nuclear Medicine and Biology* 35 (1), 11–17.

Minuzzi, L., Cumming, P., 2010. Agonist binding fraction of dopamine D_{2/3} receptors in rat brain: a quantitative autoradiographic study. *Neurochemistry International* 56 (6–7), 747–752.

Narendran, R., Hwang, D., Slifstein, M., Hwang, Y., Huang, Y., Ekelund, J., Guillin, O., Scher, E., Martinez, D., Laruelle, M., 2005. Measurement of the proportion of D₂ receptors configured in state of high affinity for agonists *in vivo*: a positron emission tomography study using [¹¹C]N-propyl-norapomorphine and

[¹¹C]raclopride in baboons. *Journal of Pharmacology and Experimental Therapeutics* 315 (1), 80–90.

Van der Werf, J.F., Sebens, J.B., Korf, J., 1984. *In vivo* binding of N-n-propylnorapomorphine in the rat striatum: quantification after lesions produced by kainate, 6-hydroxydopamine and decortication. *European Journal of Pharmacology* 102 (2), 251–259.

Ex Vivo Evaluation of the Serotonin 1A Receptor Partial Agonist [³H]CUMI-101 in Awake Rats

MIKAEL PALNER,^{1,2,3*} MARK D. UNDERWOOD,^{1,2} DILEEP J.S. KUMAR,^{1,2} VICTORIA ARANGO,^{1,2} GITE M. KNUDSEN,³ J. JOHN MANN,^{1,2} AND RAMIN V. PARSEY^{1,2}

¹Division of Molecular Imaging and Neuropathology, New York State Psychiatric Institute, New York, New York

²Department of Psychiatry, Columbia University College of Physicians and Surgeons, New York, New York

³Center for Integrated Molecular Brain Imaging, Rigshospitalet, Copenhagen, Denmark

AQ1

KEY WORDS 5-HT_{1A}; serotonin; positron emission tomography (positronemission tomography); citalopram; fenfluramine; 4-chloro-DL-phenylalanine; depletion; ex vivo; CUMI-101; MMP

ABSTRACT [³H]CUMI-101 is a 5-HT_{1A} partial agonist, which has been evaluated for use as a positron emission tracer in baboon and humans. We sought to evaluate the properties of [³H]CUMI-101 ex vivo in awake rats and determine if [³H]CUMI-101 can measure changes in synaptic levels of serotonin after different challenge paradigms. [³H]CUMI-101 shows good uptake and good specific binding ratio (SBR) in frontal cortex 5.18 and in hippocampus 3.18. Binding was inhibited in a one-binding-site fashion by WAY100635 and unlabeled CUMI-101. The ex vivo B_{\max} of [³H]CUMI-101 in frontal cortex (98.7 fmol/mg) and hippocampus (131 fmol/kg) agree with the ex vivo B_{\max} of [³H]MPPF in frontal cortex (147.1 fmol/mg) and hippocampus (72.1 fmol/mg) and with in vitro values reported with 8-OH-DPAT. Challenges with citalopram, a selective serotonin reuptake inhibitor, fenfluramine, a serotonin releaser, and 4-chloro-DL-phenylalanine, a serotonin synthesis inhibitor, did not show any effect on the standardized uptake values (SUVs) in any region. Citalopram did alter SBR, but this was due to changes in cerebellar SUVs. Our results indicate that [³H]CUMI-101 is a good radioligand for imaging 5-HT_{1A} high-density regions in rats; however, the results from pharmacological challenges remain inconclusive. **Synapse 00:000–000, 2010.** © 2010 Wiley-Liss, Inc.

INTRODUCTION

Serotonin 1A receptors (5-HT_{1A}) are implicated in numerous neurobiological functions and in the pathophysiology of mood disorders, sleep, eating, schizophrenia, anxiety, and degenerative brain diseases (Borg, 2008; Brunelli et al., 2009; Ebenezer et al., 2007a,b; Sumiyoshi et al., 2008; Wilson et al., 2005). To date, all human PET studies have been performed with 5-HT_{1A} antagonists tracers, most commonly, [¹¹C]WAY100635 and [¹⁸F]MPPF. We have recently reported the successful development and in vivo evaluation of a novel 5-HT_{1A} agonist tracer (Milak et al., 2008a). Carbon-11-labeled CUMI-101, also known as [¹¹C]MMP, is a 5-HT_{1A} partial agonist in vitro, with a K_i of 0.15 nM and EC_{50} of 0.1 nM, reaching 80% of the [³⁵S]GTP γ S binding measured by serotonin (Kumar, 2007). [¹¹C]CUMI-101 has recently been approved for human use (Milak et al., 2008b). 5-HT_{1A} is, like other G-protein-coupled receptors (GPCR),

believed to exist in at least two different affinity states with regard to agonist binding, a high-affinity state coupled with intracellular G-protein, and a low-affinity state decoupled from intracellular G-protein. Although this two-state model has been clearly established in vitro for the 5-HT_{1A} receptor (Clawges et al., 1997; Gozlan et al., 1995; Mongeau et al., 1992) and other GPCRs (Fitzgerald et al., 1999; Richfield et al., 1989), it is still unknown if these different states are relevant in vivo. An agonist PET tracer will help to elucidate this. In this study, we evaluate the uptake, distribution, and selectivity of [³H]CUMI-101 in a series of ex vivo experiments in awake rats. An issue

*Correspondence to: Mikael Palner, BioNano, Nano-Science Center, University of Copenhagen, Universitetsparken 5, 2100 København Ø, Denmark. E-mail: mikael.palner@nano.ku.dk

Received 13 September 2010; Accepted 11 November 2010

DOI 10.1002/syn.20888

Published online in Wiley Online Library (wileyonlinelibrary.com).

© 2010 WILEY-LISS, INC.

ID: subramaniank

Date: 29/12/10

Time: 12:10

Path: N:/3b2/SYN#/Vo100000/100143/APPFfile/JW-SYN#100143

NOTE TO AUTHORS: This will be your only chance to review this proof. Once an article appears online, even as an EarlyView article, no additional corrections will be made.

with small animals is dosing of PET tracers without exceeding tracer dose to be confident that the following experiments were done at tracer doses, we determined the maximum binding of [³H]CUMI-101 and compared it to the maximum binding of [³H]MPPF.

Theory predicts that an agonist or partial agonist PET tracer should be more likely to be sensitive to competition from endogenous neurotransmitter than an antagonist PET tracer, studies with [¹¹C]WAY100635 and [¹⁸F]MPPF have previously shown minimal changes after acutely induced serotonin release (Ceglia et al., 2004; Günther et al., 2008; Udo De Haes et al., 2005; Zimmer et al., 2002) or depletion (Zimmer et al., 2003). The theory is supported by dopamine (DA) D₂ agonist PET tracers, which have been shown to be more sensitive to competition from endogenous DA than DA D₂ antagonist PET tracers (Cumming et al., 2002; Narendran et al., 2005). To evaluate the sensitivity of [³H]CUMI-101 to competition from endogenous serotonin, we measured the *ex vivo* changes in the standardized uptake value (SUV), specific binding (SB), and the specific binding ratio (SBR) of [³H]CUMI-101 after acute increase in serotonin, either with citalopram (a serotonin reuptake inhibitor) or fenfluramine (a serotonin releaser), and after acute depletion of serotonin with 4-chloro-DL-phenylalanine (pCPA, a serotonin synthesis inhibitor).

MATERIALS AND METHODS

General

Male Sprague–Dawley rats, weighing 318 ± 19 SD g on the day of the experiments, were used. Rats were maintained on a 12-h light–dark cycle with free access to food and water for at least 5 days before the experiments. The animals were kept three to four a cage, except where noted. On the day of the experiment, they were transported to the laboratory and only removed briefly from the cage to perform injections and decapitations. Awake animals were used in the experiments for several reasons; anesthetics are known to change neurotransmitter levels, which would confound the kinetics of radioligand and pharmaceuticals; anesthetics are not used in humans, and so experiment conditions without anesthetics are more comparable; depth of anesthesia in individual animals can be variable, and so absence of anesthesia allows for more experiments to be carried out at one time and is thereby likely to reduce variability; the administration of drugs and ligands was considered not likely to elicit more than momentary stress and did not require sustained, extended, and/or repeated anesthesia; and repeated anesthesia may have been comparatively more stressful than no anesthesia, because the treatments were brief, and animals were returned to their home cages in the interim. The experiments were conducted in accordance with the

guidelines of the Columbia University and New York State Psychiatric Institute's Animal Care and Use Committee and the Danish Council for Animal Ethics (Journal No. 2006/561-1155). WAY100635 (*N*-(2-(4-(2-methoxyphenyl)-1-piperazinyl)ethyl)-*N*-(2-pyridyl)cyclohexanecarboxamide trihydrochloride) and CUMI-101 (2-[4-[4-methyl-2-methoxyphenyl]piperazin-1-yl]butyl)-4-methyl-1,2,4-triazine-3,5-(2*H*,4*H*)dione) were synthesized by the Radioisotope and Radioligand Production Laboratory at Columbia University College of Physicians and Surgeons, 8-OH-DPAT (8-hydroxy-2-(di-*n*-propylamino)tetralin), (+)-fenfluramine hydrochloride, pCPA, and MPPF (4-(2'-methoxyphenyl)-1-[2'-(*N*-2"-pyridinyl)-*p*-fluorobenzamido]-ethylpiperazine) were purchased from Sigma-Aldrich, (*S*)-citalopram was supplied by Lundbeck A/S. [³H]CUMI-101 was synthesized by the NIMH Chemical Synthesis and Drug Supply Program, specific activity 2.87 TBq/mmol, radiochemical purity of 99.9%. High-specific activity [³H]MPPF, specific activity 2.89 TBq/mmol, was purchased from Perkin-Elmer.

Time activity curve of [³H]CUMI-101 binding

The uptake of [³H]CUMI-101 over time was examined in awake rats. Rats were divided into six groups ($n = 4$ per group). All animals were injected in the tail vein with [³H]CUMI-101 (0.26 ± 0.003 SEM nmol/kg, 0.75 ± 0.008 MBq/kg). The groups were decapitated at 15, 30, 45, 60, 90, and 120 min postinjection of tracer, the brain was removed from the skull, rinsed for excess blood by a quick dip in dH₂O, placed on an ice cold glass plate, and dissected into regions of interests (ROIs); cerebellum, frontal cortex, hippocampus, and striatum. Blood from the trunk was collected in heparinized vials, and the plasma was then isolated by centrifugation (10 min at 16,000g). All brain tissue samples and plasma samples were collected in tared counting vials and weighed, then 1 ml solvable (Perkin Elmer) was added, and the samples were left overnight to dissolve. The following day, 2 ml Ultima Gold Scintillation fluid (Perkin Elmer) was added, and the vials were shaken and then left overnight before counting in a liquid scintillation counter (Tri-Carb 2300TR, Packard) with automatic quench correction. Blank samples and aliquots of the injected dose were also measured in the scintillation counter. $SUV = (\text{injected activity}/\text{rat weight})/(\text{activity in ROI}/\text{ROI weight})$ and $SBR = (\text{activity in ROI} - \text{activity in cerebellum})/\text{activity in cerebellum}$ were calculated and presented as time activity curve (TAC).

Binding density of [³H]CUMI-101 and [³H]MPPF-binding sites

The *ex vivo* 5-HT_{1A} receptor-binding density (B_{max}) and affinity (K_D) of [³H]CUMI-101 and [³H]MPPF was examined. Awake rats (27 rats for [³H]CUMI-

101, 30 rats for [³H]MPPF) were injected in the tail vein with either compound. The specific activity of the injected tracer was changed by the addition of unlabeled CUMI-101 or MPPF, thereby changing the total mass of injected compound: total CUMI-101 ([³H]CUMI-101 + CUMI-101) mass injected was between 0.02 and 500 nmol/kg; total MPPF ([³H]MPPF + MPPF) mass injected was between 0.1 and 1100 nmol/kg. All rats were decapitated after 90 min, based on the results from the time activity experiments of [³H]CUMI-101; for comparison reasons, [³H]MPPF-injected rats were also decapitated at 90 min. Brains were dissected into the same ROIs as above; cerebellum, frontal cortex, hippocampus, and striatum. Blood from the trunk was collected, and the plasma was isolated as described earlier. For each ROI, the total amount of labeled + unlabeled compound was calculated, then plotted against the injected dose, and subsequently fitted with a one-binding-site model (Graphpad Prism 5). This resulted in a ROI-specific estimate of receptor density (B_{max}) and the injected dose needed to give 50% occupancy (ID_{50}). Furthermore, we calculated the Hill slope using the fitted curve. The in vivo K_D was calculated using the relationship $SBR = B_{max}/K_D$ and a density for tissue of 0.8 g/ml (Hume et al., 1994).

Pharmacological inhibition of [³H]CUMI-101 binding

The inhibition of [³H]CUMI-101 binding to the 5-HT_{1A} receptor was examined. Awake rats were injected i.v. through the tail vein with different doses of the selective 5-HT_{1A} antagonist WAY100635 (0.1, 1, 10, and 4000 nmol/kg, $n = 3$ for each) or a single dose of the 5-HT_{1A} agonist 6-OH-DPAT (4000 nmol/kg, $n = 5$) 5 min before injection i.v. of [³H]CUMI-101 (0.22 ± 0.01 SEM nmol/kg). Second, as described in the above experiment, awake rats were coinjected i.v. with CUMI-101 (same doses as in B_{max} experiment above, $n = 3$ for each) and [³H]CUMI-101 (0.22 ± 0.01 SEM nmol/kg). Control animals were injected i.v. with saline 5 min before the tracer. All rats were decapitated 90 min after tracer injection, brains were dissected, plasma samples were processed, and the SUV, SBR, and SB = (activity in ROI – activity in cerebellum) were calculated as described earlier.

Endogenous serotonin challenges of [³H]CUMI-101 binding

The changes in binding of [³H]CUMI-101 after a pharmacological challenge were examined. Awake rats were injected with different doses of the serotonin reuptake inhibitor citalopram (0.4, $n = 3$ and 4 mg/kg, $n = 7$, i.p., 60 min before tracer) or the serotonin release fenfluramine (10 mg/kg, i.p. 60 min before the tracer $n = 6$ or 10 mg/kg i.v. 5 min before

the tracer $n = 5$) before an i.v. injection of [³H]CUMI-101 (0.18 ± 0.003 SEM nmol/kg). Control animals were injected i.p. with saline 60 min before the tracer. All rats were decapitated 90 min after tracer injection, brains were dissected, plasma samples were processed, and the SUV, SBR, and SB were calculated.

Serotonin depletion effects on [³H]CUMI-101 binding

The binding of [³H]CUMI-101 after depletion of endogenous serotonin was examined. Awake rats were treated with pCPA (190 mg/kg i.p. $n = 6$) and placed in isolation 24-h before experiment, as described by Kornum et al. (2006). Isolation was used, because rats treated with pCPA tend to be more aggressive and fight more than untreated rats. Naive control animals received a saline i.p. injection and were isolated for 24 h before injection of tracer, and normal control animals were housed in groups and received tracer according to the above experiments. On the day of the experiment, all rats received an i.v. injection of [³H]CUMI-101 (0.18 ± 0.003 SEM nmol/kg) and were decapitated 90 min later, brains were dissected, plasma samples were processed, and the SUV, SBR, and SB were calculated as described earlier.

Statistics

Microsoft Office Excel 2003 SP3 and Graphpad Prism v 5.00 were used for calculations and statistics. Saturation curve fitting was done with Graphpad Prism's built in nonlinear regression. Comparisons between groups were done with a two-tailed *t*-test and significant differences marked as * $P < 0.05$, ** $P < 0.01$, and *** $P < 0.001$.

RESULTS

TAC of [³H]CUMI-101 binding

Following injection of [³H]CUMI-101, the brain uptake was highest in the serotonin 5-HT_{1A} rich regions of the hippocampus and frontal cortex, whereas uptake in cerebellum was the lowest. Individual TACs for each region calculated on the basis of the SUV are presented in Figure 1A. The hippocampus displays a peak uptake at 60 min with a SUV of 3.81 ± 0.44 SEM. The uptake in frontal cortex peaked at 15 min, reaching a SUV of 5.18 ± 1.1 SEM. The uptake in striatum peaked at 15 min, reaching a SUV 2.32 ± 0.5 SEM. Cerebellum and plasma uptake/concentration also peaked at 15 min with a SUV of 1.10 ± 0.7 SEM for cerebellum and a SUV of 0.26 ± 0.01 SEM for plasma. Individual SBR for each region is presented in Figure 1B. The SBR in hippocampus increased until 60 min after which it leveled out, with a peak SBR of 6.30 ± 0.21 SEM at 120 min. The SBR in frontal cortex peaked at 60 min with a SBR of

F1

Synapse

5.19 ± 0.15 SEM equal to the SBR in hippocampus at 60 min after which it slowly declined throughout the experiment. For all subsequent studies, the 90-min time point was chosen, because it was between the SBR peaks in the frontal cortex and hippocampus and still within a time range for future comparison with a carbon-11-labeled ligand.

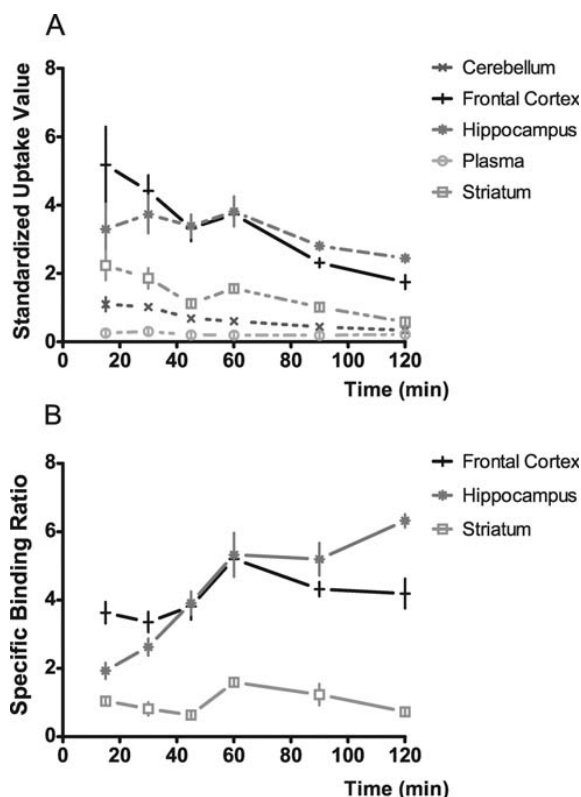


Fig. 1. Ex vivo time activity curves (TAC) in regions of interest (ROI) of [^3H]CUMI-101 in awake rats. **A:** Standardized uptake value (SUV) as a function of time. **B:** Specific binding ratio (SBR) as a function of time. Data are shown as mean \pm SEM.

Binding density of [^3H]CUMI-101 and [^3H]MPPF-binding sites

It was possible to saturate the binding of [^3H]CUMI-101 (the combined amount of [^3H]CUMI-101 and CUMI-101) and [^3H]MPPF (the combined amount of [^3H]MPPF and MPPF) in the frontal cortex, hippocampus, and striatum. Data were best fitted with a one-binding-site model, as the two binding-site model did not fit any of the ROIs. The calculated data are presented in Table I. Based on the injected dose, without correction for free fraction, it was possible to estimate the ID_{50} and in vivo K_D of [^3H]CUMI-101 and [^3H]MPPF binding, but the values came out with high variation and only one estimate, and so no significance could be calculated. Regardless, the ID_{50} of [^3H]CUMI-101 was similar in the hippocampus and frontal cortex (33.4 and 34.2 nmol/kg rat, respectively) and higher in the striatum (188.3 nmol/kg rat), suggesting different binding properties in striatum. Similar results were found when calculating the in vivo K_D in the hippocampus and frontal cortex (17.0 and 18.2 nM, respectively), whereas, in striatum, the K_D was 32.1 nM. In line with this, the Hill slope for [^3H]CUMI-101 saturation in the hippocampus and frontal cortex was close to one, but in the striatum, it was 10.44, suggesting multiple-binding sites. The cerebellum and plasma were nonsaturable. The estimated ID_{50} of [^3H]MPPF in hippocampus and frontal cortex was 20 times higher than for [^3H]CUMI-101; this was expected, because [^3H]MPPF is known to have very poor blood-brain barrier penetration and is a known p-gp substrate (Elsinga et al., 2005), which is also reflected in the poor in vivo K_D of 99 nM in frontal cortex and 33 nM in hippocampus. The estimation of ID_{50} and in vivo K_D of [^3H]MPPF in the striatum was difficult to fit with any binding model, supporting the claim that there is no real binding sites for [^3H]MPPF in the striatum. The Hill slope of [^3H]MPPF in hippocampus and frontal cortex was close to one, suggesting a single binding site as with [^3H]CUMI-101. As with [^3H]CUMI-101, there

T1

TABLE I. Regional estimates of B_{max} , ID_{50} , Hill Slope, SBR, and in vivo K_D from ex vivo saturation studies in awake rats

	Frontal Cortex	Hippocampus	Striatum
[^3H]CUMI-101			
B_{max}	98.7 ± 17.1 fmol/mg	131.3 ± 22.9 fmol/mg	80.9 ± 26.0 fmol/mg
ID_{50}	34.2 ± 20.6 nmol/kg	33.4 ± 20.4 nmol/kg	188.3 ± 134.6 nmol/kg
R^2	0.81	0.76	0.90
Hill slope	0.96 ± 0.82	1.048 ± 0.99	10.44 ± 25.26
SBR	4.64 ± 0.83	5.78 ± 1.04	2.02 ± 0.84
In vivo K_D	17.0 nM	18.2 nM	32.1 nM
[^3H]MPPF			
B_{max}	147.1 ± 31.01 fmol/mg	72.1 ± 15.0 fmol/mg	118.3 ± 46.7 fmol/mg
ID_{50}	743.6 ± 292.6	622.2 ± 245.4	163.0 ± 198.2
R^2	0.95	0.95	0.45
Hill slope	1.46 ± 0.50	0.78 ± 0.44	-
SBR	1.18 ± 1.2	1.72 ± 1.69	1.14 ± 1.21
In vivo K_D	99.7 nM	33.5 nM	83.0 nM

B_{max} , binding maximum, fmol/mg receptors, wet weight. ID_{50} , the injected dose giving 50% occupancy, nmol/kg rat. R^2 , the goodness of the curve fit. SBR, specific binding ratio (ROI-cerebellum/ROI). In vivo K_D ; $K_D = B_{max}/\text{SBR} \times \text{density}$ (0.8 g/ml). Data are shown as mean \pm SEM when possible.

Synapse

was no saturable binding in cerebellum and plasma with [³H]MPPF.

The estimated B_{\max} values are presented in Table I. [³H]CUMI-101 displayed the highest binding in hippocampus and frontal cortex and lowest binding in the striatum. [³H]MPPF showed a slightly different pattern, the highest binding region was the frontal cortex, lower binding in the striatum, and lowest binding in the hippocampus. However, these differences were not significant in either case. Generally, all the saturation curves fitted with a $R^2 > 0.90$. However, [³H]CUMI-101 binding in the hippocampus did not fit well ($R^2 = 0.76$), due to higher variation in the experimental value. [³H]MPPF binding in the striatum was only barely fitted with $R^2 = 0.46$, suggesting that there is no real binding for [³H]MPPF in the striatum. It is a limitation to this comparison that we did not calculate the TAC for [³H]MPPF; however, the estimated B_{\max} values of [³H]MPPF in the frontal cortex and hippocampus should be valid despite the late time-point, as the binding was saturable and fitted well to a one binding site model.

Pharmacological inhibition of [³H]CUMI-101 binding

Pretreatment with the antagonist WAY100365 or parent compound CUMI-101 reduced the SBR in frontal cortex and hippocampus in a dose-response relationship with one-binding site kinetics (Table II and Fig. 2). The LogIC_{50} of WAY100635 was 3.88 ± 0.05 SEM nmol/kg in the frontal cortex and 4.04 ± 0.14 SEM nmol/kg in the hippocampus. The LogIC_{50} of CUMI-101 was 1.39 ± 0.64 SEM nmol/kg in the frontal cortex and 1.52 ± 0.69 SEM nmol/kg in the hippocampus, significantly higher than the corresponding values for WAY100635 (frontal cortex $P = 0.005$, hippocampus $P = 0.007$). At the highest dose, WAY100365 reduced the SBR in hippocampus by 90% and in frontal cortex by 72%, while the SBR in the striatum was the same after treatment. Pretreatment with the agonist 8-OH-DPAT (Table II) reduced the SBR in hippocampus by 48% and in frontal cortex by 23%, while the binding in the striatum was the same after treatment. However, CUMI-101 reduced the SBR in hippocampus by 89%, in frontal cortex by 87%, and also reduced the binding in striatum by 40%, supporting the claim from the previous experiment that a second binding site is present in the striatum. Plasma levels showed small, but significant changes after treatments with CUMI-101 and 8-OH-DPAT, but not after WAY100365.

Endogenous serotonin challenges of [³H]CUMI-101 binding

The rise in intrasynaptic serotonin levels induced by citalopram or fenfluramine (Fig. 3 and Table II)

TABLE II. Percent change in [³H]CUMI-101 uptake and binding after different treatments in comparison with normally group-housed controls

Treatment	n	% change in the cerebellum			% change in frontal cortex			% change in hippocampus		
		SUV	SBR	SB	SUV	SBR	SB	SUV	SBR	SB
CUMI-101 (0.18 mg/kg)	3	-24.8 ± 1.8*	-87.3 ± 11.7***	-90.3 ± 7.1***	-83.1 ± 4.7***	-89.1 ± 11.7***	-91.6 ± 5.9***			
WAY100635 (1.6 mg/kg)	3	-4.3 ± 9.8	-72.9 ± 11.0***	-73.2 ± 7.8***	-80.0 ± 5.1***	-90.9 ± 11.8***	-91.1 ± 5.9***			
8-OH-DPAT (0.9 mg/kg)	5	-21.8 ± 3.3*	-23.7 ± 9.2**	-39.4 ± 5.7***	-47.9 ± 4.1***	-39.4 ± 9.7***	-51.8 ± 4.9***			
Citalopram (0.4 mg/kg)	3	21.7 ± 2.2	-10.7 ± 9.8	+11.3 ± 6.8	+10.9 ± 8.1	-12.5 ± 10.8	+9.4 ± 9.1			
Citalopram (4 mg/kg)	7	15.1 ± 7.1**	-19.4 ± 10.4	-2.1 ± 9.7	+5.1 ± 9.0	-10.9 ± 11.7	+3.6 ± 9.9			
Fenfluramine (10 mg/kg i.v.)	6	-32.1 ± 6.2**	+35.3 ± 10.7*	-5.2 ± 11.9	-0.1 ± 12.1	+48.9 ± 13.2**	+4.6 ± 12.9			
Fenfluramine (10 mg/kg i.p.)	5	-28.9 ± 3.9*	+29.7 ± 9.6**	-5.9 ± 6.7	+5.5 ± 6.9	+52.0 ± 11.4**	+10.5 ± 7.3			
24-h isolation	3	-4.8 ± 4.6	-3.5 ± 18.4	-8.1 ± 11.6	-10.1 ± 12.3	-6.4 ± 19.2	-10.9 ± 12.9			
pCFA + 24 h Iso. (190 mg/kg)	6	-2.4 ± 3.9	-5.8 ± 14.1	-8.1 ± 8.6	-14.1 ± 7.1	-13.7 ± 13.1	-15.76 ± 7.7			

SUV, standardized uptake value; SBR, specific binding ratio ((ROI-cerebellum)/ROI). Stars mark significant changes in relation to the control group.

* $P < 0.05$,

** $P < 0.01$,

*** $P < 0.001$. Data are shown as mean ± SEM.

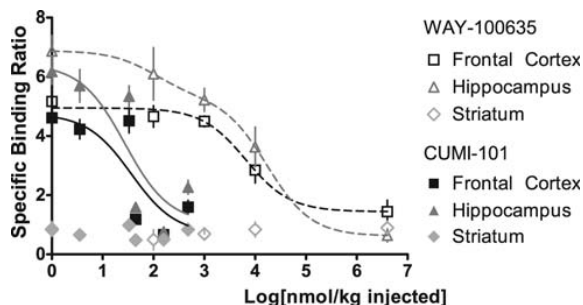


Fig. 2. Inhibition of [^3H]CUMI-101 binding by the antagonist WAY100635 or the parent compound CUMI-101. The binding is inhibited by a one binding-site function with a LogIC_{50} of WAY100635 at 3.88 ± 0.05 SEM nmol/kg in the frontal cortex and 4.04 ± 0.14 SEM nmol/kg in the hippocampus and a LogIC_{50} of CUMI-101 at 1.39 ± 0.64 SEM nmol/kg in the frontal cortex and 1.52 ± 0.69 SEM nmol/kg in the hippocampus.

did not change the SUV of [^3H]CUMI-101 in any of the ROIs. However, citalopram and fenfluramine significantly lowered the concentration of tracer in plasma and fenfluramine concomitantly lowered the SUV in cerebellum. The changes in plasma and cerebellum were relatively small in comparison with the total SUV in frontal cortex and hippocampus, but as SBR is a ratio of SUV in the ROI and the reference region and the reference region SUV is very small, these small changes in cerebellar SUV have profound effects on the SBR. Citalopram treatment did not affect the SBR of [^3H]CUMI-101 in frontal cortex and hippocampus significantly, but there was an overall dose dependent trend for reductions in SBR of 10–20%. Fenfluramine treatment significantly increased the SBR in frontal cortex and hippocampus between 30 and 50%, driven by the reduction in cerebellum uptake as there was no change in the SUV in frontal cortex or hippocampus. There was no apparent difference in giving fenfluramine i.p. 60 min prior or i.v. 5 min prior. Neither citalopram nor fenfluramine treatments significantly changed the SB in any ROI.

Serotonin depletion effects on [^3H]CUMI-101 binding

Twenty-four hours of isolation and treatment with pCPA did not alter SUV, SB, or SBR of [^3H]CUMI-101 in any region (Table II) compared to isolated saline-treated controls. However, there was a significant 15% lower SUV of [^3H]CUMI-101 in the isolated pCPA-treated group compared to normally group housed controls; this difference was also apparent between the isolated saline-treated group and normally housed controls; however, it did not reach significance.

DISCUSSION

[^3H]CUMI-101 is a good tracer in rats, with an uptake comparable to the uptake of [^3H]WAY100635

in rat brain (Hume et al., 1994), a widely used 5-HT $_{1A}$ receptor antagonist, suggesting that [^3H]CUMI-101 could be an alternative to [^3H]WAY100635. [^3H]CUMI-101 has a high uptake in the 5-HT $_{1A}$ receptor rich areas of frontal cortex and hippocampus in awake rat. The uptake in awake rats is similar to the uptake in anesthetized baboon (Kumar et al., 2007). However, the hippocampus uptake in baboon peaks at 5–10 min after which it washes out, unlike the steady state in rats. The similarities between multiple species increase the likelihood of these data being relevant in humans as well.

The binding of [^3H]WAY100635 (Hume et al., 1994) and [^{18}F]MPPF (Udo de Haes et al., 2005) (another widely used 5-HT $_{1A}$ antagonist) is comparable to the pattern of distribution we found with [^3H]CUMI-101 in the frontal cortex, hippocampus, and cerebellum. However, there is almost no binding in striatum with either [^3H]WAY100635 or [^3H]MPPF. This strongly suggest that the binding of [^3H]CUMI-101 in striatum must be to another type of receptor; in fact, binding to the alpha 1A receptor was found to be present in microPET studies with [^{11}C]CUMI-101 in rat (Liow et al., 2010). The SBR of [^3H]CUMI-101 in the frontal cortex in rat peaked at 60 min while the SBR in the hippocampus was higher and kept rising throughout the experiment; at 90 min, the SBR in frontal cortex reached 4.6 and the SBR in hippocampus 5.7. This is in accordance with baboon studies where the SBR in hippocampus is also higher than in the frontal cortex at 90 min. The ex vivo SBR of [^3H]WAY100635 at 60 min in awake rats follows the same pattern, with hippocampus SBR of 14.6 being higher than frontal cortex SBR of 7.8 (Hume et al., 1994). Also, the ex vivo SBR of [^{18}F]MPPF at 30 min in awake rats follows this pattern, with hippocampus SBR of ~ 3 being higher than frontal cortex SBR of ~ 1 (Plenevaux et al., 2000). We determined the SBR of [^3H]MPPF at 90 min in awake rats, with a hippocampus SBR of 1.7 and a frontal cortex SBR of 1.5.

The 5-HT $_{1A}$ receptor rich areas of hippocampus and frontal cortex were saturable with CUMI-101 and MPPF, the binding density was approximately the same with the two compounds, and the average injected dose of [^3H]CUMI-101 was at tracer levels. The saturation binding was best fitted with a one-binding site equation model for both compounds, whereas a two-binding site equation was expected with [^3H]CUMI-101 based on results from the in vitro saturation binding of [^3H]8-OH-DPAT (Mongeau et al., 1992). However, the reported difference between B_{maxH} (high state) and B_{maxL} (low state) with [^3H]8-OH-DPAT was relatively small, and so it might be difficult to distinguish these states in vivo with a saturation experiment. The B_{max} in frontal cortex and hippocampus is considerably higher than are reported ex vivo with [^3H]WAY 100635 in awake rats

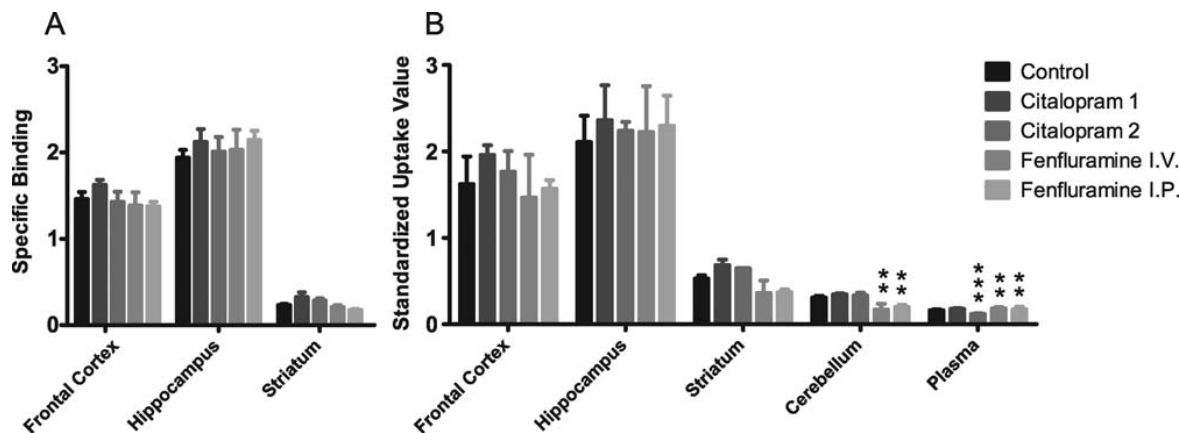


Fig. 3. A the *ex vivo* Specific Binding of [³H]CUMI-101. B represents the *ex vivo* standardized uptake value of [³H]CUMI-101. Both in awake rats after treatment with the serotonin reuptake inhibitor citalopram [(1) 0.4 mg/kg and (2) 4 mg/kg] or the serotonin releaser

fenfluramine (i.v. 10 mg/kg or i.p. 10 mg/kg). Stars mark significant changes in relation to the control group. **P* < 0.05, ***P* < 0.01, ****P* < 0.001. Data are shown as mean ± SEM.

(Hume et al., 1994) but similar to the calculated B_{\max} for the antagonist [³H]MPPF and to the *in vitro* B_{\max} reported with the agonist [³H]8-OH-DPAT (Mongeau et al., 1992). The saturation in striatum was best fit with a one-binding site model; however, calculation of the Hill slope was greater than one, suggesting multiple-binding sites; in fact, it has been reported that a second binding site of [³H]CUMI-101 in rats is mainly due to α -1 adrenoceptors receptors (Liow et al., 2010).

Tracer doses were confirmed by measuring the average occupancy in relation to the binding density of 5-HT_{1A} receptors in frontal cortex and hippocampus. The binding maximum in hippocampus and frontal cortex was estimated to be between 72 and 147 fmol/mg, whereas [³H]CUMI-101 only occupied an average of 0.2 ± 0.03 fmol/mg receptors in the frontal cortex and 0.3 ± 0.03 fmol/mg in the hippocampus, giving an occupancy of less than 1%, indicating that we are actually at tracer doses in all the challenge experiments.

Displacement studies show a high degree of selectivity in the high-binding regions, where (4 μ mol/kg, 2 mg/kg) WAY100635 blocked the binding in frontal cortex and the hippocampus, 8-OH-DPAT (4 μ mol/kg, 1.3 mg/kg) at the same dose, blocked only 40% of binding. This is consistent with the inability of 8-OH-DPAT to block the *ex vivo* binding of WAY100635 (Hume et al., 1994). However, the binding in striatum was unaffected by both WAY100635 and 8-OH-DPAT treatment, but was effectively blocked by pretreatment with CUMI-101, showing that a second and different binding site are present in the striatum. *In vitro* studies of selectivity (Kumar et al., 2007) indicate that this binding site could be the α -1 adrenoceptor, for which CUMI-101 has a K_i of 6.5 nM. In fact, microPET studies of the selectivity of CUMI-101

in rodents show a degree of α -1 adrenoceptor binding (Liow et al., 2010). This binding in striatum has not been found in baboons or humans (Kumar et al., 2007; Milak et al., 2008), leaving the possibility of a species difference.

Acute treatment with citalopram, a SSRI, has been estimated to increase the level of intrasynaptic serotonin by 200–400% above basal level, peaking after 40 min, and remaining elevated for hours (Ceglia et al., 2004; Huang et al., 2006; Mørk et al., 2003). We did not detect changes in the SUV, SBR, or SB of [³H]CUMI-101 after citalopram treatment. However, there was a nonsignificant trend of 10–20% lower SBR after citalopram and a dose-response effect between 0.4 and 4 mg/kg. The 10–20% decline in SBR is in agreement with the recent findings in baboon (Kumar et al., 2010), where a 15–30% decline in SBR was found. The increase in synaptic serotonin after acute treatment with fenfluramine is reported to be 500–900%, reaching a peak after 30–40 min, and remaining elevated for several hours (Laferrere and Wurtman, 1989; Rocher and Gardier, 2001). Paradoxically, fenfluramine increased the SBR of [³H]CUMI-101 in frontal cortex and hippocampus by 30–50%. This increase in SBR was driven by a lower SUV of [³H]CUMI-101 in the non-SB region of cerebellum, as we did not find any SB in the cerebellum in the saturation experiments, this change must be due to changes in metabolism or blood flow after fenfluramine treatment. A combination of a high K_{off} of [³H]CUMI-101 to the 5-HT_{1A} receptor and increased blood flow would increase the washout of the non-SB region without changes in the binding. With a low non-SB, even a small change in this region results in big change in the SBR, while the SUV and SB remain more resistant to these changes. This is confirmed by

the SB where no change is seen. These findings are in agreement with other studies that have reported no change or a small decline in the binding of WAY100635 (Hume et al., 2001; Maeda et al., 2001; Rice et al., 2001) or MPPF (Udo De Haes et al., 2005; Zimmer et al., 2002).

Treatment with pCPA has been shown to decrease the level of endogenous and presumably intrasynaptic serotonin after 24 h by 30–50% (Datla et al., 1996; Kornum et al., 2006). We housed rats individually in this experiment to avoid aggressive behaviors associated with lowered serotonin levels. There was no difference in the SUV, SBR, or SB of [³H]CUMI-101 after treatment with pCPA compared to individually housed controls. However, there was an effect on SUV from the combined treatment with pCPA compared to the group-housed controls. The SUV was lowered by 14% in the hippocampus, and, concomitantly, the SBR was lowered 15%. In contrast to our result, recent studies have shown that isolation housing is associated with an upregulation of serotonin 5-HT_{1A} receptors measured with [³H]8-OH-DPAT (Günther et al., 2008), and serotonin depletion has been shown to increase the binding of MPPF in the hippocampus (Zimmer et al., 2003).

There are several possible explanations for the lack of responsiveness of CUMI-101 to changes in endogenous neurotransmitter levels. CUMI-101 is a partial agonist and as such is likely to be less responsive than a full agonist would be to displacement by endogenous neurotransmitter. However, a partial agonist should still be more responsive than an antagonist ligand under the same conditions. There is also a lack of specificity in rats that will lower the sensitivity of CUMI-101, but the amount of specifically bound CUMI-101 in hippocampus and frontal cortex, the regions with the highest amount of 5-HT_{1A} receptors, is still high compared to the amount of alpha 1A receptors, and the observed proportion of selective and specific receptors should be available for competition. A full kinetic study, preferably as a bolus-infusion, is needed to conclude on the sensitivity of CUMI-101 to endogenous changes in 5-HT levels; however, it seems that measuring changes in serotonin release is challenging (Paterson et al., 2010).

CONCLUSION

We have shown that [³H]CUMI-101 is a usable radioligand in rats. [³H]CUMI-101 shows uptake in the 5-HT_{1A} receptor rich areas of frontal cortex and hippocampus where it has a high signal-to-noise ratio of 4.6 and 5.8, respectively. We found nondisplaceable binding in striatum, which may be α -1 adrenoceptor binding. The *in vivo* B_{max} of [³H]CUMI-101 in frontal cortex and hippocampus correlates well with *in vitro* values reported with 8-OH-DPAT, and

the average occupancy of [³H]CUMI-101 was around 0.1%. Our results do not support the claim that [³H]CUMI-101 is susceptible to pharmacological challenges; however, we did notice a dose-response effect after citalopram treatment, further experiments with full kinetic measurements would be needed to make a conclusion.

ACKNOWLEDGMENTS

The authors acknowledge the financial support for this project by The Capital Region of Denmark, Foundation for Health Research and The United States of America, National Institute of Mental Health.

REFERENCES

- Borg J. 2008. Molecular imaging of the 5-HT_{1A} receptor in relation to human cognition. *Behav Brain Res* 195:103–111.
- Brunelli SA, Aviles JA, Gannon KS, Branscomb A, Shacham S. 2009. PRX-00023, a selective serotonin 1A receptor agonist, reduces ultrasonic vocalizations in infant rats bred for high infantile anxiety. *Pharmacol Biochem Behav* 94:8–15.
- Ceglia I, Acconcia S, Fracasso C, Colovic M, Caccia S, Invernizzi RW. 2004. Effects of chronic treatment with escitalopram or citalopram on extracellular 5-HT in the prefrontal cortex of rats: Role of 5-HT_{1A} receptors. *Br J Pharmacol* 142:469–478.
- Clawges HM, Depree KM, Parker EM, Graber SG. 1997. Human 5-HT₁ receptor subtypes exhibit distinct G protein coupling behaviors in membranes from SF9 cells. *Biochemistry* 36:12930–12938.
- Cumming P, Wong DF, Gillings N, Hilton J, Scheffel U, Gjedde A. 2002. Specific binding of [(11)C]raclopride and N-[(3)H]propyl-norapomorphine to dopamine receptors in living mouse striatum: Occupancy by endogenous dopamine and guanosine triphosphate-free G protein. *J Cereb Blood Flow Metab* 22:596–604.
- Datla KP, Curzon G. 1996. Effect of *p*-chlorophenylalanine at moderate dosage on 5-HT and 5-HIAA concentrations in brain regions of control and *p*-chloroamphetamine treated rats. *Neuropharmacology* 35:315–320.
- Ebenezer IS, Arkle MJ, Tite RM. 2007a. 8-Hydroxy-2-(di-*n*-propylamino)-tetralin inhibits food intake in fasted rats by an action at 5-HT_{1A} receptors. *Methods Find Exp Clin Pharmacol* 29:269–272.
- Ebenezer IS, Surujbally A. 2007b. The effects of 8-hydroxy-2-(di-*n*-propylamino)-tetralin (8-OH-DPAT) on food intake in non-deprived C57BL6 mice. *Eur J Pharmacol* 559:184–188.
- Elfving B, Bjørnholm B, Knudsen GM. 2003. Interference of anaesthetics with radioligand binding in neuroreceptor studies. *Eur J Nucl Med Mol Imag* 30:912–915.
- Elsinga PH, Hendrikse NH, Bart J, van Waarde A, Vaalburg W. 2005. Positron emission tomography studies on binding of central nervous system drugs and *p*-glycoprotein function in the rodent brain. *Mol Imaging Biol* 7:37–44.
- Fitzgerald LW, Conklin DS, Krause CM, Marshall AP, Patterson JP, Tran DP, Iyer G, Kostich WA, Largent BL, Hartig PR. 1999. High-affinity agonist binding correlates with efficacy (intrinsic activity) at the human serotonin 5-HT_{2A} and 5-HT_{2C} receptors. Evidence favoring the ternary complex and two-state models of agonist action. *J Neurochem* 72:2127–2134.
- Gozlan H, Thibault S, Laporte AM, Lima L, Hamon M. 1995. The selective 5-HT_{1A} antagonist radioligand [3H]WAY 100635 labels both G-protein-coupled and free 5-HT_{1A} receptors in rat brain membranes. *Eur J Pharmacol* 288:173–186.
- Günther L, Liebscher S, Jähkel M, Oehler J. 2008. Effects of chronic citalopram treatment on 5-HT_{1A} and 5-HT_{2A} receptors in group- and isolation-housed mice. *Eur J Pharm* 593:49–61.
- Huang M, Ichiwaka J, Li Z, Dai J, Meltzer HY. 2006. Augmentation by citalopram of risperidone-induced monoamine release in rat prefrontal cortex. *Psychopharmacology* 185:274–281.
- Hume SP, Ashworth S, Opacka-Juffry J, Ahier RG, Lammertsma AA, Pike VW, Cliffe IA, Fletcher A, White AC. 1994. Evaluation of [O-methyl-3H]WAY-100635 as an *in vivo* radioligand for 5-HT_{1A} receptors in rat brain. *Eur J Pharmacol* 271:515–523.

AQ2

- Hume SP, Hirani E, Opacka-Juffry J, Myers R, Townsend C, Pike VW, Grasby P. 2001. Effect of 5-HT on Binding of WAY 100635 to receptors in rat brain, assessed using in vivo microdialysis. *Synapse* 41:150–159.
- Kornum BR, Licht CL, Weikop P, Knudsen GM, Aznar S. 2006. Central serotonin depletion affects rat brain areas differently: A qualitative and quantitative comparison between different treatment schemes. *Neurosci Lett* 392:129–134.
- Kumar JS, Prabhakaran J, Majo VJ, Milak MS, Hsiung SC, Tamir H, Simpson NR, Van Heertum RL, Mann JJ, Parsey RV. 2007. Synthesis and in vivo evaluation of a novel 5-HT_{1A} receptor agonist radioligand [*O*-methyl-¹¹C]2-(4-(4-(2-methoxyphenyl)piperazin-1-yl)butyl)-4-methyl-1,2,4-triazine-3,5(2H,4H)dione in nonhuman primates. *Eur J Nucl Med Mol Imag* 34:1050–1060.
- Laferrere B, Wurtman RJ. 1989. Effect of D-fenfluramine on serotonin release in brains of anaesthetized rats. *Brain Res* 504:258–263.
- Liow J, Lu S, Zoghbi S, Shrestha S, Gladding R, Morse C, Hirvonen J, Parsey RV, Pike V, Innis R. 2010. Selectivity in rodents and monkeys of ¹¹C-CUMI-101, an agonist radioligand for serotonin 5-HT_{1A} receptors. *Soc Nucl Med Annu Meet Abstr* 51:164.
- Maeda J, Suhara T, Ogawa M, Okauchi T, Kawabe K, Zhang MR, Semba J, Suzuki K. 2001. In vivo binding properties of [carbonyl-¹¹C]WAY-100635: Effect of endogenous serotonin. *Synapse* 40:122–129.
- Milak MS, Kumar JS, Prabhakaran J, Majo VJ, Mann JJ, Parsey RV. 2008a. [¹¹C]CUMI-101 an agonist 5-HT_{1A} positron emission tomography (PET) tracer in human: Preliminary test-retest data. *Neuroreceptor Mapp* 49:587–596.
- Milak MS, Severance AJ, Ogden RT, Prabhakaran J, Kumar JS, Majo VJ, Mann JJ, Parsey RV. 2008b. Modeling considerations for ¹¹C-CUMI-101, an agonist radiotracer for imaging serotonin 1A receptor in vivo with PET. *J Nucl Med* 49:587–596.
- Mongeau R, Welner SA, Quirion R, Suranyi-Cadotte BE. 1992. Further evidence for differential affinity states of the serotonin_{1A} receptor in rat hippocampus. *Brain Res* 590:229–238.
- Mørk A, Kreilgaard M, Sánchez C. 2003. The R-enantiomer of citalopram counteracts escitalopram-induced increase in extracellular 5-HT in the frontal cortex of freely moving rats. *Neuropharmacology* 45:167–173.
- Narendran R, Hwang D, Slifstein M, Hwang Y, Huang Y, Ekelund J, Guillin O, Scher E, Martinez D, Laruelle M. 2005. Measurement of the proportion of D₂ receptors configured in state of high affinity for agonists in vivo: A positron emission tomography study using [¹¹C]*N*-propyl-norapomorphine and [¹¹C]raclopride in baboons. *J Pharm Exp Therapeut* 315:80–90.
- Paterson LM, Tyacke RJ, Nutt DJ, Knudsen GM. 2010. Measuring endogenous 5-HT release by emission tomography: Promises and pitfalls. *J Cereb Blood Flow Metab* 30:1682–1706.
- Plenevaux A, Lemaire C, Aerts J, Lacan G, Rubins D, Melega WP, Brihaye C, Degueldre C, Fuchs S, Salmon E, Maquet P, Laureys S, Damhaut P, Weissmann D, Le Bars D, Pujol JF, Luxen A. 2000. [(18F)*p*-MPPF: A radiolabeled antagonist for the study of 5-HT_{1A} receptors with PET. *Nucl Med Biol* 27:467–471.
- Rice OV, Gatley SJ, Shen J, Huemmer CL, Rogoz R, DeJesus OT, Volkow ND, Gifford AN. 2001. Effects of endogenous neurotransmitters on the in vivo binding of dopamine and 5-HT radiotracers in mice. *Neuropsychopharmacology* 25:679–689.
- Richfield EK, Penney JB, Young AB. 1989. Anatomical and affinity state comparisons between dopamine D₁ and D₂ receptors in the rat central nervous system. *Neuroscience* 30:767–777.
- Rocher C, Gardier AM. 2001. Effects of repeated systemic administration of *d*-fenfluramine on serotonin and glutamate release in rat ventral hippocampus: Comparison with methamphetamine using in vivo microdialysis. *Naunyn-Schmiedeberg's Arch Pharmacol* 363:422–428.
- Sumiyoshi T, Bubenikova-Valesova V, Horacek J, Bert B. 2008. Serotonin_{1A} receptors in the pathophysiology of schizophrenia: Development of novel cognition-enhancing therapeutics. *Adv Ther* 25:1037–1056.
- Udo De Haes JI, Cremers TI, Bosker F, Postema F, Tiemersma-Wegman TD, den Boer JA. 2005. Effect of increased serotonin levels on [¹⁸F]MPPF binding in rat brain: Fenfluramine vs the combination of Citalopram and ketanserin. *Neuropsychopharmacology* 30:1624–1631.
- Wilson SJ, Bailey JE, Rich AS, Nash J, Adrover M, Tournoux A, Nutt DJ. 2005. The use of sleep measures to compare a new 5HT_{1A} agonist with buspirone in humans. *J Psychopharmacol* 19:609–613.
- Zimmer L, Le Bars D, Mauger G, Luxen A, Bonmarchand G, Pujol J. 2002. Effect of endogenous serotonin on the binding of the 5-HT_{1A} PET ligand 18F-MPPF in the rat hippocampus: Kinetic beta measurements combined with microdialysis. *J Neurochem* 80:278–286.
- Zimmer L, Rbahl L, Giacomelli F, Le Bars D, Renaud B. 2003. A reduced extracellular serotonin level increases the 5-HT_{1A} PET ligand 18F-MPPF binding in the rat hippocampus. *J Nucl Med* 44:1495.

Author Proof

Radiosynthesis and Evaluation of ^{11}C -CIMBI-5 as a 5-HT_{2A} Receptor Agonist Radioligand for PET

Anders Ettrup¹, Mikael Palner¹, Nic Gillings², Martin A. Santini¹, Martin Hansen³, Birgitte R. Kornum¹, Lars K. Rasmussen³, Kjell Någren², Jacob Madsen², Mikael Begtrup³, and Gitte M. Knudsen¹

¹Neurobiology Research Unit and Center for Integrated Molecular Brain Imaging (CIMBI), Copenhagen University Hospital, Rigshospitalet, Copenhagen, Denmark; ²PET and Cyclotron Unit, Copenhagen University Hospital, Rigshospitalet, Copenhagen, Denmark; and ³Department of Medicinal Chemistry, Faculty of Pharmaceutical Sciences, University of Copenhagen, Copenhagen, Denmark

PET brain imaging of the serotonin 2A receptor (5-hydroxytryptamine receptor 2A [5-HT_{2A} receptor]) has been widely used in clinical studies, and currently, several well-validated radiolabeled antagonist tracers are used for in vivo imaging of the cerebral 5-HT_{2A} receptor. Access to 5-HT_{2A} receptor agonist PET tracers would, however, enable imaging of the active, high-affinity state of receptors, which may provide a more meaningful assessment of membrane-bound receptors. In this study, we radiolabel the high-affinity 5-HT_{2A} receptor agonist 2-(4-iodo-2,5-dimethoxyphenyl)-N-(2-[^{11}C -OCH₃]methoxybenzyl)ethanamine (^{11}C -CIMBI-5) and investigate its potential as a PET tracer. **Methods:** The in vitro binding and activation at 5-HT_{2A} receptors by ^{11}C -CIMBI-5 was measured with binding and phosphoinositide hydrolysis assays. Ex vivo brain distribution of ^{11}C -CIMBI-5 was investigated in rats, and PET with ^{11}C -CIMBI-5 was conducted in pigs. **Results:** In vitro assays showed that ^{11}C -CIMBI-5 was a high-affinity agonist at the 5-HT_{2A} receptor. After intravenous injections of ^{11}C -CIMBI-5, ex vivo rat studies showed a specific binding ratio of 0.77 ± 0.07 in the frontal cortex, which was reduced to cerebellar levels after ketanserin treatment, thus indicating that ^{11}C -CIMBI-5 binds selectively to the 5-HT_{2A} receptor in the rat brain. The PET studies showed that the binding pattern of ^{11}C -CIMBI-5 in the pig brain was in accordance with the expected 5-HT_{2A} receptor distribution. ^{11}C -CIMBI-5 gave rise to a cortical binding potential of 0.46 ± 0.12 , and the target-to-background ratio was similar to that of the widely used 5-HT_{2A} receptor antagonist PET tracer ^{18}F -altanserin. Ketanserin treatment reduced the cortical binding potentials to cerebellar levels, indicating that in vivo ^{11}C -CIMBI-5 binds selectively to the 5-HT_{2A} receptor in the pig brain. **Conclusion:** ^{11}C -CIMBI-5 showed a cortex-to-cerebellum binding ratio equal to the widely used 5-HT_{2A} antagonist PET tracer ^{18}F -altanserin, indicating that ^{11}C -CIMBI-5 has a sufficient target-to-background ratio for future clinical use and is displaceable by ketanserin in both rats and pigs. Thus, ^{11}C -CIMBI-5 is a promising tool for investigation of 5-HT_{2A} agonist binding in the living human brain.

Key Words: PET tracer development; agonist; porcine; serotonin receptors

J Nucl Med 2010; 51:1-8

DOI: 10.2967/jnumed.109.074021

Received Jan. 26, 2010; revision accepted Aug. 11, 2010.
For correspondence or reprints contact: Anders Ettrup, Neurobiology Research Unit, Blegdamsvej 9, Rigshospitalet, Bldg. 9201, DK-2100 Copenhagen, Denmark.
E-mail: ettrup@nru.dk
COPYRIGHT © 2010 by the Society of Nuclear Medicine, Inc.

Serotonin 2A receptors (5-hydroxytryptamine receptor [AQ1] 2A [5-HT_{2A} receptor]) are implicated in the pathophysiology of human diseases such as depression, Alzheimer disease, and schizophrenia. Also, 5-HT_{2A} receptor stimulation exerts the hallucinogenic effects of recreational drugs such as lysergic acid diethylamide and 1-(2,5-dimethoxy-4-iodophenyl)-2-aminopropane (1), and atypical antipsychotics have antagonistic or inverse agonistic effects on the 5-HT_{2A} receptor (2).

Currently, there are 3 selective 5-HT_{2A} antagonistic PET ligands— ^{18}F -altanserin (3), ^{18}F -deuteroaltanserin (4), and ^{11}C -MDL100907 (5)—in use for mapping and quantifying 5-HT_{2A} receptor binding in the human brain. However, whereas 5-HT_{2A} antagonists bind to the total pool of receptors, 5-HT_{2A} agonists bind only to the high-affinity state of the receptor (6,7). Thus, a 5-HT_{2A} receptor agonist ligand holds promise for the selective mapping of 5-HT_{2A} receptors in their functional state; therefore, alterations in agonist binding measured in vivo with PET may be more relevant for assessing dysfunction in the 5-HT_{2A} receptor system in specific patient or population groups. Furthermore, because many of the 5-HT_{2A} receptors are intracellularly localized (8,9), combining measurements with antagonist and agonist PET tracers would enable determination of the ratio of the high-affinity, membrane-bound, and active receptors to the low-affinity, intracellular, and inactive receptors (10). Thus, quantification of functionally active 5-HT_{2A} receptors in vivo using an agonist PET tracer is hypothesized to be superior to antagonist measurements of total number of 5-HT_{2A} receptors for studying alterations in receptor function in human diseases such as depression.

D₂ receptor agonist radiotracers are now known to be superior to antagonist radiotracers in measuring dopamine release in vivo in monkeys (11) and mice (10). In humans, most studies have found that 5-HT_{2A} receptor antagonist PET tracers are not displaceable by elevated levels of endogenous serotonin (5-HT) (12). This suggests that agonist PET tracers may be better suited for measuring endogenous competition than antagonist tracers, so that 5-HT_{2A} receptor agonists would be more prone to displacement by

competition with endogenously released 5-HT. Monitoring the release of endogenous 5-HT is highly relevant in relation to human diseases such as depression and Alzheimer disease, which involve dysfunction of the 5-HT system.

2-(4-iodo-2,5-dimethoxyphenyl)-*N*-(2-methoxybenzyl) ethanamine (25I-NBOMe, or CIMBI [Center for Integrated Molecular Brain Imaging]-5) has recently been described as a potent and selective 5-HT_{2A} receptor agonist, and phosphoinositide hydrolysis assays revealed that it has a 12-fold lower median effective concentration (EC₅₀) than 5-HT itself (13). Although this compound is tritiated (14), its in vivo biologic distribution and possible PET tracer potential have not been investigated.

Here, we present the synthesis of ¹¹C-labeled CIMBI-5 and biologic evaluation of this novel PET tracer. The compound was characterized in vitro, and ¹¹C-CIMBI-5 was investigated after intravenous injection both ex vivo in rats and in vivo in pigs with PET.

MATERIALS AND METHODS

In Vitro Binding and Activation

[AQ2] [Table 1] Inhibitory constant (K_i) determinations against various neuroreceptors (Table 1) were provided by the Psychoactive Drug Screening Program (PDSP; experimental details are provided at <http://pdsp.med.unc.edu/>). In our laboratory, competition binding experiments were performed on a NIH-3T3 cell line (GF62) stably transfected with the rat 5-HT_{2A} receptor as previously described (15) using 0.2 nM ³H-MDL100907 (kindly provided by Prof. Christer Halldin) and 8 different concentrations of CIMBI-5 (1 μM to 1 pM) in a total of 1 mL of buffer (500 mM Tris base, 1,500 mM NaCl, and 200 mM ethylenediaminetetraacetic acid). Nonspecific binding was determined with 1 μM ketanserin. Incubation was performed for 1 h at 37°C.

The 5-HT_{2A} receptor activation by CIMBI-5 was measured on GF62 cells using a phosphoinositide hydrolysis assay as previ-

ously described (16). Briefly, cells were incubated with myo-(1,2)-³H-inositol (Amersham) in labeling medium. Subsequently, the cells were washed and incubated at 37°C with CIMBI-5 (1 μM to 0.1 pM). The formed inositol phosphates were extracted and counted with a liquid scintillation counter.

Radiochemical Synthesis of ¹¹C-CIMBI-5

¹¹C-methyl trifluoromethanesulfonate (triflate) produced using a fully automated system was transferred in a stream of helium to a 1.1-mL vial containing 0.3–0.4 mg of the labeling precursor (3; Fig. 1) and 2 μL of 2 M NaOH in 300 μL of acetonitrile, and the resulting mixture was heated at 40°C for 30 s. Subsequently, 250 μL of trifluoroacetic acid:CH₃CN (1:1) were added and the mixture heated at 80°C for 5 min (Fig. 2). After neutralization with 750 μL of 2 M NaOH, the reaction mixture was purified by high-performance liquid chromatography (HPLC) on a Luna C18 column (Phenomenex Inc.) (250 × 10 mm; 40:60 acetonitrile:25 mM citrate buffer, pH 4.7; and flow rate, 5 mL/min). The chemical synthesis of the labeling precursor is described in detail in the supplemental data (supplemental materials are available online only at <http://jnm.snmjournals.org>).

The fraction corresponding to the labeled product (~12.5 min) was collected in 50 mL of 0.1% ascorbic acid, and the resulting solution was passed through a solid-phase C18 Sep-Pak extraction column (Waters Corp.), which had been preconditioned with 10 mL of ethanol, followed by 20 mL of 0.1% ascorbic acid. The column was flushed with 3 mL of sterile water. Then, the trapped radioactivity was eluted with 3 mL of ethanol, followed by 3 mL of 0.1% ascorbic acid into a 20-mL vial containing 9 mL of phosphate buffer (100 mM, pH 7), giving a 15-mL solution of ¹¹C-CIMBI-5 with a pH of approximately 7. In a total synthesis time of 40–50 min, 1.5–2.5 GBq of ¹¹C-CIMBI-5 were produced, with radiochemical purity greater than 97% and specific radioactivity in the range 64–355 GBq/μmol. The lipophilicity of CIMBI-5 was calculated using 2 different programs, which were in good agreement (CSLogD [ChemSilico], cLogD_{7.4} = 3.33; Pallas 3.5 [CompuDrug Inc.], cLogD_{7.4} = 3.21).

Ex Vivo Uptake in Rats

Twenty-two Sprague–Dawley rats (mean weight, 295 ± 53 g; Charles River) were included in the study. All animal experiments were performed in accordance with the European Communities Council Resolves of November 24, 1986 (86-609/ECC), and approved by the Danish State Research Inspectorate (journal no. 2007/561-1320). Rats were maintained on a 12-h light–dark cycle, with free access to food and water.

The ex vivo uptake and brain distribution were evaluated as previously described (17). Briefly, rats were injected in the tail vein with ¹¹C-CIMBI-5 (3.9 ± 3.5 MBq/kg; specific radioactivity, 30.9 GBq/μmol). The rats were decapitated at 5 (*n* = 2), 15 (*n* = 2), 30 (*n* = 4), 45 (*n* = 2), and 60 min (*n* = 10); the brains were quickly removed, placed on ice, and dissected into frontal cortex (first 3 mm of the brain) and cerebellum. Blood from the trunk was collected immediately, and plasma was isolated by centrifugation (1,500 rpm, 10 min). All brain tissue samples were collected in tared counting vials and counted for 20 s in a γ-counter (Cobra 5003; Packard Instruments).

For ex vivo blocking studies, rats were divided in vehicle (saline) and ketanserin-treated groups (*n* = 5–6). Rats were intravenously injected with vehicle or 1 mg of ketanserin (Sigma) per kilogram 45 min before tracer administration. ¹¹C-CIMBI-5 was

TABLE 1. PDSP Screening Result: Inhibitory Constants (K_i) for CIMBI-5 Versus Serotonin and Other Receptors

Receptor	K _i (nM)
5-HT _{2A}	2.2 ± 0.1
5-HT _{2B}	2.3 ± 0.2
5-HT _{2C}	7.0 ± 1.0
5-HT ₆	58 ± 17
5-HT _{1A}	85 ± 16
D ₃	117 ± 14
α _{2C}	348 ± 17
D ₄	647 ± 37
Serotonin transporter	1,009 ± 84
α _{2A}	1,106 ± 206
M ₅	1,381 ± 231
D ₂	1,600 ± 333
5-HT ₇	1,670 ± 125
5-HT _{5A}	2,200 ± 385
D ₁	3,718 ± 365
5-HT _{1B}	3,742 ± 553
Norepinephrine transporter	4,574 ± 270
Dopamine transporter	5,031 ± 343
D ₅	7,872 ± 933

[AQ10]

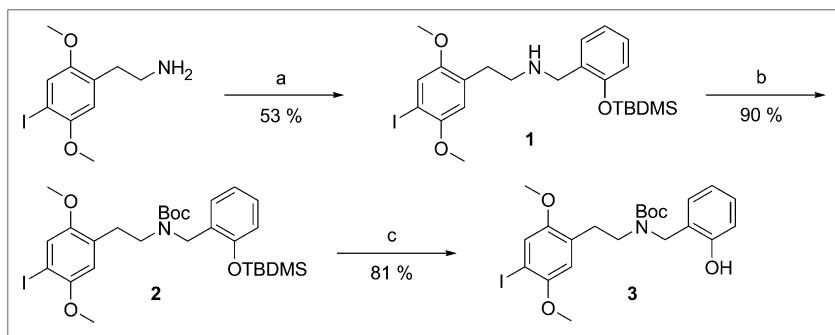


FIGURE 1. Synthesis of labeling precursor for ^{11}C -CIMBI-5 (3): (a) 2-(tert-butylidimethylsilyloxy)benzaldehyde, NaBH_4 , MeOH ; (b) Boc_2O , THF ; and (c) TBAF , NH_4Cl , THF . OTBDMS = ; THF = .

injected in the tail vein, and after 30 min, the rats were decapitated. Brain regions and plasma were extracted and counted.

PET in Pigs

Six female Danish Landrace Pigs were used in this study (mean weight, 17.8 ± 1.4 kg). After arrival, animals were housed under standard conditions and were allowed to acclimatize for 1 wk before scanning. On the scanning day, pigs were tranquilized by intramuscular injection of 0.5 mg of midazolam per kilogram. Anesthesia was induced by 0.1 mL/kg intramuscular injections of Zoletil veterinary mixture (Virbac Animal Health; 125 mg of tiletamine and 125 mg of zolazepam in 8 mL of 5 mg/mL midazolam). After induction, anesthesia was maintained by a 10 mg/kg/h intravenous infusion of propofol (B. Braun Melsugen AG). During anesthesia, animals were endotracheally intubated and ventilated (volume, 250 mL; frequency, 15 per min). Venous access was granted through 2 Venflons (Becton Dickinson) in the peripheral milk veins, and an arterial line for blood sampling measurement was obtained by a catheter in the femoral artery after a minor incision. Vital signs including blood pressure, temperature, and heart rate were monitored throughout the duration of PET. Immediately after scanning, animals were sacrificed by intravenous injection of pentobarbital–lidocaine. All animal procedures were approved by the Danish Council for Animal Ethics (journal no. 2006/561-1155).

PET Protocol

In 5 pigs, ^{11}C -CIMBI-5 was given as intravenous bolus injections, and the pigs were subsequently PET-scanned for 90 min in list mode with a high-resolution research tomography scanner (Siemens AG). Scanning began at the time of injection. After the baseline scan, 3 pigs were maintained in anesthesia and scanned a second time using the same PET protocol. The 5-HT_{2A} receptor antagonist ketanserin tartrate (Sigma) was administered at 30 min before the second scan (3 mg/kg bolus, followed by 1 mg/kg/h infusion for the duration of the scan). For all ^{11}C -CIMBI-5 PET scans, the injected radioactivity was on average 238 MBq (range, 96–418 MBq; $n = 9$), the specific radioactivity at the time of injection was 75 GBq/ μmol (range, 28–133 GBq/ μmol ; $n = 9$), the average injected mass was 1.85 μg (range, 0.37–5.49 μg ; $n = 9$), and there were no significant differences in these parameters between the baseline and blocked scans. In 2 pigs, arterial whole-blood samples were taken throughout the entire scan. During the first 15 min after injection, radioactivity in whole blood was continuously measured using an ABSS Autosampler (Allogg Technology) counting coincidences in a lead-shielded detector. Concurrently, blood samples were manually drawn at 2.5, 5, 10, 20, 30, 50, 70, and 90 min, and the radioactivity in whole blood

[AQ4]

and plasma was measured using a well counter (Cobra 5003; Packard Instruments) that was cross-calibrated to the high-resolution research tomography scanner and autosampler. Also, radiolabeled parent compound and metabolites were measured in plasma as in the “Quantification of PET Data” section.

The free fraction of ^{11}C -CIMBI-5 in plasma, f_p , was estimated using an equilibrium dialysis chamber method as previously described (18). Briefly, the dialysis was conducted in chambers (Harvard Biosciences) separated by a cellulose membrane with a protein cutoff of 10,000 Da. Small amounts of ^{11}C -CIMBI-5 (~ 10 MBq) were added to a 5-mL plasma sample from the pig. Plasma (500 μL) was then dialyzed at 37°C against an equal volume of buffer (135 mM NaCl, 3.0 mM KCl, 1.2 mM CaCl_2 , 1.0 mM MgCl_2 , and 2.0 mM KH_2PO_4 , pH 7.4). Counts per minute in 400 μL of plasma and buffer were determined in a well counter after various dialysis times, and f_p of ^{11}C -CIMBI-5 was calculated as counts per minute in buffer divided by counts per minute in plasma. The samples were taken from the dialysis chambers after equilibrium had been obtained between the 2 chambers.

HPLC Analysis of Pig Plasma and Pig Brain Tissue

Whole-blood samples (10 mL) drawn during PET were centrifuged (3,500 rpm, 4 min), and the plasma was passed through a 0.45- μm filter before HPLC analysis with online radioactivity detection, as previously described (19).

Also, the presence of radioactive metabolites of ^{11}C -CIMBI-5 in the pig brain was investigated. Twenty-five minutes after intravenous injection of approximately 500 MBq of ^{11}C -CIMBI-5, the pigs were killed by intravenous injection of pentobarbital and decapitated, and the brain was removed. At the same time, a blood sample was drawn manually. Within 30 min of decapitation, brain tissue was homogenized in 0.1N perchloric acid (Bie and Bentsen) saturated with sodium–ethylenediaminetetraacetic acid (Sigma) for 2×30 s using a Polytron homogenizer (Kinematic, Inc.). After centrifugation, the supernatant was neutralized using phosphate buffer, filtered (0.45 μm), and analyzed by HPLC as described.

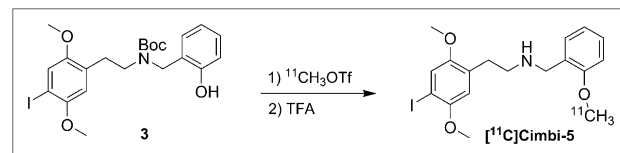


FIGURE 2. Radiochemical synthesis of ^{11}C -CIMBI-5. OTf = triflate; TFA = trifluoroacetic acid.

A plasma sample taken at the time of decapitation was analyzed concurrently.

Quantification of PET Data

Ninety-minute high-resolution research tomography, list-mode PET data were reconstructed into 38 dynamic frames of increasing length (6×10 , 6×20 , 4×30 , 9×60 , 3×120 , 6×300 , and 4×600 s). Images consisted of 207 planes of 256×256 voxels of $1.22 \times 1.22 \times 1.22$ mm. A summed image of all counts in the 90-min scan was reconstructed for each pig and used for coregistration to a standardized MRI-based statistical atlas of the Danish Landrace pig brain, similar to that previously reported for the Göttingen minipig (20), using the program Register as previously described (18). The temporal radioactivity in volumes of interest (VOI), including the cerebellum, cortex (defined in the MRI-based atlas as entire cortical gray matter), hippocampus, lateral and medial thalamus, caudate nucleus, and putamen, was calculated. Radioactivity in all VOIs was calculated as the average of radioactive concentration (Bq/mL) in the left and right sides. Outcome measure in the time-activity curves was calculated as radioactive concentration in VOI (in kBq/mL) normalized to the injected dose corrected for animal weight (in kBq/g), yielding standardized uptake values (g/mL).

In 1 pig in which full arterial input function, including metabolite correction, was measured, we calculated ^{11}C -CIMBI-5 distribution volumes (V_T) for VOIs based on either 1-tissue- or 2-tissue-compartment models (1TC or 2TC, respectively) using plasma corrected for parent compound as the arterial input function (Supplemental Table 1). Cortical nondisplaceable binding potential (BP_{ND}) was calculated as $\text{BP}_{\text{ND}} = V_T/V_{\text{ND}} - 1$ (21), assuming that specific 5-HT_{2A} receptor binding in the cerebellum was negligible and that the V_{ND} was equal to the cerebellar V_T (3). For all 5 pigs, BP_{ND} was also calculated with the simplified reference tissue model (SRTM) (22), both at baseline and in the ketanserin-blocked condition, with the cerebellum as the reference region (Supplemental Table 1). Kinetic modeling was done with PMOD software (version 3.0; PMOD Technologies Inc.). Goodness of fit was evaluated using the Akaike information criterion.

Statistical Analysis

All statistical tests were performed using Prism (version 5.0; GraphPad Software). *P* values below 0.05 were considered statistically significant. Results are expressed in mean \pm SD unless otherwise stated.

RESULTS

Chemistry

The labeling precursor was synthesized in 3 steps (Fig. 1): reductive amination with TBDMS-protected salicylaldehyde, followed by boc protection of the secondary amine and removal of the TBDMS group, which gave the labeling precursor (3). Synthesis of the reference compound has been described previously (13).

In Vitro Binding Affinity

CIMBI-5 had the highest affinity for the 5-HT_{2A} receptor, in agreement with previous studies (14). Between the subtypes of the 5-HT₂ receptors, CIMBI-5 did not show a higher affinity toward 5-HT_{2A} receptors than it did toward 5-HT_{2B} receptors; however, approximately a 3-fold higher affinity of CIMBI-5 for 5-HT_{2A} receptors than for 5-HT_{2C}

receptors was found. Against targets other than 5-HT₂ receptors, CIMBI-5 showed at least a 30-fold lower affinity for any other of the investigated receptors than for 5-HT_{2A} receptors (Table 1). In vitro binding assays conducted in our laboratory determined K_i of CIMBI-5 against 2 nM ^3H -MDL100907 at 1.5 ± 0.7 nM, thus confirming nanomolar affinity of CIMBI-5 for 5-HT_{2A} receptors.

In Vitro Functional Characterization

The functional properties of CIMBI-5 toward the 5-HT_{2A} receptor were assessed by measuring its effect on phosphoinositide hydrolysis in GF62 cells overexpressing the 5-HT_{2A} receptor. CIMBI-5 was found to be an agonist with an EC_{50} of 1.02 ± 0.17 nM (Supplemental Fig. 1), in agreement with previous reports (13). Pretreatment with 1 μM ketanserin completely inhibited CIMBI-5-induced phosphoinositide hydrolysis (data not shown). Furthermore, CIMBI-5 showed $84.6\% \pm 1.9\%$ of the 5-HT_{2A} activation achieved by 10 μM 5-HT, demonstrating that CIMBI-5 functioned nearly as a full agonist.

Ex Vivo Distribution in Rats

After injection of ^{11}C -CIMBI-5 in awake rats, the time-activity curves measured as standardized uptake values showed highest uptake in the frontal cortex, whereas uptake in the cerebellum (equivalent to nondisplaceable uptake) was lower and paralleled the plasma time-activity curve. The brain uptake peaked in all regions at 15 min after injection and thereafter slowly declined (data not shown).

The specific binding ratio (SBR) in the frontal cortex region of interest, calculated as $\text{SBR} = (\text{region of interest} - \text{cerebellum})/\text{cerebellum}$, peaked 30 min after injection, reaching a level of 0.77 ± 0.07 , after which the SBR slowly declined (Fig. 3A). Thus, 30 min after injection was chosen as a reference time point and used in the blocking experiment with ketanserin. Ketanserin pretreatment reduced the SBR in the frontal cortex to levels not significantly different from zero (0.076 ± 0.12) (Fig. 3B).

In Vivo Distribution and Ketanserin Blockade in Pig Brain

^{11}C -CIMBI-5 showed high cortical uptake in vivo in the pig brain with PET, medium uptake in striatal and thalamic regions, and low uptake in the cerebellum (Fig. 4). Furthermore, the time-activity curves demonstrated a substantial separation between the cortical and cerebellar time-activity curves (Fig. 5A). The time-activity curves peaked at approximately 10 min after injection and thereafter decreased, implying that ^{11}C -CIMBI-5 binding is reversible over the 90-min scan time used in this study.

After ketanserin treatment, the concentration of ^{11}C -CIMBI-5 in the cortex was reduced almost completely to cerebellar levels (Fig. 5A). The cerebellar time-activity curve was unaltered by ketanserin administration (Fig. 5A).

Kinetic Modeling

With the SRTM, baseline cortical BP_{ND} of ^{11}C -CIMBI-5 was 0.46 ± 0.11 ($n = 5$). After the ketanserin bolus and

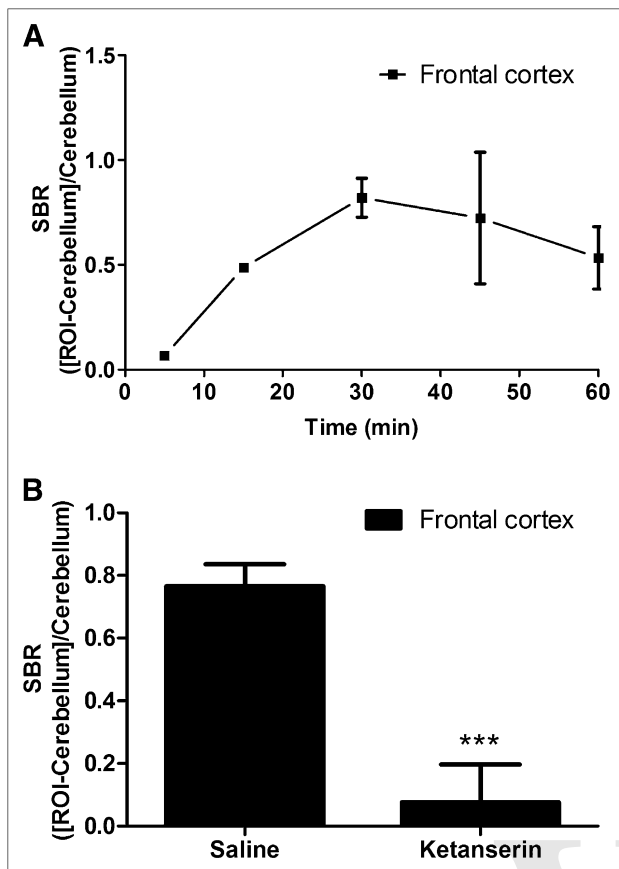


FIGURE 3. Time-dependent ex vivo distribution of ^{11}C -CIMBI-5 and displacement by ketanserin. (A) SBRs in frontal cortex in rats are shown relative to time after injection. (B) After ketanserin pretreatment (1 mg/kg intravenously), SBR in frontal cortex at 30 min after ^{11}C -CIMBI-5 injection is significantly decreased. $***P < 0.0001$ in Student t test of ketanserin vs. saline. ROI = region of interest.

infusion, the cortical BP_{ND} was significantly decreased by 75% (mean blocked BP_{ND} , 0.11 ± 0.06 ; $n = 3$). For the fitted SRTM, no significant difference in goodness of fit was found between baseline and blocked condition (Supplemental Table 1). In 1 pig in which full metabolite-corrected arterial input was measured, V_T was calculated from 1TC and 2TC models. Ratios between V_T in the cortex and cerebellum were 1.57 and 1.61, corresponding to a BP_{ND} of 0.57 and 0.61 with the 1TC and 2TC model, respectively. After ketanserin blockade, cortical ^{11}C -CIMBI-5 BP_{ND} was reduced to 0.13 and 0.11 in the 1TC and 2TC, respectively (Supplemental Table 1).

Radiolabeled Metabolites

In the radio-HPLC analysis, 1 lipophilic radioactive metabolite accounting for up to 20% of the total plasma radioactivity was found, and it maintained stable plasma [Fig. 6] levels after 20 min and throughout the scan (Fig. 6). The HPLC retention time of ^{11}C -CIMBI-5 and its metabolite in

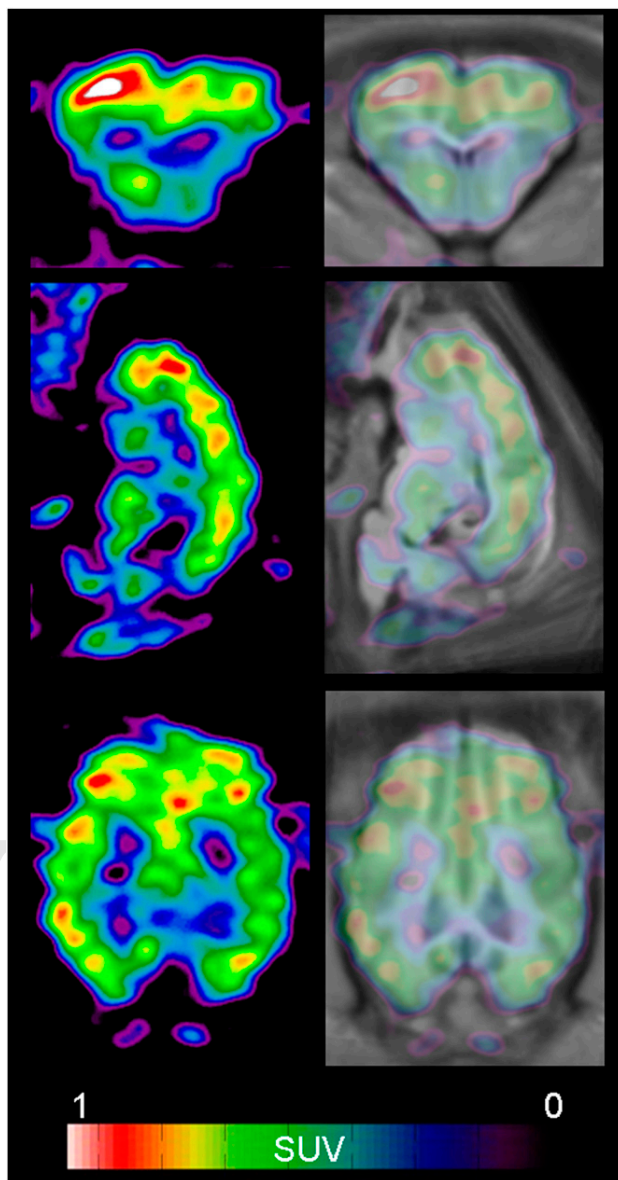


FIGURE 4. Representative coronal (top), sagittal (middle), and horizontal (bottom) PET images summed from 0 to 90 min of scanning showing distribution of ^{11}C -CIMBI-5 in pig brain. Left column shows PET images after $3 \times 3 \times 3$ mm gaussian filtering. Right column shows same PET images aligned and overlaid on standard pig brain after coregistration and transformation. SUV = standardized uptake value.

the HPLC column suggest that the metabolite is slightly less lipophilic than ^{11}C -CIMBI-5 itself (Fig. 7). However, this metabolite was found only in negligible amounts in homogenized pig brain tissue, compared with plasma from the same animal (Fig. 7).

The free fraction of ^{11}C -CIMBI-5 in pig plasma at 37°C was $1.4\% \pm 0.3\%$ using a dialysis chamber method, in which equilibrium between chambers was reached after 60 min.

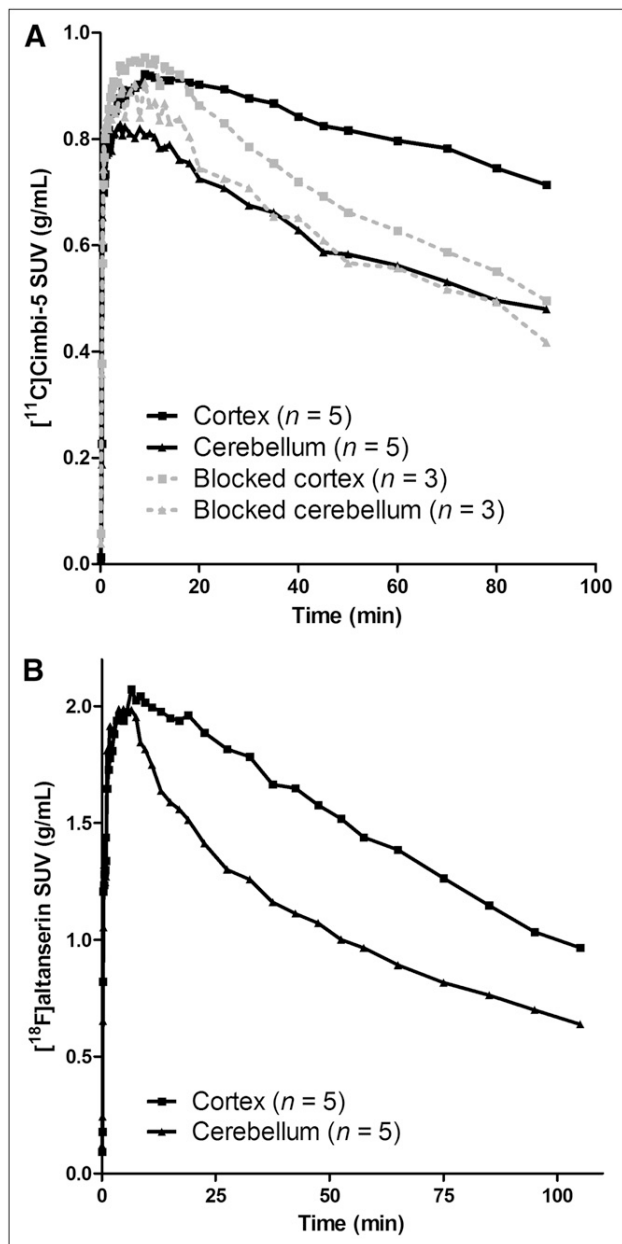


FIGURE 5. Time-activity curves of 5-HT_{2A} agonist and antagonist PET tracers in pig brain. (A) ¹¹C-CIMBI-5 time-activity curves in Danish Landrace pig brain at baseline (black solid line) or after intravenous ketanserin (3 mg/kg bolus, 1 mg/kg/h infusion) blockade (gray dotted line). (B) ¹⁸F-altanserin time-activity curves in minipigs. Mean standardized uptake values normalized to injected dose per body weight are shown. SUV = standardized uptake value.

[AQ8] **DISCUSSION**

In the current study, we report the *in vitro*, *ex vivo*, and *in vivo* validation of ¹¹C-CIMBI-5, a novel 5-HT_{2A} receptor agonist PET tracer. To our knowledge, this is the first agonist 5-HT_{2A} receptor PET tracer that has been developed. In

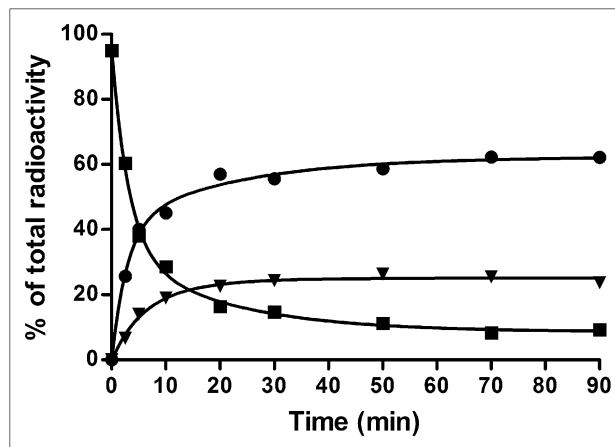
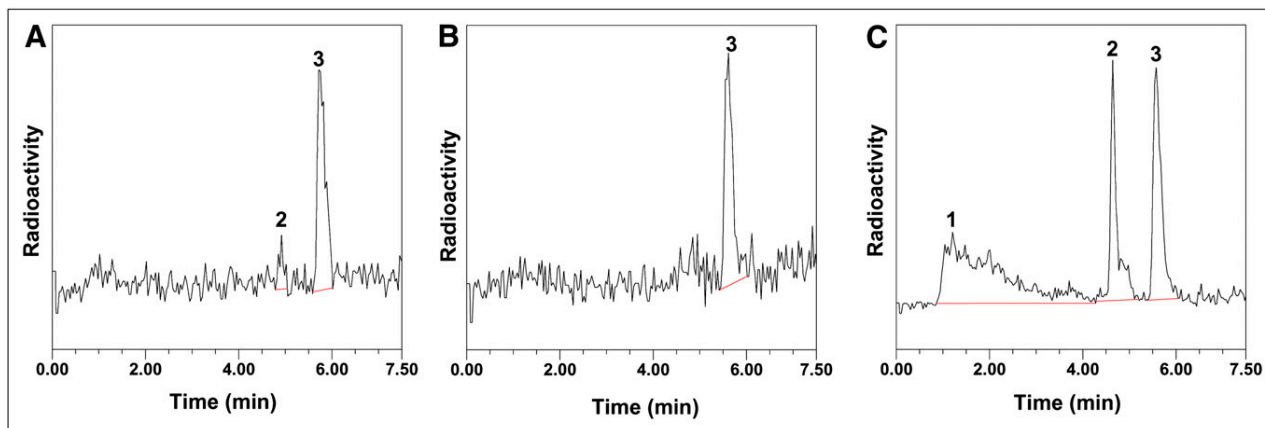


FIGURE 6. HPLC analysis of radioactive metabolites in pig plasma after intravenous injection of ¹¹C-CIMBI-5. ■ = parent compound ¹¹C-CIMBI-5; ▼ = lipophilic metabolite; ● = polar metabolites.

in vitro assays performed at our laboratory, along with assays performed through the PDSP screening program, confirmed the nanomolar affinity of CIMBI-5 for the 5-HT_{2A} receptor as previously reported (13,14). In the current study, the K_i for CIMBI-5 against ³H-MDL100907 was 1.5 ± 0.7 nM, in agreement with the PDSP value of 2.2 nM for K_i of CIMBI-5 against ³H-ketanserin. The somewhat lower value (K_i = 0.15 nM against ³H-ketanserin) previously reported (13) may have been because that assay was performed at 25°C, whereas the value reported here were obtained at 37°C. We also confirmed that CIMBI-5 has agonistic properties at the 5-HT_{2A} receptor, with an EC₅₀ value of 1.02 ± 0.17 nM, in agreement with previous reports (13). In addition, we showed that CIMBI-5 is nearly a full agonist, with 85% of the 5-HT_{2A} activation, compared with 5-HT itself. The data on binding and receptor activation, taken together with the PDSP screening for CIMBI-5 (Table 1), show that CIMBI-5 is a high-affinity agonist for 5-HT_{2A} receptors. CIMBI-5 had similar affinity to the 5-HT_{2A} and the 5-HT_{2B} receptors and a 3-fold lower affinity to the 5-HT_{2C} receptor. The eventual presence and distribution of 5-HT_{2B} receptors in the brain is still questionable, and specific 5-HT_{2B} receptor binding in the brain has to our knowledge not yet been demonstrated. For 5-HT_{2C} receptors, density of this subtype of receptors in cortical areas, compared with density of 5-HT_{2A} receptors, is negligible (23,24). Therefore, the cortical ¹¹C-CIMBI-5 binding signal stems from its 5-HT_{2A} receptor binding.

¹¹C-CIMBI-5 uptake and distribution in the rat brain after *ex vivo* dissection were similar to those in previous rat studies with ¹⁸F-altanserin (25), showing high uptake in the frontal cortex and no displaceable binding in the cerebellum. Also, the specific uptake in the frontal cortex of the rat brain was blocked by ketanserin pretreatment, indicating that ¹¹C-CIMBI-5 binding is selective for the 5-HT_{2A}



RGB

FIGURE 7. HPLC analysis of brain extracts and plasma at 25 min after injection of ^{11}C -CIMBI-5: frontal cortex (A), cerebellum (B), and plasma (C). Peaks: 1 = polar metabolites, 2 = lipophilic metabolites, and 3 = parent compound.

receptor. Similarly, ^{11}C -CIMBI-5 distributed in the pig brain in a pattern resembling the 5-HT_{2A} receptor distribution as measured with 5-HT_{2A} receptor antagonist PET tracers in pigs (25) and in humans (5,26), with high cortical uptake and low cerebellar uptake. Further, the 5-HT_{2A} selectivity of in vivo cortical ^{11}C -CIMBI-5 binding in the pig was confirmed in the blocking study in which cortical ^{11}C -CIMBI-5 binding was decreased by a ketanserin bolus and infusion whereas the cerebellar uptake was unaffected.

BP_{ND} for ^{11}C -CIMBI-5 with the cerebellum as a reference region was calculated using compartmental models, reference tissue approaches, and noninvasive Logan methods (Supplemental Table 1). For 5-HT_{2A} receptor antagonist PET tracers, such as ^{18}F -altanserin, the cerebellum is generally regarded as a valid reference region (3). Also, because negligible amounts of 5-HT_{2A} receptors are present in the cerebellum, compared with cortical areas, the preferential binding of a 5-HT_{2A} receptor PET ligand, as measured, for example, by the $\text{SRTM BP}_{\text{ND}}$, is indicative of the target-to-background ratio of 5-HT_{2A} PET ligands. At baseline, ^{11}C -CIMBI-5 showed an average $\text{SRTM BP}_{\text{ND}}$ of 0.46. Given that an agonist PET tracer, compared with the antagonist, would bind only a high-affinity subpopulation of 5-HT_{2A} receptors, the maximum number of binding sites for such an agonist tracer would be lower than the antagonist, and—given that the radioligand affinities are comparable—it is anticipated that a lower BP_{ND} for an agonist tracer would be found. When compared with human data from 5-HT_{2A} receptor antagonist PET tracers (5,26), the cortical binding potential of ^{11}C -CIMBI-5 was indeed lower, but further studies are required to explore whether the somewhat low binding potential measured in pigs will translate to humans.

[AQ9]

To compare the time–activity curves for ^{11}C -CIMBI-5 to a known 5-HT_{2A} antagonist PET tracer in the same animal species, we compared it to ^{18}F -altanserin pig data obtained from our laboratory (25). ^{11}C -CIMBI-5 and ^{18}F -altanserin

in pigs showed similar cortex-to-cerebellum uptake and equal $\text{SRTM BP}_{\text{ND}}$, 0.46 ± 0.11 and 0.47 ± 0.10 , respectively. Thus, in the pig brain ^{11}C -CIMBI-5 and ^{18}F -altanserin have similar target-to-background binding ratios, and ^{11}C -CIMBI-5 therefore holds promise for clinical use.

After injection of ^{11}C -CIMBI-5, a radiolabeled metabolite only slightly less lipophilic than ^{11}C -CIMBI-5 appeared in the pig plasma. On the basis of previous studies describing the metabolism of the 5-HT_{2A} receptor agonist compound 1-(2,5-dimethoxy-4-iodophenyl)-2-aminopropane (27) in rats, we speculated that this metabolite is the result of *O*-demethylation at a methoxy group in the iododimethoxyphenyl moiety of the tracer. Lipophilic radiolabeled metabolites impose a problem if they cross the blood–brain barrier because their presence will contribute to nonspecific binding. This has been observed for other antagonistic PET tracers in the serotonin system (3). Our brain homogenate experiments suggested that the lipophilic metabolite does not enter the pig brain, at least not to any large extent, and consequently the radiolabeled metabolite does not contribute to the nonspecific binding of ^{11}C -CIMBI-5.

Taken together, the results indicate that ^{11}C -CIMBI-5 is a promising tracer for visualization and quantification of high-affinity 5-HT_{2A} receptor agonist binding sites using PET. More specifically, studies of ^{11}C -CIMBI-5 could reveal differences in the maximum number of binding sites measured with an agonist versus antagonist tracer, thus giving insights to whether high- and low-affinity states of 5-HT_{2A} receptors coexist in vivo as is described for the dopamine system (28). Optimally, a larger cortical BP_{ND} and higher brain uptake of the PET tracer is preferred. Also, the time–activity curves of ^{11}C -CIMBI-5 suggested relatively slow kinetics, which potentially would be a more pronounced phenomenon in primates and humans complicating quantification. Therefore, it may be worthwhile to pursue development of ^{11}C -CIMBI-5 analogs with modified chemical structures to improve these PET tracer properties.

CONCLUSION

The novel high-affinity 5-HT_{2A} receptor agonist PET tracer ¹¹C-CIMBI-5 distributes in the brain in a pattern compatible with the known 5-HT_{2A} receptor distribution, and its binding can be blocked by ketanserin treatment. ¹¹C-CIMBI-5 is a promising PET tracer for in vivo imaging and quantification of high-affinity-state 5-HT_{2A} receptors in the human brain.

ACKNOWLEDGMENTS

The study was financially supported by the Lundbeck Foundation, the Faculty of Health Sciences and the Faculty of Pharmaceutical Sciences at the University of Copenhagen, and by the EU 6th Framework program DiMI (LSHB-CT-2005-512146). K_i determinations were generously provided by the NIMH PDSP. A reference sample of CIMBI-5 was kindly provided by David Nichols, Purdue University.

REFERENCES

- Gonzalez-Maesos J, Weisstaub NV, Zhou M, et al. Hallucinogens recruit specific cortical 5-HT_{2A} receptor-mediated signaling pathways to affect behavior. *Neuron*. 2007;53:439–452.
- Kim SW, Shin IS, Kim JM, et al. The 5-HT₂ receptor profiles of antipsychotics in the pathogenesis of obsessive-compulsive symptoms in schizophrenia. *Clin Neuropharmacol*. 2009;32:224–226.
- Pinborg LH, Adams KH, Svarer C, et al. Quantification of 5-HT_{2A} receptors in the human brain using [¹⁸F]altanserin-PET and the bolus/infusion approach. *J Cereb Blood Flow Metab*. 2003;23:985–996.
- Soares JC, van Dyck CH, Tan P, et al. Reproducibility of in vivo brain measures of 5-HT_{2A} receptors with PET and [¹⁸F]deuterioaltanserin. *Psychiatry Res*. 2001;106:81–93.
- Ito H, Nyberg S, Halldin C, Lundkvist C, Farde L. PET imaging of central 5-HT_{2A} receptors with carbon-11-MDL 100,907. *J Nucl Med*. 1998;39:208–214.
- Fitzgerald LW, Conklin DS, Krause CM, et al. High-affinity agonist binding correlates with efficacy (intrinsic activity) at the human serotonin 5-HT_{2A} and 5-HT_{2C} receptors: evidence favoring the ternary complex and two-state models of agonist action. *J Neurochem*. 1999;72:2127–2134.
- Song J, Hanniford D, Doucette C, et al. Development of homogeneous high-affinity agonist binding assays for 5-HT₂ receptor subtypes. *Assay Drug Dev Technol*. 2005;3:649–659.
- Cornea-Hebert V, Watkins KC, Roth BL, et al. Similar ultrastructural distribution of the 5-HT_{2A} serotonin receptor and microtubule-associated protein MAP1A in cortical dendrites of adult rat. *Neuroscience*. 2002;113:23–35.
- Peddie CJ, Davies HA, Colyer FM, Stewart MG, Rodriguez JJ. Colocalisation of serotonin_{2A} receptors with the glutamate receptor subunits NR1 and GluR2 in the dentate gyrus: an ultrastructural study of a modulatory role. *Exp Neurol*. 2008;211:561–573.
- Cumming P, Wong DF, Gillings N, Hilton J, Scheffel U, Gjedde A. Specific binding of [¹¹C]raclopride and *N*-[³H]propyl-norapomorphine to dopamine receptors in living mouse striatum: occupancy by endogenous dopamine and guanosine triphosphate-free G protein. *J Cereb Blood Flow Metab*. 2002;22:596–604.
- Narendran R, Hwang DR, Slifstein M, et al. In vivo vulnerability to competition by endogenous dopamine: comparison of the D₂ receptor agonist radiotracer (–)-*N*-[¹¹C]propyl-norapomorphine ([¹¹C]NPA) with the D₂ receptor antagonist radiotracer [¹¹C]raclopride. *Synapse*. 2004;52:188–208.
- Pinborg LH, Adams KH, Yndgaard S, et al. [¹⁸F]altanserin binding to human 5HT_{2A} receptors is unaltered after citalopram and pindolol challenge. *J Cereb Blood Flow Metab*. 2004;24:1037–1045.
- Braden MR, Parrish JC, Naylor JC, Nichols DE. Molecular interaction of serotonin 5-HT_{2A} receptor residues Phe339(6.51) and Phe340(6.52) with superpotent *N*-benzyl phenethylamine agonists. *Mol Pharmacol*. 2006;70:1956–1964.
- Nichols DE, Frescas SP, Chemel BR, Rehder KS, Zhong D, Lewin AH. High specific activity tritium-labeled *N*-(2-methoxybenzyl)-2,5-dimethoxy-4-iodophenethylamine (INBMeO): a high-affinity 5-HT_{2A} receptor-selective agonist radioligand. *Bioorg Med Chem*. 2008;16:6116–6123.
- Herth MM, Kramer V, Piel M, et al. Synthesis and in vitro affinities of various MDL 100907 derivatives as potential ¹⁸F-radioligands for 5-HT_{2A} receptor imaging with PET. *Bioorg Med Chem*. 2009;17:2989–3002.
- Kramer V, Herth MM, Santini MA, Palner M, Knudsen GM, Rosch F. Structural combination of established 5-HT receptor ligands: new aspects of the binding mode. *Chem Biol Drug Des*. July 15, 2010 [Epub ahead of print].
- Palner M, McCormick P, Gillings N, Begtrup M, Wilson AA, Knudsen GM. Radiosynthesis and ex vivo evaluation of (R)-(–)-2-chloro-*N*-[1-¹¹C-propyl]n-propylnorapomorphine. *Nucl Med Biol*. 2010;37:35–40.
- Kornum BR, Lind NM, Gillings N, Marnier L, Andersen F, Knudsen GM. Evaluation of the novel 5-HT₄ receptor PET ligand [¹¹C]SB207145 in the Gottingen minipig. *J Cereb Blood Flow Metab*. 2009;29:186–196.
- Gillings N. A restricted access material for rapid analysis of [¹¹C]-labeled radiopharmaceuticals and their metabolites in plasma. *Nucl Med Biol*. 2009;36:961–965.
- Watanabe H, Andersen F, Simonsen CZ, Evans SM, Gjedde A, Cumming P. MR-based statistical atlas of the Gottingen minipig brain. *Neuroimage*. 2001;14:1089–1096.
- Innis RB, Cunningham VJ, Delforge J, et al. Consensus nomenclature for in vivo imaging of reversibly binding radioligands. *J Cereb Blood Flow Metab*. 2007;27:1533–1539.
- Lammertsma AA, Hume SP. Simplified reference tissue model for PET receptor studies. *Neuroimage*. 1996;4:153–158.
- Kristiansen H, Elfving B, Plenge P, Pinborg LH, Gillings N, Knudsen GM. Binding characteristics of the 5-HT_{2A} receptor antagonists altanserin and MDL 100907. *Synapse*. 2005;58:249–257.
- Marazziti D, Rossi A, Giannaccini G, et al. Distribution and characterization of [³H]mesulergine binding in human brain postmortem. *Eur Neuropsychopharmacol*. 1999;10:21–26.
- Syvanen S, Lindhe O, Palner M, et al. Species differences in blood-brain barrier transport of three positron emission tomography radioligands with emphasis on P-glycoprotein transport. *Drug Metab Dispos*. 2009;37:635–643.
- Adams KH, Pinborg LH, Svarer C, et al. A database of [¹⁸F]-altanserin binding to 5-HT_{2A} receptors in normal volunteers: normative data and relationship to physiological and demographic variables. *Neuroimage*. 2004;21:1105–1113.
- Ewald AH, Fritschi G, Maurer HH. Metabolism and toxicological detection of the designer drug 4-iodo-2,5-dimethoxy-amphetamine (DOI) in rat urine using gas chromatography-mass spectrometry. *J Chromatogr B Analyt Technol Biomed Life Sci*. 2007;857:170–174.
- Laruelle M. Imaging synaptic neurotransmission with in vivo binding competition techniques: a critical review. *J Cereb Blood Flow Metab*. 2000;20:423–451.